Response to the Executive Editor and two anonymous reviewers:

SC1: 'Executive Editor Comment on "Gas-phase chemistry in the online multiscale NMMB/BSC Chemical Transport Model: Description and evaluation at global scale"', Astrid Kerkweg, 16 Jun 2016

Dear authors,
In my role as Executive editor of GMD, I would like to bring to your attention our Editorial version 1.1:

http://www.geosci-model-dev.net/8/3487/2015/gmd-8-3487-2015.html

This highlights some requirements of papers published in GMD, which is also available on the GMD website in the 'Manuscript Types' section:
http://www.geoscientific-model-development.net/submission/manuscript_types.html
In particular, please note that for your paper, the following requirement has not been met in the Discussions paper:

 • "The main paper must give the model name and version number (or other unique identifier) in the title."

Please add the version number for your model to which the description and evaluation applies in the title upon your revised submission to GMD. Yours, Astrid Kerkweg

Response: Following the Editorial guidelines we have included the model version in the title.

Note that we have decided to rename our model following a comment from reviewer #2 about avoiding the use of CTM for an online model. Thus, the new name is NMMB-MONARCH, where MONARCH stands for "Multiscale Online Nonhydrostatic AtmospheRe CHemistry model". In the responses to the reviewer's comments we keep the NMMB/BSC-CTM name to keep consistency with the manuscript submitted to GMDD, but in the revised manuscript the new name, NMMB-MONARCH, is used.

Now, the revised manuscript is entitled "Description and evaluation of the Multiscale Online Nonhydrostatic AtmospheRe CHemistry model (NMMB-MONARCH) version 1.0: gas-phase chemistry at global scale".

RC1: 'Reviewer Comments', Anonymous Referee #1, 01 Aug 2016

The authors present a detailed description and evaluation of the tropospheric chemistry transport model NMMB/BSC-CTM. This model domain has been expanded from regional to global. The focus of their evaluation is gas-phase chemistry with emphasis on tropospheric ozone and its precursors. Several ground-based, aircraft and satellite data are used to show model strengths and weaknesses. The paper is well-written and is within the scope of the journal. I would recommend the publication of this paper after my minor comments below have been addressed:

Response: The authors wish to thank anonymous reviewer #1 for his/her valuable comments and suggestions.

Note that we have decided to rename our model following a comment from reviewer #2 about avoiding the use of CTM for an online model. Thus, the new name is NMMB-MONARCH, where MONARCH stands for "Multiscale Online Nonhydrostatic AtmospheRe CHemistry model". In the responses to the reviewer's comments we keep the NMMB/BSC-CTM name to keep consistency with the manuscript submitted to GMDD, but in the revised manuscript the new name, NMMB-MONARCH, is used.

Now, the revised manuscript is entitled "Description and evaluation of the Multiscale Online Nonhydrostatic AtmospheRe CHemistry model (NMMB-MONARCH) version 1.0: gas-phase chemistry at global scale".

Page 2, line 15: replace "fed by emission inventories" with "emissions of chemical species".
Response: Amended.

Page 2, Line 31: Define NMMB/BSC here.
Response: In the revised manuscript MONARCH is now defined there.

Page 3, line 19: replace "main reactions occurring in the atmosphere by" with "atmospheric composition". It would be helpful to give a motivation for choosing year 2004 for evaluation.
Response: Amended. 2004 is a reference year for our modeling group that we already considered in previous studies (e.g., Pay et al. 2010; Baldasano et al. 2011). Therefore, our choice is based on the amount and variety of quality controlled and quality assured observations available in our group. We don't think this information is relevant for the manuscript.

Pay, M. T., et al. "A full year evaluation of the CALIOPE-EU air quality modeling system over Europe for 2004." Atmospheric Environment 44.27 (2010): 3322-3342.
Baldasano, J. M., et al. "An annual assessment of air quality with the CALIOPE modeling system over Spain." Science of the Total Environment 409.11 (2011): 2163-2178.

Page 3, line 28: Insert "direct" before radiative effect.
Response: Amended.

Page 5, line 10: A reference is needed here.
Response: The reference of Yarwood (2005) is now included.

Page 5, line 17: 1.85 ppm is too high for this year of simulation. Can you please provide a justification for using this number? Also, is the CH4 concentration constant throughout the troposphere in the model or only at the surface?

Response: Considering a global background concentration of methane is a common practice in air quality modeling. Following this approach, current practices set the methane background level either as a default background concentration (i.e. 1.76 ppm, e.g. Shindell et al, 2006), or as the background level for the Northern Hemisphere (i.e. 1.85 ppm, used for instance within CMAQ). Including either of those concentrations would lead to differences with respect to reality, and we decided to select the latter, which on the other hand is the closest to the present time global background concentration (1.83 ppm, see WMO 2015, or Dlugokencky, 2016). The global average for 2004 is reported to be 0.06 to 0.07 ppm lower, around 4%. This small difference is not expected to cause any sizeable differences in the results shown here.

Shindell et al. Multimodel simulations of carbon monoxide: Comparison with observations and projected near-future changes. Journal of Geophysical Research Atmospheres. VOL. 111, D19306, doi:10.1029/2006JD007100, 2006
WMO Greenhouse Gas Bulletin Nº 11: November 2015
Ed Dlugokencky, NOAA/ESRL www.esrl.noaa.gov/gmd/ccgg/trends_ch4/, viewed on 30/09/2016

Page 8, section 2.2.6: Where does the MEGAN model implemented in this CTM derive the leaf-area index needed to calculate biogenic emissions?

Response: The leaf-area index is obtained from the MEGANv2.04 databases (http://lar.wsu.edu/megan/guides.html). The data is originally at 150 sec horizontal resolution and it is averaged to the NMMB/BSC-CTM model grid. It is described in Guenther et al. (2006).

Guenther, A. et al. Estimates of global terrestrial isoprene emissions using MEGAN (Model of Emissions of Gases and Aerosols from Nature). Atmos. Chem. Phys 1–30 (2006).

Page 8, line 29: Need a period after "parameters".
Response: Amended.

Page 9, section 3: What is the size of the bottom-most layer in the model? Also provide an estimate of the time it takes to run a year's simulation.

Response: The size of the bottom-most layer in the model is below 40 m. This information is now included in the revised manuscript. The time to run a yearly simulation is about 2 weeks using 132 cores in the Marenostrum supercomputer based on Intel SandyBridge-EP E5-2670/1600 20M 8-core at 2.6 GHz.

Page 9, lines 12-13: Since emissions after year 2000 were not provided by Lamarque et al., which projection (RCP?) was used for 2010 emissions to perform linear interpolation?

Response: Thanks for pointing this out. There was an error in the description of the methodology used to derive the 2004 anthropogenic and biomass burning emissions. We stated that these emissions were obtained by interpolation between years 2000 and 2010. In reality we considered the emissions for year 2000 from Lamarque et al. (2010). This issue has been clarified in the revised manuscript, as follows: "Note that this methodology involves

Page 10, line 25: Any particular reason why only two aircraft campaigns were used for the evaluation instead of several others available in Emmons et al. (2000).

Response: The model was evaluated against all the campaigns available in Emmons et al. (2000). However, for the paper we selected the two closest campaigns to year 2004. Figure 1 shows the comparison of the model with the PEM-Tropics and POLINAT-2 campaigns for HNO3, NOx and PAN. We have included Figure 1 in the supplementary material (see Figure S5) and additional text describing the results in the main manuscript (see also Table 5).
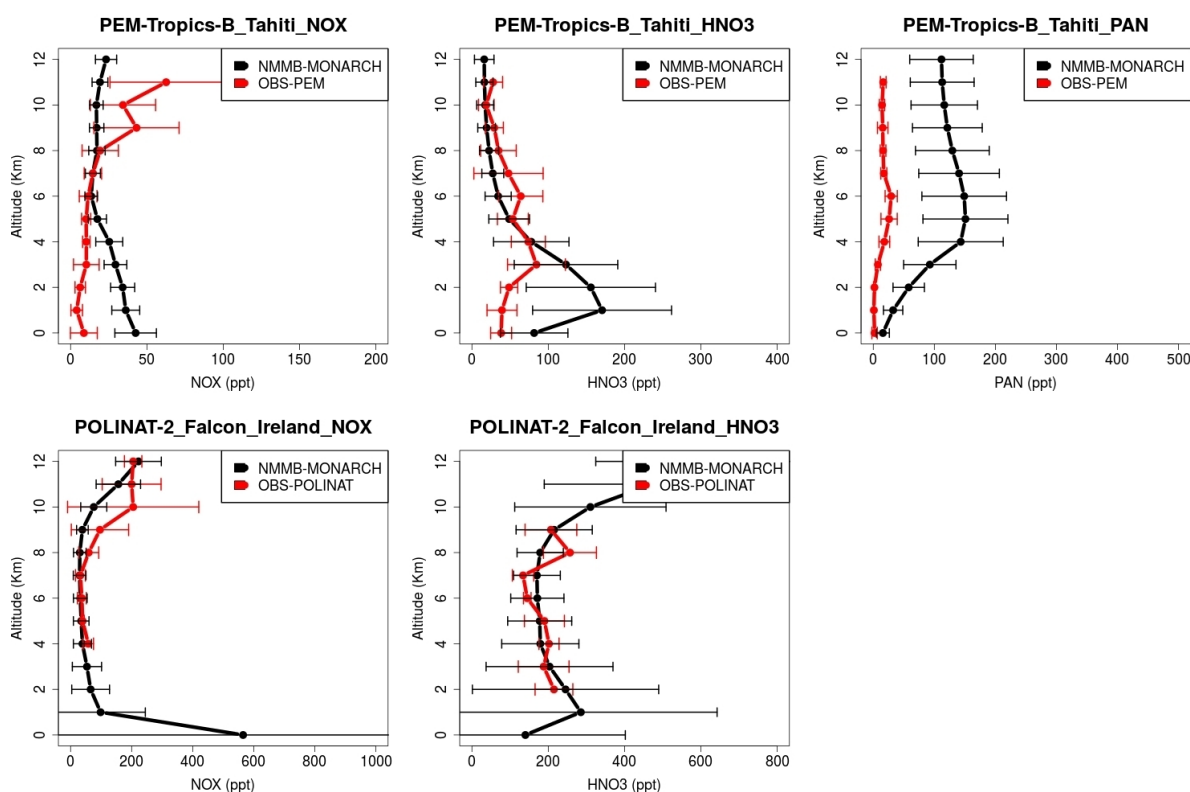

Figure 1. Comparison of modeled (black lines) and observed (red lines) vertical profiles of NOx and HNO3 and PAN for Tahiti and Ireland. Horizontal lines show the standard deviations.

Page 12, section 5.1: What is the simulated tropospheric lifetime of methane in the model and how does it compare with that from multi-model studies (e.g., Naik et al 2013a)?

Response: Methane lifetime was not explicitly calculated during model execution. While the burden can be calculated in post processing the estimation of the mean tropospheric methane – OH oxidation flux (needed to calculate lifetime) would require repeating the simulations. Therefore, we can neither include this information, nor discuss it at present in the manuscript.
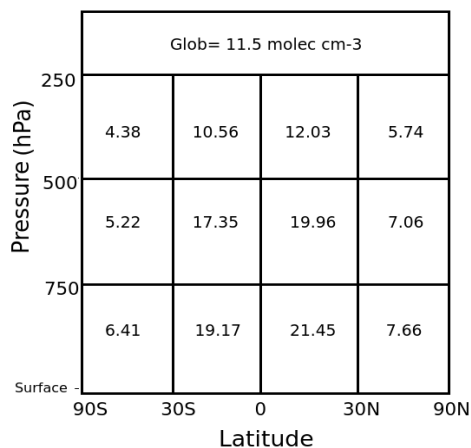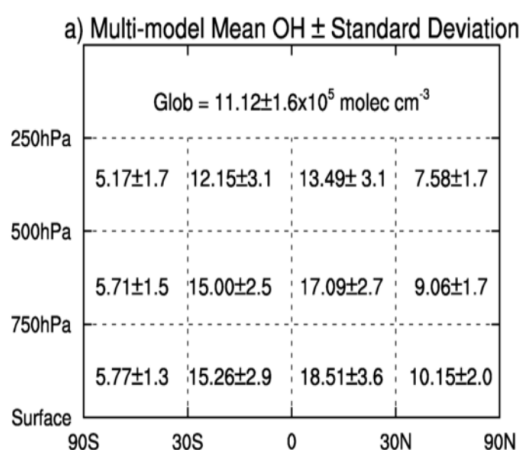
How does the simulated OH interhemispheric ratio compare with other studies (Naik et al., 2013a; Patra et al., 2014).

Response: The mean OH inter-hemispheric (N/S) ratio of the model is 1.18. This quantity is comparable with the present-day multi-model mean ratio (1.28 ± 0.1) shown in Naik et al., (2013). This information is now included in the revised manuscript.

Naik, V., Voulgarakis, A., Fiore, A. M., Horowitz, L. W., Lamarque, J.-F., Lin, M., Prather, M. J., Young, P. J., Bergmann, D., Cameron-Smith, P. J., Cionni, I., Collins, W. J., Dalsøren, S. B., Doherty, R., Eyring, V., Faluvegi, G., Folberth, G. A., Josse, B., Lee, Y. H., MacKenzie, I. A., Nagashima, T., van Noije, T. P. C., Plummer, D. A., Righi, M., Rumbold, S. T., Skeie, R., Shindell, D. T., Stevenson, D. S., Strode, S., Sudo, K., Szopa, S., and Zeng, G.: Preindustrial to present-day changes in tropospheric hydroxyl radical and methane lifetime from the Atmospheric Chemistry and Climate Model Intercomparison Project (ACCMIP), Atmos. Chem. Phys., 13, 5277-5298, doi:10.5194/acp-13-5277-2013, 2013.

Lightning NOx emissions have been shown to contribute significantly to tropospheric OH concentrations (Murray et al., 2013). Lightning NOx emissions are not considered in the current model set-up. Please explain how the simulated OH concentrations match closely with those of other modeling studies that include lightning NOx emissions.

Response: We calculated the regional mean air mass-weighted OH concentrations and they are close to the multi-model values in Naik et al. (2013a) (see Fig. 2). Over the tropics (30S-30N) our OH is slightly higher, and above 500 hPa, is lower than the multi-model mean. Labrador et al. (2004) studied the sensitivity of OH to NOx from lightning. They showed that OH increases mostly in the middle to upper troposphere (500-200 hPa) when lightning emissions are considered. Accordingly, the lack of lightning emissions in our model could explain the lower OH values above 500 hPa reported here. This discussion is now included in the revised manuscript and Fig. 2 (right panel) is included in the supplementary material as Figure S2.

a) Multi-model Mean OH ± Standard Deviation

Glob = 11.12±1.6x10^5 molec cm^{-3}

Pressure	90S–30S	30S–0	0–30N	30N–90N
250hPa – 500hPa	5.17±1.7	12.15±3.1	13.49±3.1	7.58±1.7
500hPa – 750hPa	5.71±1.5	15.00±2.5	17.09±2.7	9.06±1.7
750hPa – Surface	5.77±1.3	15.26±2.9	18.51±3.6	10.15±2.0

Naik et al. 2013

Glob= 11.5 molec cm-3

Pressure (hPa)	90S–30S	30S–0	0–30N	30N–90N
250 – 500	4.38	10.56	12.03	5.74
500 – 750	5.22	17.35	19.96	7.06
750 – Surface	6.41	19.17	21.45	7.66

Latitude

NMMB/BSC-CTM

Figure 2. Comparison between the model and Naik et al., (2013) regional mean airmass-weighted OH concentrations (× 10^5 molecule cm^{-3}).

Labrador, L. J., R. von Kuhlmann, and M. G. Lawrence (2004), Strong sensitivity of the global mean OH concentration and the tropospheric oxidizing efficiency to the source of NOx from lightning, Geophys. Res. Lett., 31, L06102, doi:10.1029/2003GL019229

Naik, V., Voulgarakis, A., Fiore, A. M., Horowitz, L. W., Lamarque, J.-F., Lin, M., Prather, M. J., Young, P. J., Bergmann, D., Cameron-Smith, P. J., Cionni, I., Collins, W. J., Dalsøren, S. B., Doherty, R., Eyring, V., Faluvegi, G., Folberth, G. A., Josse, B., Lee, Y. H., MacKenzie, I. A., Nagashima, T., van Noije, T. P. C., Plummer, D. A., Righi, M., Rumbold, S. T., Skeie, R., Shindell, D. T., Stevenson, D. S., Strode, S., Sudo, K., Szopa, S., and Zeng, G.: Preindustrial to present-day changes in tropospheric hydroxyl radical and methane lifetime from the Atmospheric Chemistry and Climate Model Intercomparison Project (ACCMIP), Atmos. Chem. Phys., 13, 5277-5298, doi:10.5194/acp-13-5277-2013, 2013.

Page 12, line 28: Need a reference for aerosol influence on OH. Also, a larger oxidizing capacity would be simulated if lightning NOx emissions were included in these simulations.

Response: Real and Sartelet (2011) studied the effect of aerosols in the photolysis rates and gaseous species, showing that differences in photolysis rates lead to changes in gas concentrations, with the largest impact simulated on OH and NO concentrations. At the ground, monthly mean concentrations of both species were reduced over Europe by around 10 to 14% and their tropospheric burden by around 10%. The decrease in OH led to an increase of the lifetime of several species such as VOC. On the other hand, Bian et al. (2003) evaluated the effect of aerosols on the global budgets of O3, OH and CH4 through their alteration of photolysis rates. The impact identified was to increase tropospheric O3 by 0.63 Dobson units and increase tropospheric CH4 by 130 ppb (via tropospheric OH decreases of 8%). Although the CH4 increases were global, the changes in tropospheric OH and O3 were mainly regional, with the largest impacts in northwest Africa for January and in India and southern Africa for July.

As we have described in a previous comment, a larger oxidizing capacity would be simulated, especially above 500 hPa, if lightning NOx emissions were included in our model run (Labrador et al., 2004).

Both aspects, and corresponding references, are now discussed in the revised version of the manuscript with the following paragraph: "Therefore, the lack of lightning emissions in our model run could at least partly explain the lower OH values above 500 hPa reported here. Another potential explanation is the lack of aerosols in our simulation, which may overestimate photolysis rates in polluted regions (e.g., Bian et al., 2003; Real and Sartelet, 2011)."

Real, E., and K. Sartelet. "Modeling of photolysis rates over Europe: impact on chemical gaseous species and aerosols." Atmospheric Chemistry and Physics 11.4 (2011): 1711-1727.

Bian, H., M. J. Prather, and T. Takemura, Tropospheric aerosol impacts on trace gas budgets through photolysis, J. Geophys. Res., 108(D8), 4242, doi:10.1029/2002JD002743, 2003.

Labrador, L. J., R. von Kuhlmann, and M. G. Lawrence (2004), Strong sensitivity of the global mean OH concentration and the tropospheric oxidizing efficiency to the source of NOx from lightning, Geophys. Res. Lett., 31, L06102, doi:10.1029/2003GL019229

Page 13, line 9-10: Please give the reason why there were low CO concentrations in 2004 despite large Alaskan and Canadian wildfires.

Response: Elguindi et al., 2010 presented a global analysis of observed CO seasonal averages and interannual variability for the years 2002-2007. They analyzed the CO concentrations during this period: "In JJA 2003, the anomalously high concentrations of CO due to the intense heat wave experienced in Europe, especially in August (Tressol et al.,2008; Ordoñez et al.,2010), are well represented in the data. Likewise, the high concentrations seen in SON 2002 are due to exceptional circumstances, namely the intense boreal forest fires which occurred over western Russia (Edwards et al.,2004; Yurganov et al., 2005; Kasischke et al.,2005)."

In summary, there were also important fires during the period 2002-2007 and meteorological conditions that could have an impact to the CO concentrations, like the intense heat wave or the photochemical conditions. This is why Elguindi et al., 2010 concluded that "despite the intense boreal forest fires that occurred during the summer in Alaska and Canada, the year 2004 had comparably lower tropospheric CO concentrations".

Elguindi, N., Clark, H., Ordóñez, C., Thouret, V., Flemming, J., Stein, O., Huijnen, V., Moinat, P., Inness, A., Peuch, V.-H., Stohl, A., Turquety, S., Athier, G., Cammas, J.-P., and Schultz, M.: Current status of the ability of the GEMS/MACC models to reproduce the tropospheric CO vertical distribution as measured by MOZAIC, Geoscientific Model Development, 3, 501–518, doi:10.5194/gmd-3-501-2010, http://www.geosci-model-dev.net/3/501/2010/, 2010.

Page 13, 11-15: Other modeling studies suggest even lower CO burden (e.g., Naik et al., 2013b). Could higher CH4 concentration prescribed in the model play a role in the simulated high CO burden?

Response: The influence of CH4 on CO has been assessed through a short sensitivity test. Changing the CH4 prescribed value from 1.85 ppm (NH background average) to 1.78 ppm (global average for 2004) lead to changes in daily average CO concentration up to ±0.12 ppb, which leads us to believe that other factors have a larger impact on CO burden (see for instance Shindell et al., 2006).

Shindell, D. T., et al. (2006), Multimodel simulations of carbon monoxide: Comparison with observations and projected near-future changes, J. Geophys. Res., 111, D19306, doi:10.1029/2006JD007100

Page 13, last paragraph: the role of seasonal CO emissions in explaining the low northern hemisphere wintertime bias has been highlighted by Stein et al., (2014), which should be noted here.

Response: Stein et al., (2014) is already discussed in the manuscript on page 14 and 15. On page 14 of the manuscript "During winter and spring, Stein et al. (2014) also obtain an underestimation of CO vertical profiles in airports located in the Northern Hemisphere (NH)" and "The wintertime negative bias (~ - 10-35 ppb) in the NH may be explained by either the lack of seasonally varying anthropogenic emissions in our simulation, an underestimation of CO emissions (Stein et al, 2014), or a combination thereof". On page 15 "Stein et al. (2014) suggests that the persistent negative bias in northern mid-latitude CO in models is most likely due to a combination of too low road traffic emissions and dry deposition errors."

Stein et al., (2014) On the wintertime low bias of Northern Hemisphere carbon monoxide found in global model simulations, Atmos. Chem. Phys., 14, 9295-9316, doi:10.5194/acp-14-9295-2014.

Page 15, line 25: Give the lifetime of NOx.

Response: The lifetime of NOx varies considerably with altitude, being only a few hours near the PBL and up to a few days in the upper troposphere (Tie et al., 2001 and 2002). This information is now included in the revised manuscript with the following sentence: "It has a relatively short lifetime (a few hours near the PBL and up to a few days in the upper troposphere; Tie et al., 2001 and 2002)".

Tie, X., R. Zhang, G. Brasseur, L. Emmons, and W. Lei (2001), Effects of lightning on reactive nitrogen and nitrogen reservoir species in the troposphere, J. Geophys. Res., 106(D3), 3167–3178, doi:10.1029/2000JD900565.
Tie, X., Zhang, R., Brasseur, G. et al. Journal of Atmospheric Chemistry (2002) 43: 61. doi:10.1023/A:1016145719608

Page 18, line 13-18: How do the calculated dry deposition estimates compare with those from more recent chemistry-climate model simulations (e.g., Naik et al., 2013b).

Response: The calculated dry deposition (1209 Tg O3) is higher than in TM5 (829 Tg O3) and MOZART-2 (857 Tg O3) and similar to LMDz-INCA (1261 Tg O3) and the multimodel ensemble in Stevenson et al. (2006) (1003 -+ 200 Tg O3). In addition, the model shows similar results to the GFDL AM3 chemistry-climate model (Naik et al., 2013b). The reference to GFDL AM3 model is now added in the revised manuscript.

Naik et al., 2013b, Impact of preindustrial to present day changes in short-lived pollutant emissions on atmospheric composition and climate forcing, J. Geophys. Res., doi: 10.1002/jgrd.50608.

Page 19: What fraction of model O3 biases could be related to biases in the simulated meteorological fields (e.g., temperature)?

Response: This is not an easy question to answer. Ozone is sensitive to temperature, solar radiation and vertical mixing. It is clear that biases in the meteorology will have a significant impact on the ozone biases. Another study would be required to provide a thorough quantification of the biases and this is beyond the scope of the present work. In any case, the NMMB meteorological skills are under constant improvement at NCEP and the authors consider the computed meteorology to lie within the skills of current state-of-the-art meteorological models.

Map figures: Please remove the grey background on the maps as this makes it difficult to read the colours.

Response: We think that the color scale is readable, according to the figure´s purpose, and if we remove the grey background the white dots in the figure would not be visible. Therefore, we kept the figures with the grey background.

Figure 6, 10: Colour bar text is too small to read.

Response: Amended.

RC2: 'Review of Badia et al. 2016', Anonymous Referee #2, 02 Aug 2016

Review of "Gas-phase chemistry in the online multiscale NMMB/BSC Chemical Transport Model: Description and evaluation at global scale" by Badia et al.

Overview:

The paper is a description and an evaluation of a one-year (2004) global simulation of what is called the NMMB/BSC Chemical Transport Model. The model results for CO, O3 and NO2/PAN/HNO3 are compared against surface observations, profile observations and satellite retrievals. The comparison shows that the NMMB/BSC model gives acceptable results but both CO and ozone are overestimated on the global scale.

General remarks:

My two main concerns with the presented model run for 2004 is (i) that NOx emissions from lightning were not considered in the model run and (ii) that no specific biomass burning emissions for 2004 were used. A parameterisation of lightning emissions is scientific standard in global CTMs and there is no good reason, why such an important contribution to global tropospheric chemistry can be omitted. Getting daily or 8-daymean 2004 biomass emission data (GFED, GFAS etc.) would not have been difficult. Also the lack of seasonality of the anthropogenic emissions is an unnecessary simplification. Against the backdrop of these omissions it becomes difficult to draw conclusion from the model results and it severely undermines the scientific credibility of the paper.

Response: The authors wish to thank anonymous reviewer #2 for the valuable comments and suggestions.

Note that we have decided to rename our model following a comment from reviewer #2 about avoiding the use of CTM for an online model. Thus, the new name is NMMB-MONARCH, where MONARCH stands for "Multiscale Online Nonhydrostatic AtmospheRe CHemistry model". In the responses to the reviewer's comments we keep the NMMB/BSC-CTM name to keep consistency with the manuscript submitted to GMDD, but in the revised manuscript the new name, NMMB-MONARCH, is used.

Now, the revised manuscript is entitled "Description and evaluation of the Multiscale Online Nonhydrostatic AtmospheRe CHemistry model (NMMB-MONARCH) version 1.0: gas-phase chemistry at global scale".

We agree with the reviewer that the model run presented in the manuscript has some shortcomings. However, we disagree that they undermine the scientific credibility of the paper. This contribution describes a first major step in the development of a new multiscale chemical weather prediction system and its thorough evaluation, all of which is within the scope of GMD. Improvements to the system are conducted on a regular basis in our group, and the inclusion of NOx emissions from lightning is planned for the next version of the model. The selection of the emissions was an intentional decision. Not only the thorough evaluation with observations but also the comparison to other scientific studies was our priority. Considering the timeline of the Atmospheric Chemistry and Climate Model

Intercomparison Project (ACCMIP) initiative, we made use of the emissions presented in Lamarque et al. (2010). Thus, we took advantage of this excellent opportunity to evaluate the NMMB/BSC-CTM model in a way that can be consistently compared to other modeling systems contributing to ACCMIP. In this sense, emissions representative of the 2000 decade were used both for anthropogenic and biomass burning sources. This decision implied some drawbacks in our work, such as the non specificity of the emissions for year 2004, or the lack of seasonal variability on anthropogenic emissions. We consider those limitations as minor compared to the benefits of comparing our simulations to those of the ACCMIP experiment. The selected year of simulation provides a reference to identify the skills and limitations of the methods applied, but it is not intended to reproduce exactly the same episodes observed during 2004. Our goal is to reproduce the annual trends and patterns of the main atmospheric chemistry components. In the manuscript, all the limitations of our simulations are identified and described. In the revised manuscript version, we have provided additional discussion on these issues along with their implications. For example, the lack of lightning emissions helps explaining the underestimation of OH in the middle to upper troposphere. The results of this evaluation and comparison have allowed us identifying the next steps that will be required to improve the modeling system.

The lack of seasonality in the anthropogenic emissions is considered a minor limitation. Currently, there are still important uncertainties on the estimation of anthropogenic emissions at global scale, and most of the available modeling studies of atmospheric chemistry at global scales run the experiments with constant profiles. This can be explained by the resolution of study, as models are configured at global horizontal resolutions of a few degrees. Under such conditions, the daily variability of the emissions may not be the most important issue to address. Regarding biomass burning emissions, Marlier et al. (2014) showed that going from monthly to daily fire emissions does not change the atmospheric composition very drastically, especially for gases. This supports our initial approach of not using specific daily emissions of biomass burning for 2004.

We believe that the constructive discussion of the model's behavior in the absence of the aforementioned processes can provide useful insight into the importance of those processes.

Lamarque, J.-F., Bond, T. C., Eyring, V., Granier, C., Heil, A., Klimont, Z., Lee, D., Liousse, C., Mieville, A., Owen, B., Schultz, M. G., Shindell, D., Smith, S. J., Stehfest, E., Van Aardenne, J., Cooper, O. R., Kainuma, M., Mahowald, N., McConnell, J. R., Naik, V., Riahi, K., and van Vuuren, D. P.: Historical (1850–2000) gridded anthropogenic and biomass burning emissions of reactive gases and aerosols: methodology and application, Atmos. Chem. Phys., 10, 7017-7039, doi:10.5194/acp-10-7017-2010, 2010.
Marlier, M.E., A. Voulgarakis, D.T. Shindell, G. Faluvegi, C.L. Henry, and J.T. Randerson, 2014: The role of temporal evolution in modeling atmospheric emissions from tropical fires. Atmos. Environ., 89, 158-168, doi:10.1016/j.atmosenv.2014.02.039.

On the other hand, the presented model had two advanced properties, namely the online calculation of VOC emissions using the MEGAN model and the fact that the presented model is an on-line coupled chemistry – meteorological model (or ChemistryGCM). The term CTM, which the authors choose, is commonly used for off-line model without the simulation of meteorology (see Baklanov et al. 2014, ACP). I therefore recommend not to use the term CTM in the name of the model because it is an on-line coupled model. Unfortunately, it is a missed chance that these two new aspects were not explored further in the paper.

Response: This manuscript represents our first step towards the development of a fully coupled chemistry-meteorology model. We intend to present the current state of development of the model (version 1.0) with a comprehensive evaluation using a wide variety of observations. This will serve as a baseline for further studies where more complexity will be added to the system and where specific sensitivity studies may be conducted. Future work will analyze the impact of the online nature of the model, and to assess the sensitivity to the online calculation of biogenic emissions.

Concerning the name of the model (NMMB/BSC-CTM), we have considered the suggestion of the reviewer to not use the term CTM (Chemistry Transport Model) in the model name. CTM has been used traditionally for offline chemistry models, and we agree with the reviewer that using it may lead to some confusion. Considering the nature of our model, a pure online meteorology-chemistry system, we have decided to completely rename the model. The new name is NMMB-MONARCH, where MONARCH stands for "Multiscale Online Nonhydrostatic Atmosphere Chemistry model". We believe that with the new name, all the major characteristics of the system are clearly stated. Now in the revised manuscript all the references to NMMB/BSC-CTM have been replaced with NMMB-MONARCH. We only keep a reference to the old name in the abstract and introduction section to link the previous developments with the new naming adopted. Thus, the title of the manuscript is now "Description and evaluation of the Multiscale Online Nonhydrostatic AtmospheRe CHemistry model (NMMB-MONARCH) version 1.0: gas-phase chemistry at global scale".

The evaluation is carried out with a well-balanced choice of observations but the results are too often only described with the words such as "good agreement" etc. I think this is not very meaningful, instead the results should be quantified in a better way, i.e. a bias of 10 ppb, 20% etc.

Response: The results are now better quantified in the revised manuscript, and although expressions as "good agreement" are maintained, they come with a quantification of statistics to support them.

It is a thought-provoking result that both CO and ozone are overestimated because an overestimation of the oxidation capacity is often linked with CO underestimation (see Strode et al. 2015, ACP) It is something which can not be found in other models using similar emission data, and especially for models that also use the CB05 chemical mechanism. I think this result deserves a more thorough investigation.

Response: In our case, we attribute the CO overestimation mainly to emission sources. Even, if some other models using similar emissions don't show this overestimation, we have detected significant sensitivity of the biogenic emissions from MEGAN (as discussed in the manuscript) to the temporal basis of the meteorological conditions. This could affect CO emission overestimation.

On the other hand, the O3 overestimation can be due to multiple factors, such as the lack of halogen and heterogeneous chemistry, an overestimation of the STE for some seasons, the lack of aerosols in the simulation, uncertainties in the solar radiation reproduced by the model, the lack of seasonal variation on anthropogenic emissions, and/or deviations in dry/wet deposition rates.

It is out of the scope of this work to develop specific sensitivity analysis to analyze the influence of each of those factors (as in Strode et al., 2015). Future works will be devoted specifically to these tasks.

Without carrying out sensitivity studies, it is in general problematic to come to valid conclusion on the reasons for certain aspects (bad or good) of the model performance. The authors predominately only argue (without doing sensitivity studies) that (i) defi- ciency in the emissions and/or (ii) the lack of considering aerosol in the photolysis rates are the reasons for identified model deficiencies. While there is consensus in the scientific community that emissions can be very uncertain, there is no evidence given in the paper, why the aerosol impact should be so important as the authors claim. (I am happy to be convinced otherwise by a sensitivity study or a reference to it).

Response: The authors agree that the emphasis put during the discussion on the uncertainty of emissions and the lack of aerosols in the previous version of the paper could lead to the misconception that we believe those are the only causes for the disagreements found between model and observations. The revised manuscript has been thoroughly revised to point out other known causes for poor model performance, which have been referenced in all cases.

For ozone, other factors contributing to the deviations could be the lack of halogen chemistry in the CB05 mechanism, an excess of STE towards the troposphere, or possible bias in the meteorology (solar radiation, temperature). Sherwen et al. (2016) show that the halogen chemistry reduces the global tropospheric ozone burden by 15%. On the other hand, Real and Sartelet (2011) studied the effect of aerosols on photolysis rates and gaseous species and found that "Differences in photolysis rates lead to changes in gas concentrations, with the largest impact simulated on OH and NO concentrations. At the ground, monthly mean concentrations of both species are reduced over Europe by around 10 to 14% and their tropospheric burden by around 10%. The decrease in OH leads to an increase of the lifetime of several species such as VOC". Additionally, Bian et al. (2003) evaluated the effect of aerosols on the global budgets of O3, OH and CH4 through their alteration of photolysis rates. The impact identified was to increase tropospheric O3 by 0.63 Dobson units and increase tropospheric CH4 by 130 ppb (via tropospheric OH decreases of 8%). Although the CH4 increases were global, the changes in tropospheric OH and O3 were mainly regional, with the largest impacts in northwest Africa for January and in India and southern Africa for July. These last works, supports the idea introduced in our manuscript that the role of aerosols and photolysis is also important. In the revised manuscript, we have included these possible causes for the ozone bias discussion.

Real, E. and Sartelet, K.: Modeling of photolysis rates over Europe: impact on chemical gaseous species and aerosols, Atmos. Chem. Phys., 11, 1711-1727, doi:10.5194/acp-11-1711-2011, 2011.

Bian, H., M. J. Prather, and T. Takemura, Tropospheric aerosol impacts on trace gas budgets through photolysis, J. Geophys. Res., 108(D8), 4242, doi:10.1029/2002JD002743, 2003.

Sherwen, T., Schmidt, J. A., Evans, M. J., Carpenter, L. J., Großmann, K., Eastham, S. D., Jacob, D. J., Dix, B., Koenig, T. K., Sinreich, R., Ortega, I., Volkamer, R., Saiz-Lopez, A., Prados-Roman, C., Mahajan, A. S., and Ordóñez, C.: Global impacts of tropospheric halogens (Cl, Br, I) on oxidants and composition in GEOS-Chem, Atmos. Chem. Phys. Discuss., doi:10.5194/acp-2016-424, in review, 2016.

The authors should discuss other aspect of their model setup in more detail. If there is the feeling that photolysis rates play a role, then cloud cover would be the first suspect. The

cloud cover should be checked for biases since the model simulates clouds itself. Also worth checking are the ozone total columns used in the photolysis scheme because they are not constrained by observations.

Response: This manuscript aims to describe the tropospheric gas-phase chemistry of a new modeling system. Although, the comment of the reviewer asking for information about realism of the stratospheric ozone and clouds is relevant, we believe its discussion goes beyond the scope of the paper, and we have decided not to explicitly include it in the revised manuscript. However, we provide below information about the goodness of both simulated fields. In the revised manuscript we introduce the role of STE in the O3 biases.

The stratospheric ozone in the NMMB/BSC-CTM can be computed with linear models, on one hand the COPCAT scheme and on the other, as an alternative, the Cariolle scheme. In the PhD of Dr. Alba Badia (Badia, 2014), both systems were evaluated against satellite data. Relevant biases on the COPCAT stratospheric ozone are:

1) *COPCAT underestimates the stratospheric ozone maximum between 50N-20S latitudes and the ozone above 10 hPa. This underestimation is consistent with the study by Monge-Sanz et al. (2011), which compares the annual average from the year 2000 ozone profiles between the COPCAT parameterization and the HALOE measurements in the tropics (4 N).*

2) *COPCAT also underestimate the ozone in the low stratosphere between 90N-50N during DJF and MAM.*

3) *Over high southern latitudes COPCAT tends to overestimate O3 concentrations during the months of DJF and MAM in the mid/low stratosphere below 20hPa.*

In addition, Figure 1 shows the comparison of the ozone total column computed with Cariolle and COPCAT and with SCIAMACHY satellite retrievals. Additionally, the work of Monge-Sanz et al. (2011) further describes the biases associated to the COPCAT linear model. It is important to note that COPCAT is used as the linear ozone scheme of the ECMWF global model system IFS.
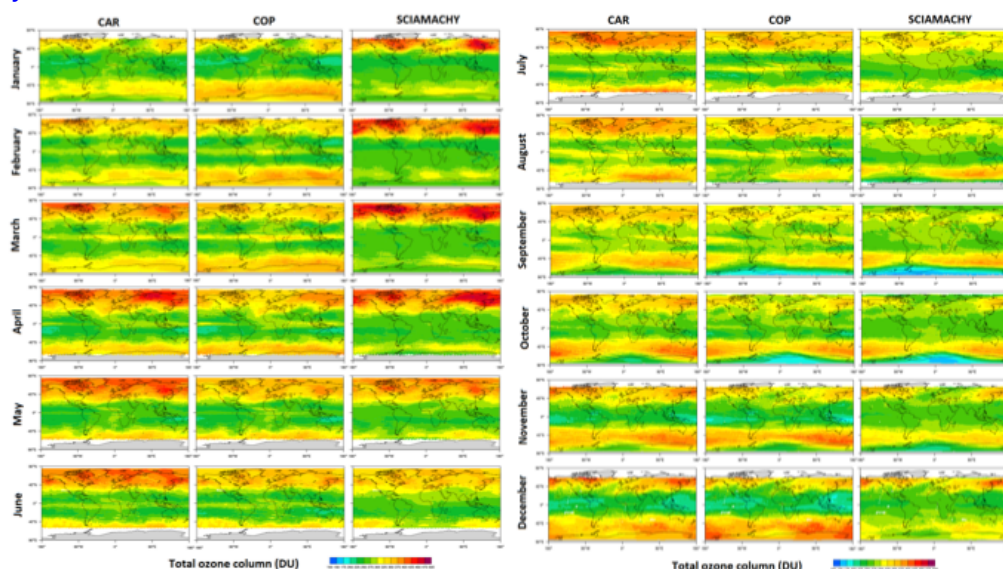

Figure 1. Comparison of the ozone total column monthly mean computed with NMMB/BSC-CTM using Cariolle scheme (CAR) and COPCAT scheme (COP), and compared with the SCIAMACHY satellite retrievals.

Regarding the clouds and possible biases. Clouds are simulated by the NMMB meteorological model. The model has been and is being extensively evaluated by NCEP in its both global and limited area configurations. Results of the skills of NMMB at global scale have widely been presented at several international conferences (e.g. AGU, EGU General Assembly). Comparisons of the NMMB initialized with GFS analysis show competitive results of the NMMB compared with GFS. For example, in Figure 2 the anomaly correlation at day 5-forecast shows excellent results with NMMB initialized with GFS or ECMWF analysis. Better results are obtained with ECMWF analysis. Such results wouldn't be possible with a poor representation of the cloud cover, and provide clear information on the skill of the NMMB as a numerical weather forecast model at global scale.

Anomaly correlation day-5 forecast

North Hemisphere

DATE	GFS	NMMB (GFS)	NMMB (ECMWF)
20110304	0.72	0.77	0.85
20110317	0.71	0.79	0.89
20110430	0.69	0.88	0.89
20110616	0.75	0.84	0.83
20110617	0.74	0.73	0.84
20110618	0.73	0.81	0.88
20110619	0.62	0.64	0.81
20110620	0.70	0.61	0.72
20110629	0.63	0.79	0.88
20110702	0.63	0.90	0.94
20110713	0.71	0.38	0.55
20110718	0.68	0.59	0.58
20110806	0.72	0.83	0.84
20110807	0.71	0.73	0.83
20110808	0.73	0.87	0.91
20110813	0.69	0.84	0.85
20110912	0.71	0.76	0.81

South Hemisphere

DATE	GFS	NMMB (GFS)	NMMB (ECMWF)
20110131	0.75	0.81	0.87
20110209	0.75	0.77	0.88
20110222	0.70	0.75	0.81
20110306	0.65	0.69	0.84
20110320	0.71	0.86	0.88
20110325	0.62	0.69	0.70
20110327	0.72	0.66	0.76
20110403	0.75	0.64	0.74
20110414	0.72	0.72	0.75
20110421	0.75	0.78	0.90
20110506	0.68	0.66	0.90
20110507	0.72	0.84	0.88
20110725	0.75	0.88	0.90
20110728	0.72	0.88	0.90
20110925	0.73	0.73	0.84

- 11/32 significant improvement with both analyses
- 12/32 significant improvement with ECMWF analysis in comparison with run with GFS analysis
- 17/32 improvement in comparison to GFS with same analysis
- 2/32 score remain less then then 0.7 with both analyses
- On average better scores with ECMWF analyses

22/09/16   Z. Janjic   33

Figure 2. Anomaly correlation day-5 forecast in the Northern and Southern Hemisphere obtained with the NMMB global model initialized with GFS and ECMWF analysis. Days selected when GFS forecast was poor. (Source: Z. Janjic personal communication).

However, some works have shown minor tropospheric effects of clouds on ozone (e.g., Voulgarakis et al., 2009; Liu et al., 2006). This points to that clouds are unlikely to have a large global effect on tropospheric gas-phase chemistry (only regionally).

Badia i Moragas, A., 2014. Implementation, development and evaluation of the gas-phase chemistry within the Global/Regional NMMB/BSC Chemical Transport Model (NMMB/BSC-CTM). PhD Dissertation, Universitat Politècnica de Catalunya.

Monge-Sanz, B. M., Chipperfield, M. P., Cariolle, D., and Feng, W.: Results from a new linear O3 scheme with embedded heterogeneous chemistry compared with the parent full-chemistry 3-D CTM, Atmos. Chem. Phys., 11, 1227-1242, doi:10.5194/acp-11-1227-2011, 2011.

Voulgarakis, A., Wild, O., Savage, N. H., Carver, G. D., and Pyle, J. A.: Clouds, photolysis and regional tropospheric ozone budgets, Atmos. Chem. Phys., 9, 8235-8246, doi:10.5194/acp-9-8235-2009, 2009.

Liu, H., et al. (2006), Radiative effect of clouds on tropospheric chemistry in a global three-dimensional chemical transport model, J. Geophys. Res., 111, D20303, doi:10.1029/2005JD006403.

Another potentially important aspect is the fact the emissions are injected uniformly in the lowest 500m (anthropogenic) or 1300 m (biomass burning). This could have a large impact on dry deposition, which depends on the surface level concentration, and ozone titration by NO during the night. The 500 m seems to be an exaggeration of the extent of the mixed layer during the night over land and the choice needs to be better motivated. One would expect that the diffusion scheme of the model simulates the vertical mixing in the PBL. Also, the 1300 m for the biomass burning injection would need to be justified, as the fire injection height can vary substantially (see for example. Remy al., 2016, ACP).

Response: The authors agree that the injection of emissions in global models is a critical point. However, there is no clear consensus within the modeling community in the approaches to be applied, as can be seen in different works where different approaches are applied from vertically distributing the emissions in height, injecting the emissions in the first model layers, or simply in the first model layer (i.e., Emmons et al., 2010, Huijnen et al., 2010). In our case, we consider that a global model with 1° of horizontal resolution and 64 vertical layers has limitations in the vertical diffusion of pollutants injected in the surface layer due to the lack of detail in the type of landuse or soil properties at specific locations. The coarse resolution strongly affects the surface concentration and we found beneficial to inject the emissions in the PBL for anthropogenic and biomass burning. In the case of anthropogenic emissions, we defined a constant injection height of 500 m that will distribute the emissions within the convective boundary layer during the day, and will trap the emissions in a stable boundary layer during nighttime. With higher resolutions this first approach might be detrimental to the model skills, and a more detailed injection of the emissions will be considered. Regarding biomass burning, the injection within the first 1300 m was considered a good approximation of injecting the emissions within the PBL and is within the range of emission heights recommended by Dentener (2006). Furthermore, some studies recommend an increase in the injection height in the tropics to 2 km based on the evidence from recent satellite observations (e.g. Labonne et al., 2007), which is a height much higher than that selected in our simulations.

Dentener, F., Kinne, S., Bond, T., Boucher, O., Cofala, J., Generoso, S., Ginoux, P., Gong, S., Hoelzemann, J. J., Ito, A., Marelli, L., Penner, J. E., Putaud, J.-P., Textor, C., Schulz, M., van der Werf, G. R., and Wilson, J.: Emissions of primary aerosol and precursor gases in the years 2000 and 1750 prescribed data-sets for AeroCom, Atmos. Chem. Phys., 6, 4321–4344, doi:10.5194/acp- 6-4321-2006, 2006b.

Emmons, L. K., Walters, S., Hess, P. G., Lamarque, J.-F., Pfister, G. G., Fillmore, D., Granier, C., Guenther, A., Kinnison, D., Laepple, T., Orlando, J., Tie, X., Tyndall, G., Wiedinmyer, C., Baughcum, S. L., and Kloster, S.: Description and evaluation of the Model for Ozone and Related chemical Tracers, version 4 (MOZART-4), Geosci. Model Dev., 3, 43-67, doi:10.5194/gmd-3-43-2010, 2010.

Huijnen, V., Williams, J., van Weele, M., van Noije, T., Krol, M., Dentener, F., Segers, A., Houweling, S., Peters, W., de Laat, J., Boersma, F., Bergamaschi, P., van Velthoven, P., Le Sager, P., Eskes, H., Alkemade, F., Scheele, R., Nédélec, P., and Pätz, H.-W.: The global chemistry transport model TM5: description and evaluation of the tropospheric chemistry version 3.0, Geosci. Model Dev., 3, 445-473, doi:10.5194/gmd-3-445-2010, 2010.

Labonne, M., Breon, F.-M., and Chevallier, F.: Injection heights of biomass burning aerosols as seen from a space borne lidar, Geophys. Res. Lett., 34, L11806, doi:10.1029/2007GL029311, 2007

The paper would greatly benefit from proofreading for English language.
Response: The final version of the manuscript has been revised in detail.

Specific comments:

P1
Title: consider not calling the model a CTM as CTM's are understood as "off-line"
Response: See the response to the general comment addressed above.

P2
L 27: a better reference for IFS-MOZART is Flemming et al. 2009, GMD
Response: Amended.

L 33: Please clarify if the non-hydrostatic option was used in the run.
Response: Yes, the nonhydrostatic option was turned on in the run although it is not necessary for the global scales used in our study. The extra computational cost of the nonhydrostatic dynamics is on the order of 10% in global applications, or nonexistent if the nonhydrostatic extension is switched off at coarser resolutions. However, the relatively low cost of the nonhydrostatic dynamics allows its application even at transitional resolutions where the benefits due to the nonhydrostatic dynamics are small or uncertain. See Janjic and Gall (2012) for further clarifications.

Janjic, Z. and Gall, R., 2012. Scientific documentation of the NCEP nonhydrostatic multiscale model on the B grid (NMMB). Part 1 Dynamics. NCAR/TN-489+ STR, 75 pp.

P3
L 26: better "in detail"
Response: Amended.

P4
L15-25: please clarify which of the options is actually used in the presented run. The other options don't need to be mentioned. They could be referenced.
*Response: Table 1 presents the specific configuration of the NMMB used in this work. A comment regarding Table 1 is now introduced in the revised manuscript.*

P 5
L 17: 1850 ppb of methane seems too high for 2004. The value should be 1775 ppb http://www.esrl.noaa.gov/gmd/ccgg/trends_ch4/
Response: In this first model version, we followed the approach to prescribe a constant methane concentration, which will be refined in future model versions. Current practices set the methane background level either as a default background concentration (i.e. 1.76 ppm, e.g. Shindell et al, 2006), or as the background level for the Northern Hemisphere (i.e. 1.85 ppm, used for instance within CMAQ). Including either of those concentrations would lead to differences with respect to reality and the choice in our case was made to include the value the closest to the present time global background concentration (1.83 ppm, see WMO 2015, or Dlugokencky, 2016), because we aim to apply this first version of the NMMB/BSC-CTM in forecast mode. The global average for 2004 is reported to be 0.06 to 0.07 ppm lower, around 4%.

Moreover, the sensitivity of the model results to the background methane concentration is relatively low. We have performed a test using a value of CH4 of 1.786 ppm (reported level by WMO for 2004) and compared it to the simulation with CH4 at 1.85 ppm. Differences in daily mean O3 and CO concentration up to ±0.6 ppb and ±0.12 ppb, respectively, are found for randomly selected days of April and August (Figure 3 depicts the differences for the 5th of August 2004 at surface level). The largest differences for O3 are not at the surface, but at higher layers (plots depict only surface level, but the maximum differences reported consider the full atmospheric column). In relative terms, differences can be considered low.
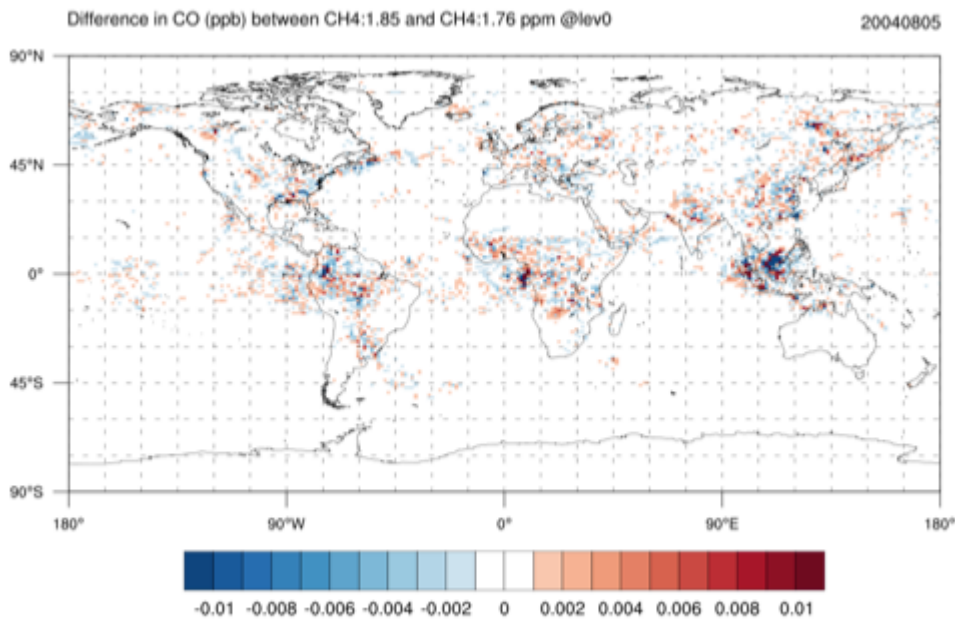
(a)
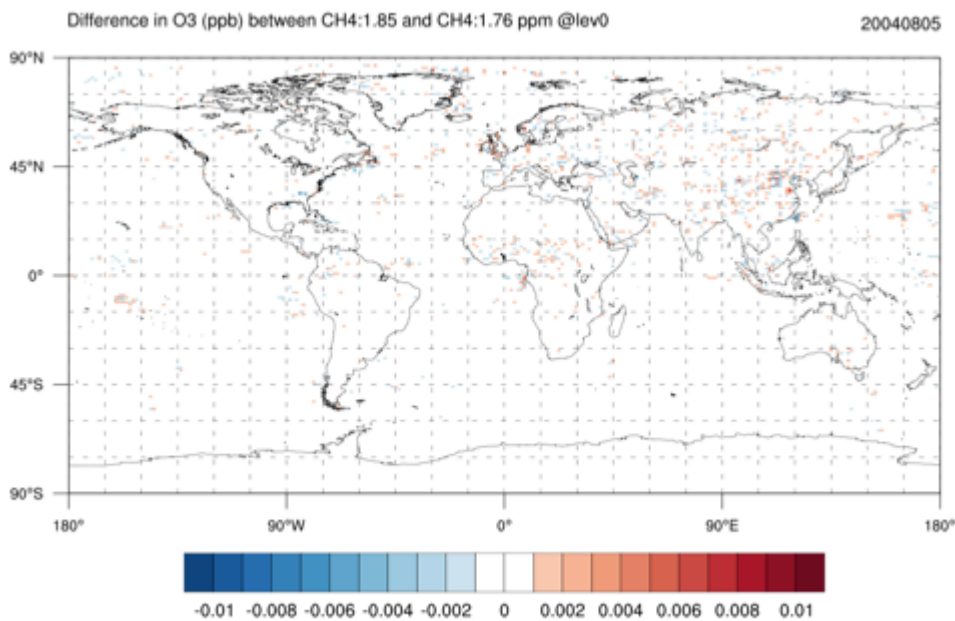
(b)

Figure 3. Difference in daily mean surface level concentration of (a) CO (ppb), and (b) O3 (ppb) for the 5th of August 2004, between a simulation with background methane concentration set to 1.85 ppm and another with 1.786 ppm.

L 22: Add more information about the realism of the two input fields (overhead ozone and clouds)
Response: This has already been addressed in the reply of a general comment above.

P 6
L 10: Is this a monthly climatology ?
Response: No. A specific value for season and landuse is provided.

L 13: "cloud processes" – does this also include wet-phase chemistry ?
Response: No. The version 1.0 of the model does not consider aqueous phase chemistry. This is now clarified in the revised manuscript.

L 14: The presented terms are not clear. Please clarify what you mean by all the mentioned processes. For example, what is wet deposition for non-precipitating cloud?
Response: The terms presented are common in the modeling context and are taken from Byun and Ching (1999) and Foley et al. (2010). The manuscript includes both references. The meaning of the terms used are:
- *Grid-scale: it refers to those processes explicitly resolved by the model at the spatial scale of the model resolution.*
- *Subgrid-scale: it refers to those processes that are parameterized in the physics, i.e., convective clouds.*
- *Grid- scale Scavenging: it refers to the removal of gases by cloud droplets of clouds explicitly resolved by a numerical model, i.e., stratiform clouds.*
- *Grid-scale Wet deposition: it refers to the deposition by precipitation produced by explicitly resolved clouds.*
- *Subgrid-scale vertical mixing: it refers to the convective mixing that is produced within convective clouds.*
- *Subgrid-scale scavenging: it refers to the removal of gases by cloud droplets of clouds parameterized with a cumulus convection parameterization.*
- *Subgrid-scale wet deposition for precipitating: it refers to the deposition by precipitation produced by parameterized convective clouds.*
  The relevant non-precipitating cloud processes are scavenging and vertical mixing. Wet deposition is possible for precipitating clouds. In order to avoid a too long section with common terminology definition the reader is referred to the scientific literature from where this terminology comes from.

Byun, D. and Ching, J.: Science algorithms of the EPA Models-3 community multiscale air quality (CMAQ) modeling system, Rep. EPA/600/R-99, 30, 1999.

Foley, K. M., Roselle, S. J., Appel, K. W., Bhave, P. V., Pleim, J. E., Otte, T. L., Mathur, R., Sarwar, G., Young, J. O., Gilliam, R. C., Nolte, C. G., Kelly, J. T., Gilliland, A. B., and Bash, J. O.: Incremental testing of the Community Multiscale Air Quality (CMAQ) modeling system version 4.7, Geoscientific Model Development, 3, 205–226, doi:10.5194/gmd-3-205-2010, http://www.geosci-model-dev.net/3/205/2010/, 2010.

L16: Why only in-cloud scavenging and not all the other processes ?

Response: The most relevant scavenging process affecting gases are the in-cloud scavenging. The American Meteorological Society glossary in its definition of scavenging by precipitation says "Rainout (or snowout), which is the in-cloud capture of particulates as condensation nuclei, is one form of scavenging. The other form is washout, the below-cloud capture of particulates and gaseous pollutants by falling raindrops. Large particles are most efficiently removed by washout. Small particles (especially those less than 1 μm in diameter) more easily follow the airstream flowing around raindrops and generally avoid capture by raindrops except in heavy rain events". In the case of gases, neglecting below-cloud scavenging is not considered a strong limitation.

L 19: How is the cloud time scale derived?

Response: Following Byun and Ching (1999) and Foley et al. (2010) the time scale of a convective cloud is assumed to be 3600s, and for explicitly resolved clouds, the model times step is applied.

Byun, D. and Ching, J.: Science algorithms of the EPA Models-3 community multiscale air quality (CMAQ) modeling system, Rep. EPA/600/R-99, 30, 1999.

Foley, K. M., Roselle, S. J., Appel, K. W., Bhave, P. V., Pleim, J. E., Otte, T. L., Mathur, R., Sarwar, G., Young, J. O., Gilliam, R. C., Nolte, C. G., Kelly, J. T., Gilliland, A. B., and Bash, J. O.: Incremental testing of the Community Multiscale Air Quality (CMAQ) modeling system version 4.7, Geoscientific Model Development, 3, 205–226, doi:10.5194/gmd-3-205-2010, http://www.geosci-model-dev.net/3/205/2010/, 2010.

P7

L2: Do you refer to large-scale and convective precipitation here?

Response: Yes, grid-scale refers to large-scale processes (those resolved by the grid information solved by the model) and subgrid-scale to convective processes.

L7: "Convective mixing" do you mean transport by convective mass fluxes ?

Response: Yes, convective mixing is referred to the processes that transport vertically within the convective cloud the air masses.

L 13: 100 hPa is a rather high tropopause for mid- and high latitudes.

Response: There is a common practice in modeling studies to implement stratospheric chemistry above 100 hPa (i.e., Lamarque et al., 2010; Voulgarakis et al., 2011). The chemistry in the tropopause is very slow and the transition within the tropospheric and stratospheric chemistry is wide. Considering the resolution of models in the upper troposphere and stratosphere makes the selection of 100 hPa a compromise solution.

Lamarque, J.-F., Bond, T. C., Eyring, V., Granier, C., Heil, A., Klimont, Z., Lee, D., Liousse, C., Mieville, A., Owen, B., Schultz, M. G., Shindell, D., Smith, S. J., Stehfest, E., Van Aardenne, J., Cooper, O. R., Kainuma, M., Mahowald, N., McConnell, J. R., Naik, V., Riahi, K., and van Vuuren, D. P.: Historical (1850–2000) gridded anthropogenic and biomass burning emissions of reactive gases and aerosols: methodology and application, Atmos. Chem. Phys., 10, 7017-7039, doi:10.5194/acp-10-7017-2010, 2010.

Voulgarakis, A., P. Hadjinicolaou, and J.A. Pyle, 2011: Increases in global tropospheric ozone following an El Niño event: Examining stratospheric ozone variability as a potential driver. Atmos. Sci. Lett., 12, 228-232, doi:10.1002/asl.318.

L 13: Were these Mozart 4 fields evaluated for the stratosphere?

Response: Yes. MOZART-4 model is described in Emmons et al., (2010) : "Mixing ratios of several species (O3, NOx, HNO3, N2O5, CO, CH4) are constrained in the stratosphere since MOZART-4 does not have complete stratospheric chemistry. These mixing ratios have been updated to zonal means from a MOZART-3 simulation." MOZART-3 is suitable for representing chemical/physical processes in stratosphere and for quantifying ozone fluxes from the stratosphere to the troposphere (Kinnison et al., 2007). The validity of STE processes in MOZART-3 has been evaluated in several studies (Park et al., 2004., Pan et al. 2007 and Liu et al., 2009). The model results in Park et al., 2004 showed good agreement for methane and water vapor, but underestimated the nitrogen oxide abundance.

Emmons, L. K., Walters, S., Hess, P. G., Lamarque, J.-F., Pfister, G. G., Fillmore, D., Granier, C., Guenther, A., Kinnison, D., Laepple, T., Orlando, J., Tie, X., Tyndall, G., Wiedinmyer, C., Baughcum, S. L., and Kloster, S.: Description and evaluation of the Model for Ozone and Related chemical Tracers, version 4 (MOZART-4), Geosci. Model Dev., 3, 43-67, doi:10.5194/gmd-3-43-2010, 2010.

Kinnison, D. E., et al. (2007), Sensitivity of chemical tracers to meteorological parameters in the MOZART-3 chemical transport model, J. Geophys. Res. , 112, D20302, doi:10.1029/2006JD007879.

Liu, Y., Liu, C. X., Wang, H. P., Tie, X. X., Gao, S. T., Kinnison, D., and Brasseur, G.: Atmospheric tracers during the 2003–2004 stratospheric warming event and impact of ozone intrusions in the troposphere, Atmos. Chem. Phys., 9, 2157-2170, doi:10.5194/acp-9-2157-2009, 2009.

Park, M., Randel, W. J., Kinnison, D. E., Garcia, R. R., and Choi, W.: Seasonal variation of methane, water vapor, and nitrogen oxides near the tropopause: Satellite observations and model simulations, J. Geophys. Res., 109, D03302, doi:10.1029/2003JD003706, 2004.

Pan, L. L., Wei, J. C., Kinnison, D. E., Garcia, R. R., Wuebbles, D. J., and Brasseur, G. P.: A set of diagnostics for evaluating chemistry-climate models in the extratropical tropopause region, J. Geophys. Res., 112, D09316, doi: 10.1029/2006JD007792, 2007.

L 18ff: There is no need to present the COPCAT scheme here, a reference to the paper is enough.

Response: Following the reviewer's comment, the description of the COPCAT linear scheme is removed from the manuscript and a reference, Monge-Sanz et al. (2011), is provided.

Monge-Sanz, B. M., Chipperfield, M. P., Cariolle, D., and Feng, W.: Results from a new linear O3 scheme with embedded heterogeneous chemistry compared with the parent full-chemistry 3-D CTM, Atmos. Chem. Phys., 11, 1227-1242, doi:10.5194/acp-11-1227-2011, 2011.

L 18: Please provide information on the biases of your stratosphere ozone simulated by the COPCAT scheme because they have an impact on the photolysis rates.

Response: As already discussed in the general comments, information on the stratospheric ozone simulated by COPCAT scheme can be found in the PhD of Dr. Alba Badia (Badia, 2014). From there, the most relevant biases on the stratospheric ozone identified are:

1) *COPCAT underestimates the stratospheric ozone maximum between 50N-20S latitudes and the ozone above 10 hPa. This underestimation is consistent with the study by Monge-Sanz et al. (2011), which compares the annual average from the year 2000 ozone profiles between the COPCAT parameterization and the HALOE measurements in the tropics (4 N).*

2) *COPCAT also underestimate the ozone in the low stratosphere between 90N-50N during DJF and MAM.*

3) *Over high southern latitudes COPCAT tends to overestimate O3 concentrations during the months of DJF and MAM in the mid/low stratosphere below 20hPa.*

In addition, Figure 1 shows the comparison of the ozone total column computed with Cariolle and COPCAT and with SCIAMACHY satellite retrievals. Additionally, the work of Monge-Sanz et al. (2011) further describes the biases associated to the COPCAT linear model. It is important to note that COPCAT is used as the linear ozone scheme of the ECMWF global model system.

In the revised manuscript the following sentence has been added "For further description of the approach and information on the biases of the stratosphere ozone simulated by the COPCAT scheme, the reader is referred to Monge-Sanz et al. (2011). "

Badia i Moragas, A., 2014. Implementation, development and evaluation of the gas-phase chemistry within the Global/Regional NMMB/BSC Chemical Transport Model (NMMB/BSC-CTM). PhD Dissertation, Universitat Politècnica de Catalunya.

Monge-Sanz, B. M., Chipperfield, M. P., Cariolle, D., and Feng, W.: Results from a new linear O3 scheme with embedded heterogeneous chemistry compared with the parent full-chemistry 3-D CTM, Atmos. Chem. Phys., 11, 1227-1242, doi:10.5194/acp-11-1227-2011, 2011.

P 8

L 14: No lightning emissions is a severe shortcoming of the simulation and the paper (see my general comment).

Response: *This has been highlighted in the revised manuscript. The following sentence has been included "The omission of lightning emissions is expected to have a significant impact in the oxidation of the middle and upper troposphere" in Section 2.2.6.*

L 15: Please explain in more detail how the MEGAN code was integrated in your model.

Response: *The authors do not fully understand the comment of the reviewer regarding the coupling of MEGAN code with the NMMB/BSC-CTM. The MEGAN code has been prepared as a subroutine that is called by the chemistry driver of the model to compute an update on the biogenic emissions. The coupling is fully on-line integrated, so the meteorological variables (temperature and solar radiation) is passed as attribute to the subroutine. The authors consider that this explanation is not required in the manuscript.*

L34: I don't understand the 24h averages here. I thought (L23) the actual hourly meteorological data were used for the calculation of the Megan emissions.

Response: *The MEGAN model uses two different pieces of information regarding meteorological conditions. On one hand the model uses the actual temperature and solar radiation provided by the meteorological model at the required time-step of the simulation. On the other hand, the MEGAN model requires information of the previous day meteorological conditions. For that, several approaches are found in the literature, from implementations providing the average of the previous day temperature and solar radiation to approaches that work with monthly averages. MEGAN shows important sensitivity on these approaches as described in the manuscript: "[...]Marais et al. (2014) performed several sensitivity model runs to study the impact of different model input and settings on isoprene estimates that resulted in differences of up to 17% compared to a baseline". In our study, weather inputs are based on previous day 24h averages and data for the hour of interest.*

Marais, E. A., Jacob, D. J., Guenther, A., Chance, K., Kurosu, T. P., Murphy, J. G., Reeves, C. E., and Pye, H. O. T.: Improved model of isoprene emissions in Africa using Ozone Monitoring Instrument (OMI) satellite observations of formaldehyde: implications for oxidants and particulate matter, Atmos. Chem. Phys., 14, 7693-7703, doi:10.5194/acp-14-7693-2014, 2014.

P 9
L3: better say "every 720 s"
Response: Amended.

L 5: Which fields are initialised (also clouds or only T, v,w,q). What is known about the biases of the 24 h forecasts?
Response: The meteorological model NMMB is initialized with the Final Analysis (FNL) of NCEP. The fields initialized are temperature, winds, specific humidity, and cloud water mixing ratio. The work developed at NCEP shows that the Anomaly Correlation at 500 hPa at 24 h of forecast is nearly 1, see Figure 4. This provides clear evidence of the skill of the model in NWP. The skills are comparable to those of GFS.
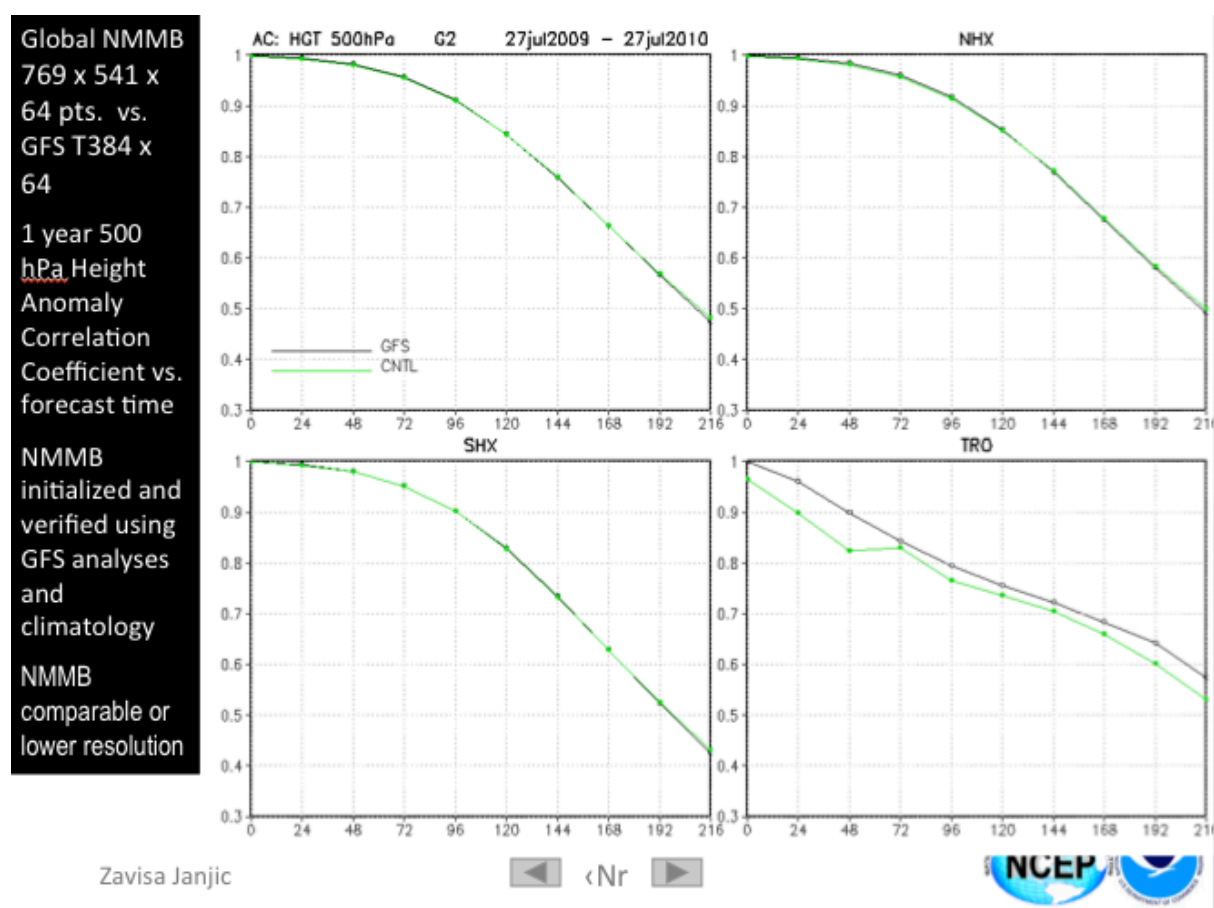
Figure 4. Anomaly Correlation of the NMMB (green lines) and GFS (black lines) 9-day forecast of the 500 hPa Height.

L 12: not using 2004 fire emissions is a severe omission (see my general comment). Please clarify what fire emissions have been used. Was it an average for the period? It is not clear what "interpolated" means. Do the fire emissions have a seasonal cycle?
Response: The anthropogenic emissions and biomass burning emissions used in our work are those described in Lamarque et al. (2010), to allow an easy intercomparison. An error

was introduced in the initial manuscript, because the emissions are not computed for the year 2004; we use the emissions derived by Lamarque et al. (2010) for the 2000. The details on how these emissions were derived can be read in Lamarque reference. Now, in the revised manuscript the sentence "Note that the 2004 emissions are derived from a linear interpolation between years 2000 and 2010" has been changed to "Note that this methodology involves assuming 2004 emissions equivalent to the best estimate reported by ACCMIP for year 2000". The biomass burning emissions provided by Lamarque et al. (2010) have a seasonal cycle, while anthropogenic emissions are constant throughout the year.

Lamarque, J.F., Bond, T.C., Eyring, V., Granier, C., Heil, A., Klimont, Z., Lee, D., Liousse, C., Mieville, A., Owen, B. and Schultz, M.G., 2010. Historical (1850–2000) gridded anthropogenic and biomass burning emissions of reactive gases and aerosols: methodology and application. Atmospheric Chemistry and Physics, 10(15), pp.7017-7039.

L 26: see my general comment, please justify the choices
Response: *The injection height of the different emissions used in our model are derived from sensitivity runs. Please, see previous discussion in the general comments about the justification of the emission heights.*

L 29: Please provide reference the strong impact of aerosol on the photolysis rates.
Response: *Real and Sartelet (2011 ACP) studied the effect of aerosols in the photolysis rates and gaseous species. They state that "Differences in photolysis rates lead to changes in gas concentrations, with the largest impact simulated on OH and NO concentrations. At the ground, monthly mean concentrations of both species are reduced over Europe by around 10 to 14% and their tropospheric burden by around 10%. The decrease in OH leads to an increase of the lifetime of several species such as VOC". ". On the other hand, Bian et al. (2003) evaluated the effect of aerosols on the global budgets of O3, OH and CH4 through their alteration of photolysis rates. The impact identified was to increase tropospheric O3 by 0.63 Dobson units and increase tropospheric CH4 by 130 ppb (via tropospheric OH decreases of 8%). Although the CH4 increases were global, the changes in tropospheric OH and O3 were mainly regional, with the largest impacts in northwest Africa for January and in India and southern Africa for July. We have included these references in the revised manuscript.*

Real, E., and K. Sartelet. "Modeling of photolysis rates over Europe: impact on chemical gaseous species and aerosols." Atmospheric Chemistry and Physics 11.4 (2011): 1711-1727.
Bian, H., M. J. Prather, and T. Takemura, Tropospheric aerosol impacts on trace gas budgets through photolysis, J. Geophys. Res., 108(D8), 4242, doi:10.1029/2002JD002743, 2003.

P 11
L27: It is not clear how missing data in the surface observations were considered. If you compare only averages without timely match give numbers of the amount of missing data.
Response: *If missing data are found in the observations, the corresponding time period is removed from the model data. Following this approach, model and observation derived averages are fully comparable (as only matching periods are used for the evaluation). This is clarified in the manuscript as follows: At the surface-level, daily O3 averages are computed from 3-hourly values of model and observations, applying a filter to model data whenever observations are missing, so as to consider timely/collocated values. Section 1 of the supplementary material presents the statistical measures calculated from the daily data.*

L 30: 1000m asl.? This could be a mountain stations near to the coast or a station on a flat plateau inland. It would be better to include the model orography in the choice of the mountain stations. (say 500 m above orography)

Response: The altitude 1000 m asl. has been shown as a clear transition from a boundary-layer to a free-tropospheric regime for ozone (Chevalier et al., 2007). We are interested in filtering mountain stations because they provide measurements that are normally representative of the local conditions, but not of the air parcel that would be included on a model grid cell, of 1.4°x1°. Applying this threshold for station filtering is a common practice for several works devoted to atmospheric chemistry-transport model evaluation (Solazzo et al., 2012; Solazzo and Galmarini 2016).

Chevalier, A., Gheusi, F., Delmas, R., Ordóñez, C., Sarrat, C., Zbinden, R., Thouret, V., Athier, G., and Cousin, J.-M.: Influence of altitude on ozone levels and variability in the lower troposphere: a ground-based study for western Europe over the period 2001–2004, Atmos. Chem. Phys., 7, 4311-4326, doi:10.5194/acp-7-4311-2007, 2007.

Efisio Solazzo, Roberto Bianconi, Robert Vautard, K. Wyat Appel, Michael D. Moran, Christian Hogrefe, Bertrand Bessagnet, Jørgen Brandt, Jesper H. Christensen, Charles Chemel, Isabelle Coll, Hugo Denier van der Gon, Joana Ferreira, Renate Forkel, Xavier V. Francis, George Grell, Paola Grossi, Ayoe B. Hansen, Amela Jeričević, Lukša Kraljević, Ana Isabel Miranda, Uarporn Nopmongcol, Guido Pirovano, Marje Prank, Angelo Riccio, Karine N. Sartelet, Martijn Schaap, Jeremy D. Silver, Ranjeet S. Sokhi, Julius Vira, Johannes Werhahn, Ralf Wolke, Greg Yarwood, Junhua Zhang, S.Trivikrama Rao, Stefano Galmarini, Model evaluation and ensemble modelling of surface-level ozone in Europe and North America in the context of AQMEII, Atmospheric Environment, Volume 53, June 2012, Pages 60-74, ISSN 1352-2310, http://dx.doi.org/10.1016/j.atmosenv.2012.01.003.
Solazzo, E. and Galmarini, S.: Error apportionment for atmospheric chemistry-transport models – a new approach to model evaluation, Atmos. Chem. Phys., 16, 6263-6283, doi:10.5194/acp-16-6263-2016, 2016.

P 12
L1: This choice of the tropopause is not consistent with the choice of the tropopause for the chemical boundary conditions (P7L13).

Response: We agree with the reviewer's comment. However, one has to bear in mind that NO_x concentrations in the tropopause region are very low, as the stratospheric NO_x layer is located considerably higher in the stratosphere, and pollution NO_x is mostly located closer to the surface. Therefore the tropospheric column does not significantly depend on the choice of tropopause level. In our work, we have considered the tropopause definition as the model level interface corresponding to approximately 100 hPa in the tropics and 250 hPa in the extratropics following Horowitz et al. (2003). In this sense, we don't think that this inconsistency has a real impact in the results discussed.

Horowitz, L. W., Walters, S., Mauzerall, D. L., Emmons, L. K., Rasch, P. J., Granier, C., Tie, X., Lamarque, J.-F., Schultz, M. G., Tyndall, G. S., Orlando, J. J., and Brasseur, G. P.: A global simulation of tropospheric ozone and related tracers: Description and evaluation of MOZART, version 2, Journal of Geophysical Research: Atmospheres, 108, doi:10.1029/2002JD002853, http://dx.doi.org/10.1029/ 2002JD002853, 2003.

L 29: see my general comment. The aerosol effect may not be the most important one. There are many other possible explanations: high CH4, water vapour, clouds and photolysis, excessive mixing of emissions etc.

Response: The authors agree with the reviewer comment. In this sense, the sentence of L29 has been reformulated in the revised manuscript in the following way: "Therefore, the

lack of lightning emissions in our model run could at least partly explain the lower OH values above 500 hPa reported here. Another potential explanation is the lack of aerosols in our simulation, which may overestimate photolysis rates in polluted regions (e.g., Bian et al., 2003; Real and Sartelet, 2011)."

P 13
L1: CH4 is also a CO source. Please also reformulate the sentence.
Response: CH4 is an hydrocarbon, so as stated in the manuscript, the photolysis of hydrocarbons are a source of CO. For clarification, "including methane" is now written in the revised manuscript.

L 14 add reference for C-IFS
Response: Amended.

L 29: Could the high methane be a reason ?
Response: The influence of CH_4 on modeled CO levels has been assessed through a sensitivity test, which resulted in a low impact (please, see our previous response). Changing the CH_4 prescribed value from 1.85 ppm to 1.78 ppm (2004 global average as reported by WMO) leads to changes in daily average CO concentration up to ±0.12 ppb, which leads us to believe that other factors have a larger impact on CO burden (see for instance Shindell et al., 2006).

Shindell, D. T., et al. (2006), Multimodel simulations of carbon monoxide: Comparison with observations and projected near-future changes, J. Geophys. Res., 111, D19306, doi:10.1029/2006JD007100

L 30: Figure 3. Please show separate plots for NH, SH mid-latitudes and tropics. The seasonality is obscured by averaging over all stations.
Response: We have only 14 stations available for CO, and only 2 of them are located in the SH. For that reason, we decided to average over all stations. The seasonality for the CO is represented in Figure 6.

P 14
L2: no seasonality of the anthropogenic emissions is an oversimplification.
Response: This limitation has been highlighted in the revised manuscript.

L3: Figure 3 shows the relative bias (%), not MB as defined in the supplement.
Response: Figure 3 shows the MB, not the relative bias (%). This information is now corrected in the revised manuscript.

L3 Please clarify correlation of which time scale is shown, i.e. of the hourly, daily monthly values? Did you filter out seasonality? How important is the diurnal cycle to the correlation.
Response: Time scale is described in the Model evaluation section: "For the surface-level comparison, three-hourly averages from the observations and model are used to compute daily O3 averages and calculate the statistical measures defined in section 1 in the supplemental material". We didn't filter out seasonality.

L 28 Stein et al. and many other authors find a general underestimation in winter and spring NH.

Response: Amended.

P 15

L8: What do you mean by overestimated emissions above the PBL ?

Response: As we described in the document, all the land-based anthropogenic emissions are emitted in the first 500 m of the model and biomass burning emissions from forests in the first 1300 m. When the PBL is lower than this altitude, emissions above the PBL can be overestimated and contribute to the positive bias identified in the CO.

L 8: Please discuss the role of convection

Response: The following sentence has been included in the revised manuscript: "Excessive vertical mixing by moist convection may explain the overestimation in the tropics".

L 32: What regime (rural, urban) was used ?

Response: Only rural stations were used in this study. This information is now included in the revised manuscript.

P 16

L 8: Please discuss also PBL mixing during the night

Response: We have included the following sentence in the revised manuscript: "Also, excessive mixing within the PBL during the night could contribute to a decrease in ozone titration by NO and partially explain the bias".

P 17

L 8: see my general comment on the use of "good agreement"

Response: More quantitative statements have been included in the revised manuscript supporting the qualitative statements initially used.

L 17: Please mention the value of the biases.

Response: The average wet deposition rates for the model and the observations are shown in Fig S4 (supporting material). Wet deposition MB for Europe, USA and Asia are -200.70 mg N/m^2, - 36.87 mg N/m^2 and -163.27 mg N/m^2, respectively. These biases are now mentioned in the revised manuscript.

L 26: What is the seasonal cycle of the biomass emissions ?

Response: The ACCMIP inventory has monthly variations for biomass burning. This is described in Lamarque et al. (2010).

Lamarque, J.F., Bond, T.C., Eyring, V., Granier, C., Heil, A., Klimont, Z., Lee, D., Liousse, C., Mieville, A., Owen, B. and Schultz, M.G., 2010. Historical (1850–2000) gridded anthropogenic and biomass burning emissions of reactive gases and aerosols: methodology and application. Atmospheric Chemistry and Physics, 10(15), pp.7017-7039.

P 18

L 1 "rural" (?) perhaps better remote

Response: Amended.

L 4: dominated by the tropics - perhaps simply because they are the largest region on earth (?)

Response: This point is now included in the revised manuscript.

L 7: TM5 has a similar chemical mechanism. Should it not be similar ?

Response: NMMB/BSC-CTM and TM5 have a similar chemical mechanism. However, other processes that are represented differently in both models, such as the deposition, vertical mixing and emissions, also have an impact on the O3 burden. These processes can explain the differences in the O3 burdens between the models.

L 16: Please clarify how the STE is calculated in your model.

Response: The stratosphere-troposphere ozone exchange flux is calculated as the annual balance of the ozone mass crossing the 100 hPa height. This approach is accurate on the global and long-term average (Hsu et al., 2005). However, there are considerable differences among the models for calculating or specifying the stratosphere-troposphere exchange of ozone. This is now indicated in the revised manuscript.

Hsu, J., M. J. Prather, and O. Wild (2005), Diagnosing the stratosphere-to-troposphere flux of ozone in a chemistry transport model, J. Geophys. Res. ,110, D19305, doi:10.1029/2005JD006045.

L 27: "all day long " ? Do you mean "throughout the year"

Response: Yes. The expression has been changed to "throughout the year".

L 27: For global models the values are commonly given in volume mixing ratios (ppb). Try to avoid mg/m3 throughout the paper.

Response: Most of the surface observations collected are in $\mu g/m^3$. For that reason, we prefer to keep the measurement units when surface comparisons are done.

L 28: The emission injection (500m) leads to a dilution of NO and therefore a reduction of the ozone titration. This could also explain the overestimation.

Response: The authors agree with the reviewer's comment. In the revised manuscript this possible explanation of the overestimation of O3 is included.

P 19
L4 Please quantify biases, what do you mean by "error".

Response: In the revised manuscript the biases are now quantified and the sentence "error" has been substituted by "root mean square errors" to clarify the text. The quantification of the biases is provided in Figure 12.

L 15. This points to biases of the COPCAT ozone, which has consequences for the photolysis rates.

Response: The authors agree with the reviewer on the possible effect of the COPCAT biases upon the tropospheric ozone. This has been introduced in the revised manuscript.

P 20
L 8: The lack of aerosol modulation of photolysis is a probably a minor aspect. Lack of heterogeneous chemistry (N2O5) might be more important. Please also mention the main

shortcomings of this simulation: (1) no lightning, (2) no 2004 biomass burning emissions and (3) no seasonal cycle for anthropogenic emissions.

Response: The authors consider that the effect of aerosols on photolysis and radiation is not a minor aspect, as the results in Real and Sartelet (2011 ACP) indicate: "Differences in photolysis rates lead to changes in gas concentrations, with the largest impact simulated on OH and NO concentrations. At the ground, monthly mean concentrations of both species are reduced over Europe by around 10 to 14% and their tropospheric burden by around 10%. The decrease in OH leads to an increase of the lifetime of several species such as VOC". Furthermore, Bian et al. (2003) evaluated the effect of aerosols on the global budgets of O3, OH and CH4 through their alteration of photolysis rates. The impact identified was to increase tropospheric O3 by 0.63 Dobson units and increase tropospheric CH4 by 130 ppb (via tropospheric OH decreases of 8%). Although the CH4 increases were global, the changes in tropospheric OH and O3 were mainly regional, with the largest impacts in northwest Africa for January and in India and southern Africa for July. We have included these references in the revised manuscript.

Following the reviewer's suggestion now the main shortcomings of the simulation presented in the manuscript are clearly stated. The following sentence has been added in the conclusions section: "We note that in this contribution, we omitted aerosols and lightning emissions; anthropogenic emissions disregard seasonality; and biomass burning emissions are not specific to 2004."

Real, E., and K. Sartelet. "Modeling of photolysis rates over Europe: impact on chemical gaseous species and aerosols." Atmospheric Chemistry and Physics 11.4 (2011): 1711-1727.

Bian, H., M. J. Prather, and T. Takemura, Tropospheric aerosol impacts on trace gas budgets through photolysis, J. Geophys. Res., 108(D8), 4242, doi:10.1029/2002JD002743, 2003.

L15: The paper provides no evidence for this claim - it can therefore not be a conclusion.

Response: The authors do not present as a conclusion the effect of aerosols on the concentrations of OH. We only suggest some possible reasons to explain why our results of OH at northern latitudes are slightly higher than the climatological mean of Spivakovsky et al. (2000). We agree with the reviewer that this cannot be a conclusion of the work, in this sense, we only highlight a possible explanation that deserves further research in the future studies with the model.

L 34 see above, no evidence in the paper

Response: Addressing the reviewer's comment, the following statement has been removed from the revised manuscript: "CO production from VOCs biogenic emissions, calculated online and depending on meteorological variables such as radiation, might be overestimated too, due to the lack of aerosol attenuation of radiation".

P 21
L 13 better "megacities"
Response: Amended.

Figure 3: better to have plots for different regions (NH, SH, Tropics) to better see the seasonal cycle. Choose a smaller y-range for more clarity. Show plot in ppb (as for the profiles) rather than microgramm/m3.

Response: We have only 14 stations available for CO, and only 2 of them are located in the SH. For that reason, we decided to average over all stations. The seasonality for the CO is represented in Figure 6. Most of the surface observations are in $\mu g/m^3$ and therefore we used $\mu g/m^3$ in the surface comparison.

Figure 4: MB (see supplement) is defined without scaling (i.e. not relative in %). Please show the MB as defined in the supplement. Use ppb as unit.
Response: In the document the MB is calculated, not the relative bias (%). This information is now corrected in the revised manuscript. Surface observations are shown in $\mu g/m^3$.

Figure 7: better y-range, use ppb
Response: Surface observations are shown in $\mu g/m^3$.

Figure 8: as for Figure 4
Response: In the document the MB is calculated, not the relative bias (%). This information is now corrected in the revised manuscript.

Figure 11: use ppb
Response: Surface observations are shown in $\mu g/m^3$.

Figure 12: see Figure 4
Response: In the document the MB is calculated, not the relative bias (%). This information is now corrected in the revised manuscript.

Figure 13: choose x-range 0-100 for better clarity in the troposphere.
Response: The x-range 0-100 has been chosen to include both the tropopause and the lower stratosphere.

Figure 14: see Figure 4
Response: In the document, the MB is calculated, not the relative bias (%). This information is now corrected in the revised manuscript.

~~Gas-phase chemistry in the online multiscale NMMB/BSC Chemical Transport Model:~~ Description and evaluation of the Multiscale Online Nonhydrostatic AtmospheRe CHemistry model (NMMB-MONARCH) version 1.0: gas-phase chemistry at global scale

Alba Badia[1,*], Oriol Jorba[1], Apostolos Voulgarakis[2], Donald Dabdub[3], Carlos Pérez García-Pando[4, 5, †], Andreas Hilboll[6,7], María Gonçalves[1, 8], and Zavisa Janjic[9]

[1]Earth Sciences Department, Barcelona Supercomputing Center, Barcelona, Spain
[2]Department of Physics, Imperial College, London
[3]Mechanical and Aerospace Engineering, University of California, Irvine
[4]NASA Goddard Institute for Space Studies, New York, USA
[5]Department of Applied Physics and Applied Math, Columbia University, New York, USA
[6]Institute of Environmental Physics, University of Bremen, Germany
[7]MARUM – Center for Marine Environmental Sciences, University of Bremen, Germany
[8]Universitat Politecnica de Catalunya, Barcelona, Spain
[9]National Centers for Environmental Prediction, College Park, MD, USA
[*]Now at the Centre for Ocean and Atmospheric Sciences, School of Environmental Sciences, University of East Anglia, Norwich, United Kingdom
[†]Now at the Barcelona Supercomputing Center, Barcelona, Spain

Correspondence to: oriol.jorba@bsc.es

Abstract.

This paper presents a comprehensive description and benchmark evaluation of the tropospheric gas-phase chemistry component of the Multiscale Online Nonhydrostatic AtmospheRe CHemistry model (NMMB-MONARCH), formerly known as NMMB/~~BSC Chemical Transport Model (NMMB/~~BSC-CTM~~), an online chemical weather prediction system conceived for~~

5 ~~both the regional and the global scale. We~~, that can be run on both regional and global domains. Here, we provide an extensive evaluation of a global annual cycle simulation using a variety of background surface stations (EMEP, WDCGG and CASTNET), ozonesondes (WOUDC, CMD and SHADOZ), aircraft data (MOZAIC and several campaigns), and satellite observations (SCIAMACHY and MOPITT). We also include an extensive discussion of our results in comparison to other state-of-the-art models.

10 The model shows a realistic oxidative capacity across the globe. The seasonal cycle for CO is fairly well represented at different locations (correlations around 0.3-0.7 in surface concentrations), although concentrations are underestimated in spring and winter in the Northern Hemisphere, and are overestimated throughout the year at 800 and 500 hPa in the Southern Hemisphere.

Nitrogen species are well represented in almost all locations, particularly NO_2 in Europe (RMSE below 9 μg m^{-3}). The modeled vertical distribution of NO_x and HNO_3 are in excellent agreement with the observed values and the spatial and sea-

sonal trends of tropospheric NO_2 columns correspond well to observations from SCIAMACHY, capturing the highly polluted areas and the biomass burning cycle throughout the year. Over Asia, the model underestimates NO_x from March to August probably due to an underestimation of NO_x emissions in the region. Overall, the comparison of the ~~modelled~~ modeled CO and NO_2 with MOPITT and SCIAMACHY observations emphasizes the need for more accurate emission rates from anthropogenic and biomass burning sources (i.e., specification of temporal variability).

The resulting ozone (O_3) burden (348 Tg) lies within the range of other state-of-the-art global atmospheric chemistry models. The model generally captures the spatial and seasonal trends of background surface O_3 and its vertical distribution. However, the model tends to overestimate O_3 throughout the troposphere in several stations. This ~~is~~ may be attributed to an overestimation of CO concentration over the ~~southern hemisphere~~ Southern Hemisphere leading to an excessive production of O_3 ~~.~~ or to the lack of specific chemistry (e.g., halogen chemistry, aerosol chemistry). Overall, O_3 correlations range between 0.6 to 0.8 for daily mean values. The overall performance of the ~~NMMB/BSC-CTM~~ NMMB-MONARCH is comparable to that of other state-of-the-art global ~~chemical transport~~ chemistry models.

1 Introduction

Tropospheric ozone (O_3) is a radiatively active gas interacting with solar and terrestrial radiation that is mainly produced during the photochemical oxidation of methane (CH_4), carbon monoxide (CO) and non-methane volatile organic compounds (NMVOC) in the presence of nitrogen oxides (NO_x) (Crutzen, 1974; Derwent et al., 1996). Downward transport from the stratosphere, where O_3 is created by photolysis of oxygen (O_2) molecules, is also an important source of tropospheric O_3 (Stohl et al., 2003; Hsu and Prather, 2009). In urban areas, O_3 is a major component of 'smog', which can cause a number of respiratory health effects (WHO, 2014). Since the pre-industrial era, changes in emissions of O_3 precursors from anthropogenic and biomass burning sources have modified the distribution of tropospheric O_3 and other trace gases (Lamarque et al., 2013). Tropospheric O_3, with an average lifetime of the order of weeks, is highly variable in space and time, and Air Quality Models (AQM) are required to predict harmful levels of O_3 along with its precursors and other trace gases.

AQMs are driven by meteorological fields and ~~fed by emission inventories~~ emissions of chemical species. They include a chemical mechanism for representing gas-phase and aerosol atmospheric chemistry, a photolysis scheme describing the photo-dissociation reactions driven by sunlight, dry and wet deposition schemes to account for the removal of pollutants from the atmosphere, and the characterization of the downward transport of stratospheric O_3. The development of AQMs and meteorological models (MM) evolved as separate fields (offline approach) due to complexity and limitations in computer resources.

The offline approach requires lower computational capacity, but involves a loss of essential information on atmospheric processes whose time-scale is smaller than the output time rate of the meteorological model (Baklanov et al., 2014). Nowadays, owing to a general increase in computer capacity, online coupled meteorology-chemistry models are being increasingly developed and used by the scientific community, who recognizes the advantages of the online approach (Byun, 1990). Overviews of online AQM-MM models are available in the literature (Zhang, 2008; Baklanov et al., 2014).

Several global AQMs have been developed during the last decades, including the multiscale GEM-AQ (online, 1.5° x 1.5°) (Gong et al., 2012), TM5-chem-v3.0 (offline, 3° x 2°) (Huijnen et al., 2010), LMDZ-INCA (offline, 3.8° x 2.5°) (Folberth et al., 2006), the GATOR-GCMM (online, 4° x 5°) (Jacobson, 2001), the IFS-MOZART used in the MACC project (online, 80 km x 80 km) (Flemming et al., 2009), C-IFS recently developed at ECMWF (online, 80 km x 80 km) (Flemming et al., 2015), and MOZART-4 (offline, 2.8° x 2.8°) (Emmons et al., 2010). Most of these models have been applied at coarse resolutions with simplified chemical schemes. Currently, the systems are being updated and prepared for higher resolution applications.

In this contribution, we describe the gas-phase chemistry of the Multiscale Online Nonhydrostatic AtmospheRe CHemistry model (NMMB-MONARCH), a chemical weather prediction system formerly known as NMMB/BSC-CTM that can be run either globally or regionally (Pérez et al., 2011; Jorba et al., 2012). The NMMB-MONARCH, developed at the Barcelona Supercomputing Center, is based on the coupling of the meteorological Nonhydrostatic Multiscale Model on the B-grid (NMMB; Janjic and Gall, 2012) with a chemistry module. We provide a thorough evaluation of the gas-phase chemistry over a one-year period for the global domain using an horizontal resolution of 1.4° x 1.4°.

The NMMB-MONARCH configured as a limited area (regional) model has recently participated in the Air Quality Model Evaluation International Initiative Phase2 (AQMEII-Phase2) intercomparison exercise (Im et al., 2014). Badia and Jorba (2014) also provided a detailed evaluation of the gas-phase chemistry for the year 2010 over Europe in the context of AQMEII-Phase2. The initial model developments focused on the implementation of the mineral dust aerosol component (NMMB/BSC-Dust; Pérez et al., 2011; Haustein et al., 2012) and the sea-salt aerosol component (Spada et al., 2013, 2015). The implementation and evaluation of other relevant aerosols will be soon described elsewhere (Spada et al., in prep). This initiative aims at developing a fully coupled chemical multiscale (global/regional) weather prediction system that resolves gas-aerosol-meteorology interactions and provides initial and boundary conditions for embedded high resolution nests in a unified dynamics-physics-chemistry environment.

The paper is organized as follows. In Sec. 2, we provide a description of the atmospheric driver, the gas-phase chemistry module, and the model configuration including the online biogenic emissions. Section 3 presents an overview of the model setup with a description of the chemical and meteorological initial conditions, and the anthropogenic and biomass burning emissions implemented for this experiment. We illustrate the capability of the NMMB-MONARCH to reproduce the atmospheric composition by evaluating the model with ground-based monitoring stations, ozonesondes, aircraft data, climatological vertical

profiles and satellite retrievals, which are described in Sec. 4. The results of the model performance are discussed in Sec. 5 for year 2004. The last section summarizes the conclusions of this work.

2 Model description

The NMMB-MONARCH is a fully online multiscale chemical weather prediction system for regional and global-scale applications (Pérez et al., 2011; Jorba et al., 2012). The system is based on the meteorological Nonhydrostatic Multiscale Model on the B-grid (NMMB; Janjic and Gall, 2012), developed at the National Centers for Environmental Prediction (NCEP). The model couples online the NMMB with the gas-phase and aerosol continuity equations to solve the atmospheric chemistry processes in detail. The model is designed to account for the feedbacks among gases, aerosol particles and meteorology. Currently, it can consider the direct radiative effect of aerosols, while ignoring cloud-aerosol interactions. In this work, only the gas-phase chemistry is used, thus no interaction between gas-phase and aerosol-phase is applied. In this section we provide a concise description of the NMMB and the gas-phase chemistry module of the NMMB-MONARCH.

2.1 The Nonhydrostatic Multiscale Model on the B-grid

The Nonhydrostatic Multiscale Model on the B-grid (NMMB; Janjic and Black, 2005; Janjic and Gall, 2012) was conceived for short- and medium-range forecasting over a wide range of spatial and temporal scales, from large eddy simulations (LES) to global simulations. Its unified nonhydrostatic dynamical core allows for running either regional or global simulations, both including embedded regional nests. The NMMB has been developed within the Earth System Modeling Framework (ESMF) at NCEP, following the general modeling philosophy of the NCEP regional Weather Research and Forecasting (WRF) Nonhydrostatic Mesoscale Model (NMM; Janjic et al., 2001; Janjic, 2003). The regional NMMB has been the operational regional North American Mesoscale (NAM) model at NCEP since October 2011. The numerical schemes used in the model were designed following the principles presented in Janjic (1977, 1979, 1984, 2003). Isotropic horizontal finite volume differencing is employed so a variety of basic and derived dynamical and quadratic quantities are conserved. Among these, the conservation of energy and enstrophy (Arakawa, 1966) improves the accuracy of the nonlinear dynamics. The hybrid pressure-sigma coordinate is used in the vertical direction and the Arakawa B-grid is applied in the horizontal direction. The global model on the latitude-longitude grid with polar filtering was developed as the reference version, and other geometries such the cubed-sphere are currently being tested. The regional model is formulated on a rotated longitude-latitude grid, with the Equator of the rotated system running through the middle of the integration domain resulting in more uniform grid distances. The nonhydrostatic component of the model dynamics is introduced through an add-on module that can be turned on or off, depending on the resolution. The operational physical package includes: (1) the Mellor-Yamada-Janjic (MYJ) level 2.5 turbulence closure for the treatment of turbulence in the Planetary Boundary Layer (PBL) and in the free atmosphere (Janjic et al., 2001), (2)

the surface layer scheme based on the Monin-Obukhov similarity theory (Monin and Obukhov, 1954) with introduced viscous sublayer over land and water (Zilitinkevich, 1965; Janjic, 1994), (3) the NCEP NOAH (Ek et al., 2003) or the LISS land surface model (Vukovic et al., 2010) for the computation of the heat and moisture surface fluxes, (4) the GFDL or RRTMG long-wave and shortwave radiation package (Fels and Schwarzkopf, 1975; Mlawer et al., 1997), (5) the Ferrier gridscale clouds and microphysics (Ferrier et al., 2002), and (6) the Betts-Miller-Janjic convective parametrization (Betts, 1986; Betts and Miller, 1986; Janjic, 1994, 2000). Vertical diffusion is handled by the surface layer scheme and by the PBL scheme. Lateral diffusion is formulated following the Smagorinsky non-linear approach (Janjic, 1990). Table 1 describes the main configuration of the meteorological model used in this work.

2.2 Gas-phase chemistry module

The tropospheric gas-phase chemistry module is coupled online within the NMMB~~code~~. Different chemical processes were implemented following a modular operator splitting approach to solve the advection, diffusion, chemistry, dry and wet deposition, and emission processes. Meteorological information is available at each time step to solve the chemical processes~~properly~~. In order to maintain consistency with the meteorological solver, the chemical species are advected and mixed at the corresponding time step of the meteorological tracers using the same numerical schemes implemented in the NMMB. The advection scheme is Eulerian, positive definite and monotone, maintaining a consistent mass-conservation of the chemical species within the domain of study (Janjic et al., 2009; Tang et al., 2009; Janjic and Gall, 2012).

2.2.1 Chemical-phase reaction mechanism

Several chemical mechanisms can be implemented within the ~~NMMB/BSC-CTM~~NMMB-MONARCH. A modular coupling with the Kinetic PreProcessor (KPP) package (Damian et al., 2002; Sandu and Sander, 2006) allows the model to maintain wide flexibility. Additionally, an Eulerian-Backward-Iterative solver (Hertel et al., 1993) was implemented as a complementary option to the KPP solvers to allow the model to run with a fast ordinary differential equation solver at global scales. For the present study, we use a Carbon-Bond family mechanism, the Carbon Bond 2005 (CB05; Yarwood et al., 2005), an updated version of the Carbon-Bond IV (CB4) lumped-structure-type mechanism (Gery et al., 1989). CB4 was formulated focusing on limited domain extent, urban and regional environments and for planetary boundary layer chemistry. CB05 extends its applicability from urban to remote tropospheric conditions and is suitable for global applications. CB05 was evaluated against smog chamber data from the University of California, Riverside and University of North Carolina (Yarwood et al., 2005). It includes 51 chemical species and solves 156 reactions (see Tables S1 and S2 in the supplementary information). Both the organic chemistry of methane and ethane, and the chemistry of methylperoxy radical, methyl hydroperoxide and formic acid are treated explicitly. The higher organic peroxides, organic acids, and peracids are treated as lumped species. Following its main design, CB05 defines proxy single and double carbon bond species, paraffin and an olefin bond respectively, and it introduces the internal olefin species. The rate constants were updated based on evaluations from Atkinson et al. (2004) and Sander et al. (2006). Organic compounds not explicitly treated are apportioned to the carbon-bond species based on the molecular structure

and following Yarwood et al. (2005) assignments from VOC species to CB05 model species. The concentration of methane is considered constant (1.85 ppm) in this study.

2.2.2 Photolysis scheme

One of the most important processes determining tropospheric composition is the photo-dissociation of trace gases. Table ~~S2~~ S3 in the supplementary information lists the photolysis reactions considered. To compute the photolysis rates, we implemented the Fast-J (Wild et al., 2000) online photolysis scheme. Fast-J has been coupled with the physics of each model layer (e.g., clouds and absorbers such as O_3). The optical depths of grid-scale clouds from the atmospheric driver are considered by using the fractional cloudiness based on relative humidity (Fast et al., 2006). The main advantages of Fast-J are the optimization of the phase function expansion into Legendre polynomials and the optimization of the integration over wavelength (Wild et al., 2000). The Fast-J scheme has been upgraded with CB05 photolytic reactions. The quantum yields and cross section for the CB05 photolysis reactions have been revised and updated following the recommendations of Atkinson et al. (2004) and Sander et al. (2006). The Fast-J scheme uses seven different wavelength bins appropriate for the troposphere to calculate the actinic flux covering from 289 to 850 nm (see Table VIII from Wild et al. (2000)). In this work, aerosols are not considered in the photolysis rate calculation. This might produce an atmosphere excessively oxidized in regions where aerosols are significant (e.g., Bian et al., 2003; Real and Sartelet, 2011).

2.2.3 Dry-deposition scheme

The dry-deposition scheme is responsible for computing the flux of trace gases from the atmosphere to the surface. It is calculated by multiplying ~~concentrations~~ the concentration in the lowest model layer by the spatially and temporally varying deposition velocity:

$$\frac{\partial C_i}{\partial t}_{dry-dep} = -C_i v_d \tag{1}$$

where t is the time, i the gas-phase species, C_i is the concentration of the gas in the lowest model layer, and v_d is the dry-deposition velocity. At each time step, v_d is calculated according to:

$$|v_d| = \frac{1}{(R_a + R_b + R_c)} \tag{2}$$

where R_a is the aerodynamic resistance (depends only on atmospheric conditions), R_b is the quasilaminar sublayer resistance (depends on friction velocity and molecular characteristics of gases), and R_c is the canopy or surface resistance (depends on surface properties and the reactivity of the gas). R_a and R_b are computed following their common definition (Seinfeld and Pandis, 1998), while R_c is simulated following Wesely (1989), where the surface resistance is derived from the resistances of the surfaces of the soil and the plants. The properties of the plants are determined using land-use data (from the meteorological

driver USGS land-use) and depend on the season. The surface resistance also depends on the diffusion coefficient, the reactivity, and water solubility of the reactive trace gases.

2.2.4 Wet-deposition scheme

We use the scheme of Byun and Ching (1999) and Foley et al. (2010) to resolve the cloud processes affecting the concentration of 36 gases from the CB05 chemical mechanism. The processes included are grid-scale scavenging and wet-deposition, subgrid-scale vertical mixing, ~~and~~ scavenging and wet-deposition for precipitating and non-precipitating clouds. Aqueous chemistry is neglected in version 1.0 of the model. At the moment, we consider only in-cloud scavenging, which is computed
using the Henry's Law equilibrium equation. The rate of change for in-cloud pollutant concentration is given by:

$$\frac{\partial C_{icld}}{\partial t} = C_{icld} \frac{e^{-\alpha_i \tau_{cld}} - 1}{\tau_{cld}} \tag{3}$$

where C_{icld} is the gas concentration within the cloud [ppm], τ_{cld} is the cloud timescale [s], and α_i is the scavenging coefficient for the gas species that is calculated as:

$$\alpha_i = \frac{1}{\tau_{washout}(1 + \frac{TWF}{H_i})}, \tag{4}$$

where ~~H_i~~ H_i is the Henry's Law coefficient for the gas species [M/atm], ~~TWF~~ $TWF = \rho_{H_2O}/(W_T R T)$ is the total water fraction (where ρ_{H_2O} is the density of water [kg/m^3], W_T is the total mean water content [~~M~~kg/~~atm~~m^3], R is the Universal gas constant, and T is the in-cloud air temperature [K]), and $\tau_{washout}$ is the washout time [s], i.e., the amount of time required to remove all of the water from the cloud volume at a specified precipitation rate~~m/s~~, which is given by:

$$\tau_{washout} = \frac{W_T \Delta Z_{cld}}{\rho_{H_2O} P_r} \tag{5}$$

where ΔZ_{cld} is the cloud thickness [m] and P_r is the precipitation rate [m/s]. Both grid-scale and subgrid-scale scavenging are computed with equation 3, where τ_{cld} is 1 hour for subgrid-scale clouds, and the chemistry timestep for grid-scale clouds. Wet deposition is computed following the algorithm of Chang et al. (1987), which depends upon P_r and the gas concentration within the cloud C_{icld}. Thus, the wet deposition is given by:

$$wdep_i = \int_0^{\tau_{cld}} C_{icld} P_r dt \tag{6}$$

The sub-grid cloud scheme implemented solves convective mixing, scavenging and wet deposition of a representative cloud within the grid cell following the CMAQ and RADMv2.6 model schemes (Byun and Ching, 1999; Chang et al., 1987). Precipitating and non-precipitating sub-grid clouds are considered. The latter are categorized as pure fair weather clouds and non-precipitating clouds and may coexist with precipitating clouds (Byun and Ching, 1999; Foley et al., 2010).

2.2.5 Upper boundary conditions

5 Because the model focuses on the troposphere, stratospheric chemistry is taken into account using a simplified approach. Above 100 hPa, mixing ratios of several species (NO, NO_2, N_2O_5, HNO_3 and CO) are initialized each day from a global chemical model MOZART-4 (Emmons et al., 2010). For O_3, an important reactive gas requiring a more refined representation in the stratosphere, we use a linear O_3 stratospheric scheme, COPCAT (Monge-Sanz et al., 2011). COPCAT is based on the approach of Cariolle and Déqué (1986), which represented the first effort to include a linearized O_3 scheme (named Cariolle v1.0) in a

10 three-dimensional model.

Following the COPCAT approach, the change in O_3 with time due to local chemistry is given by:

$$\frac{\partial C_{O_3}}{\partial t} = \frac{d\chi}{dt} = (P - L)\chi, T, \Phi$$

where $(P - L)$ represents the O_3 tendency as a linear function depending on χ, the O_3 mass mixing ratio ($kg kg^{-1}$), T, the temperature (K), and Φ, the column O_3 above the point under consideration ($kg m^{-2}$).

15 Equation (??) is expanded to first order in a Taylor Series as follows:

$$\frac{\partial C_{O_3}}{\partial t} = \frac{d\chi}{dt} = (P - L)_0 + \mathbf{a} +$$
$$\mathbf{b} + \mathbf{c}$$

The second term in the expansion represents variations in the local O_3 amount (a), the third represents temperature effects

20 (b) and the last term, called radiation term, accounts for the influence of non-local O_3 on the amount of solar radiation reaching the level under consideration (c). Specific terms in this equation (represented with the subscript 0) are coefficients applicable at the equilibrium state. In COPCAT these coefficients In COPCAT the linear coefficients are obtained at equilibrium from the TOMCAT/SLIMCAT box model (Chipperfield, 2006). These terms are presented as functions of 24 latitudes, 24 model vertical levels and 12 months.

25 Heterogeneous processes describing the polar stratospheric chemistry are non-linear and depend on the three-dimensional structure of the atmosphere. COPCAT includes complete heterogeneous processes in their coefficients, considering heterogeneous and gas-phase chemistry to be consistent when applied in this linear O_3 parameterization. This kind of parameterization is in better agreement with the current state of knowledge of stratospheric heterogeneous chemistry than previous schemes (Monge-Sanz et al., 2011). For further description of the approach and information on the biases of the stratosphere ozone simulated by the COPCAT scheme, the reader is referred to Monge-Sanz et al. (2011).

2.2.6 Online natural emissions

Natural emissions of gaseous pollutants include biogenic emissions, soil emissions, emissions from lightning, and emissions from oceans and volcanoes. Currently, soil and oceanic emissions in the model are prescribed as described in Sect. 3.1 and emission from lightning and volcanoes are not considered. The omission of lightning emissions may have a significant impact in the oxidation of the middle and upper troposphere. Only biogenic emissions, which strongly depend on meteorological fields and vegetation cover, are calculated online. They are computed using the Model of Emissions of Gases and Aerosols from Nature version 2.04 (MEGANv2; Guenther et al., 2006). MEGAN is able to estimate the net emission rate of gases and aerosols from terrestrial ecosystems into the above-canopy atmosphere. MEGAN canopy-scale emission factors differ from most other biogenic emission models, which use leaf-scale emission factors, and cover more than 130 Non-Methane Volatile Organic Compounds (NMVOCs). All the MEGAN NMVOCs are speciated following the CB05 chemical mechanism; thus, emissions for isoprene, lumped terpenes, methanol, nitrogen monoxide, acetaldehyde, ethanol, formaldehyde, higher aldehydes, toluene, carbon monoxide, ethane, ethene, paraffin carbon bond, and olefin carbon bond are considered within the model. Biogenic emissions are computed every hour to account for evolving meteorological changes in solar radiation and surface temperature. Thus, weather- driving variables considered are temperature at 2 m and incoming short wave radiation at the surface.

Figure S1 in the supplementary information shows the modeled emission for isoprene and terpenes for January and July 2004, and Table 2 lists the global annual emissions for isoprene, monoterpenes and other important NMVOCs. Biogenic isoprene emissions used in this study amount 683.16 Tg/year. While other global models have lower estimates (Huijnen et al., 2010; Horowitz et al., 2003; Emmons et al., 2010), MEGAN isoprene emissions typically range from about 500 to 750 Tg/year (Guenther et al., 2006). These estimates largely depend on the assumed land cover, emission factors, and meteorological parameters. Therefore, the emission uncertainties and their impacts upon surface O_3 are associated with uncertainties in these inputs. Ashworth et al. (2010) obtained emission reductions of 3% and 7% when using daily and monthly meteorological data, respectively, instead of hourly data, with reductions reaching up to 55% in some locations. Marais et al. (2014) performed several sensitivity model runs to study the impact of different model input and settings on isoprene estimates that resulted in differences of up to $\pm$ 17% compared to a baseline. In our study, weather inputs are based on previous day 24h averages and data of the hour of interest.

3 Model setup

The model is set up as global with a horizontal grid spacing of ~~1.4°x1°~~ 1.4° x 1° and 64 vertical layers up to 1 hPa. The depth of the bottom layer is below 40 m. The dynamics fundamental time step is set to 180s and the chemistry processes are solved every ~~4 fundamental time steps~~720s. The radiation, photolysis scheme and biogenic emissions are computed every hour. We use NCEP/Final ~~Analyzes~~ Analysis (FNL) as initial conditions for the meteorological driver, and we reinitialize the meteorology every 24 h to reproduce the observed transport. We performed a spin-up of 1-year using initial chemistry conditions from the global atmospheric model MOZART-4 (Emmons et al., 2010) prior to the 2004 annual cycle simulation that is evaluated in the

present study. Table 1 describes the main configuration of the model. The feedback between chemistry and meteorology is not considered in this study.

3.1 Emissions

The global emissions used in this study are based on the Atmospheric Chemistry and Climate Model Intercomparison Project (ACCMIP; Lamarque et al., 2013), which includes emissions from anthropogenic and biomass burning sources at 0.5° ~~x0.5x~~ 0.5° horizontal resolution (Lamarque et al., 2010). ~~Note that the~~ Note that this methodology involves assuming 2004 emissions ~~are derived from a linear interpolation between years 2000 and 2010.~~ equivalent to the best estimate reported for ACCMIP for year 2000. Therefore specific events occurred during 2004 (e.g., large summer wildfires in Alaska and Canada) are not described. The ACCMIP inventory is a combination of several existing regional and global inventories. The surface anthropogenic emissions are based on two historical emission inventories, namely RETRO (1960-2000; Schultz and Rast (2007)) and EDGAR-HYDE (1890-1990; Van Aardenne et al. (2005)) and monthly variations for biomass burning, ship and aircraft emissions are provided. One limitation is that land-based anthropogenic emissions have constant values for the entire year. Lamarque et al. (2010) presents a comparison of the annual total CO anthropogenic and biomass burning emissions (Tg(CO)/year) for different regional and global emission inventories for year 2000 (see Table 5 of this paper). Note that ACCMIP global CO anthropogenic emissions are significantly higher (610.5 Tg CO/year) than other emissions inventories (e.g. RETRO with 476 Tg CO/year, EDGAR-HYDE with 548 Tg CO/year, and GAINS with 542 Tg CO/year).

Ocean and soil natural emissions are based on the POET (Granier et al., 2005) global inventory. Lightning and volcano emissions are not considered in this simulation. Biogenic emissions are computed using MEGANv2.04 model as described in Sec. 2.2.6. NO emissions for January and July 2004 are shown in Figure S1 in the supplementary information and yearly totals for anthropogenic~~and biomass burning~~, biomass burning, biogenic, soil, and ocean emissions are summarized in Table 2.

To account for the sub-grid scale vertical diffusion within the planetary boundary layer (PBL) all the land-based anthropogenic emissions are emitted in the first 500 m of the model, biomass burning emissions from forests in the first 1300 m, biomass burning emissions from grass in the first 200 m, ocean emissions on the first 30 m and shipping emissions on the first 500 m. The model does not include the attenuation of radiation due to aerosols in the photolysis scheme. Therefore, regions with strong biomass burning emissions may significantly overestimate chemical photolysis production (e.g., Bian et al., 2003; Real and Sartelet, 2011).

4 Observational data

4.1 Surface concentration and wet deposition

For the evaluation of ground-level gas concentrations, we selected background stations having hourly data (Fig. 1 left panel) from the World Data Center for Greenhouse Gases (WDCGG; http://gaw.kishou.go.jp/wdcgg/), the European Monitoring and Evaluation Programme (EMEP; http://www.emep.int/), the Clean Air Status and Trends Network in ~~USA~~ US (CASTNET;

10

http://java.epa.gov/castnet/) and the Acid Deposition Monitoring Network in East Asia (EANET; http://www.eanet.asia/). For
O$_3$, we used data from 41 WDCGG, 52 EMEP, 64 CASTNET and 11 EANET stations, covering Europe, United States (US),
and a few locations in ~~east~~ East Asia. We also selected 21 EMEP stations for NO$_2$, 10 EANET stations for NO$_x$ and 14
WDCGG stations for CO.

The simulated wet deposition of HNO$_3$ is also compared against observed nitrate (HNO$_3$ and aerosol nitrate) wet deposition,
including 260 measurements from the National Atmospheric Deposition Program (NADP; http://nadp.sws.uiuc.edu/) network
in North America, 51 from the EMEP network in Europe and 28 from EANET in East Asia.

4.2 Vertical structure: ozonesondes~~and~~, MOZAIC and measurement campaigns

The surface evaluation is complemented with an assessment of the vertical structure of O$_3$ using ~~ozonosondes~~ ozonesondes
from the World Ozone and Ultraviolet Radiation Data Center ~~ozonosonde~~ ozonesonde network (WOUDC;http://www.woudc.
org/), the Global Monitoring Division (GMD; ftp://ftp.cmdl.noaa.gov/ozwv/ozone/) and the Southern Hemisphere ADditional
OZonesondes (SHADOZ; http://croc.gsfc.nasa.gov/shadoz/; Thompson et al., 2003a, b). Most stations provide between 4 and
12 profiles per month each year with a precision of ± 3-8 % in the troposphere (Tilmes et al., 2012). We followed the method-
ology of Tilmes et al. (2012) for the selection and treatment of the measurements. Table 3 lists the locations and the number of
available measurements per season of the 39 ozonesonde stations used (also displayed in Fig. 1), as well as the regions where
stations with similar O$_3$ profiles were aggregated~~)~~.

Additional observations considered in this study are CO vertical profiles from Measurement of Ozone, Water Vapor, Carbon
Monoxide, Nitrogen Oxide by Airbus In-Service Aircraft (MOZAIC; http://http://www.iagos.fr). Based on the availability of
data, we selected 14 airports (displayed in Fig. 1 right panel) covering different regions of the world during 2004. The number
of vertical profiles available per season are provided in Table 4.

Nitric oxide (NO$_x$), peroxyacetyl nitrate (PAN) and acid nitric (HNO$_3$) vertical profiles are used from ~~two~~ four different
measurement campaigns: TOPSE (Atlas et al., 2003; Emmons et al., 2003)~~and~~, TRACE-P (Jacob et al., 2003), PEM-Tropics-B
(Raper et al., 2001) and POLINAT-2 (Schumann et al., 2000). Tropospheric data from these ~~two~~ four previous campaigns were
gridded onto global maps with resolution 5° ~~x5~~ x 5° ~~x1km~~ x 1 km, forming data composites of important chemical species in
order to provide a picture of the global distributions (Emmons et al., 2000).

~~When running an AQM model, it is preferable to compare the model output with an observational database from the same
year as the model simulation. Nevertheless, in our case, there are insufficient global observations to achieve this goal for
any full year. Hence, in this model evaluation,~~ In this study, all the observations ~~are for~~ considered are within the simulated
year (2004~~, except for the~~), with the exception of the vertical profiles obtained from measurement campaigns. ~~Hence, in this
study, model output from selected regions are compared with this campaign from the same regions regardless of the year of
the measurements. In addition, it is valuable to compare the same regions for different species which allows identification of
systematic differences between the model results and observations . Details of these campaigns describing their geographical
region and period~~ Details on the geographical regions and periods for these campaigns are described in Table 5, and the ~~location~~
locations are displayed in Fig. 1 (right panel).

4.3 Satellite data

~~Modelled~~ Modeled tropospheric NO_2 columns are compared with SCanning Imaging Absorption spectroMeter for Atmospheric CHartographY (SCIAMACHY, http://www.sciamachy.org/) satellite data. SCIAMACHY (on board of ENVISAT, which was operational from March 2002 to April 2012) is a passive remote sensing spectrometer measuring backscattered, reflected, transmitted or emitted radiation from the atmosphere and Earth's surface with a wavelength range between 240-2380 nm. The SCIAMACHY instrument has a spatial resolution of typically 60 km x 30 km^2, and has three different viewing geometries: nadir, limb, and sun/moon occultation. Alternating nadir and limb views, global coverage is achieved in six days.

NO_2 daily data was obtained from the Institute of Environmental Physics, the University of Bremen (http://www.iup.uni-bremen.de/doas/scia_no2_data_tropos.htm), based on Version 3.0 data product (Hilboll et al., 2013). This dataset is an improved extension of the data presented in Richter et al. (2005). Validation of the data product was performed in several studies ~~(e. g., ,).~~ (e.g., Petritoli et al., 2004; Heue et al., 2005). We used daily satellite overpasses of cloud-free (<20% cloud fraction) tropospheric vertical column densities (VCDtrop NO_2) from SCIAMACHY measurements using the limb/nadir matching approach, whose total uncertainty is estimated to vary between 35 and 60% in heavily polluted cases and >100% in clean scenarios ~~()~~(Boersma et al., 2004).

Additionally, CO mixing ratios at 800 and 500 hPa were evaluated with the Measurement of Pollution in the Troposphere (MOPITT~~:~~, http://www2.acd.ucar.edu/mopitt) instrument retrievals. ~~The MOPITT, aboard~~ MOPITT, on board of the NASA EOS-Terra satellite, is a gas filter radiometer and measures thermal infrared (near 4.7 μm) and near-infrared (near 2.3 μm) radiation, only during clear-sky conditions, with a ground footprint of about 22 km x 22 km. We used the MOPITT Version 5 (V5) Level 2 data product, which provides daily CO mixing ratios. MOPITT CO mixing ratios have been validated with in situ CO profiles measured from numerous NOAA/ESRL aircraft profiles in Deeter et al. (2013), and they were found to be positively biased by about 1% and highly correlated (r = 0.98) at ~~the surface level~~surface levels.

5 Model evaluation

This section presents the ~~evaluation~~ model evaluation with observations of relevant trace gases~~from the NMMB/BSC-CTM using the observations described in the previous section. It also~~, and compares the results with other modeling studies available in the literature. ~~For the~~

~~For the~~ evaluation of daily surface-level ~~comparison, three-hourly averages from~~ O_3, we considered averages of temporally collocated 3-hourly values from the model and ~~the observations and model are used to compute daily O_3 averages and calculate the statistical measures defined in section~~ observations. Section 1 ~~in the supplemental material~~ of the supplementary material presents the statistical measures calculated from the daily data. Ground-monitoring stations were selected with a maximum altitude of 1000 meters. ~~In the case of ozonesondes and MOZAIC the comparison is made only when vertical profile observations are available, i.e., the data from the model and the observations are collocated/simultaneous. Similar criteria is used in the case of~~ Temporal collocation was also considered when comparing to ozonesondes, MOZAIC, MOPITT and SCIAMACHY~~for~~ ~~NO_2. Moreover.~~ For CO, averaging kernels ~~for CO are accounted~~ were considered to represent the observational sensitivity at

different pressure levels. When computing the ~~modelled~~ modeled tropospheric columns of NO_2 the tropopause was assumed to be fixed at 100 hPa in the tropics and 250 hPa in the extratropics.

Similarly, ~~when comparing model data with data composites from aircraft campaigns the same period of the year at the same location is selected and mapped into the same grid resolution ,~~ the evaluation with aircraft campaigns was performed after remapping the model output to the resolution of the observed data composites (5° x 5° x ~~1km, before the comparison is made~~1 km). For some species, the model evaluation is given per seasons: ~~DJF for~~ December-January-February ~~, MAM for~~ (DJF), March-April-May ~~, JJA for~~ (MAM), June-July-August ~~and SON for~~ (JJA) and September-October-November (SON).

5.1 Hydroxyl Radical (OH)

One of the means for characterizing the general properties of an AQM is through its ability to simulate OH oxidation. OH is the main oxidant in the troposphere and is responsible for the removal of many compounds, thereby controlling their atmospheric abundance and lifetime. OH is mostly found in the tropical lower and mid troposphere ~~with a strong dependence~~ and strongly depends on the levels of ultraviolet radiation and water ~~vapour~~vapor. Tropospheric OH formation is mainly due to O_3 photolysis, dominated by the tropics. Also, OH is directly connected to the chemistry of O_3 production since the initial reactions of O_3 formation (VOC+OH and CO+OH) are driven by OH. Hence, O_3 production rates depend on the sources and sinks of odd hydrogen radicals. Primary OH formation also includes the photolysis of HCHO and secondary VOC.

The tropospheric mean (air mass weighted) OH derived by the model is 11.5 ~~molec~~ x 10^5 molec cm^{-3}, assuming a tropospheric domain ranging from 200 hPa to the surface. ~~(~~Note that previous studies suggest that the estimation of the mean OH does not depend on the definition of the tropopause (Voulgarakis et al., 2013). ~~)~~ This value is in good agreement with other studies, e.g., Voulgarakis et al. (2013) where the mean OH concentration from 14 models for 2000 was estimated to be 11.1±1.8 x 10^5 molec cm^{-3}; Spivakovsky et al. (2000) with 11.6 x 10^5 molec cm^{-3}, and Prinn et al. (2001) with 9.4 ± 0.13 x 10^5 molec cm^{-3}.

The zonal mean OH concentrations for January, April, July and October 2004 are shown in Fig 2. Seasonal differences reflect the impact of water vapor concentration and stratospheric O_3 column upon incident ultraviolet (UV) radiation (Spivakovsky et al., 2000; Lelieveld et al., 2002). The highest OH concentrations arise in the tropics throughout the year. In northern midlatitudes, the highest OH concentrations are found during summer in the lower to middle troposphere. The latitudinal and seasonal variations are similar to the climatological mean in Spivakovsky et al. (2000), particularly the lower values in the extratropics. Peak concentrations are slightly larger compared to this climatology and other studies (e.g., Horowitz et al., 2003; Huijnen et al., 2010). During January and October the peaks appear in the southern tropics between 700-1000 hPa and 800-1000 hPa, respectively. The peak in April and July is found in the northern tropics between 800-1000 hPa and 700-1000 hPa, respectively. ~~The larger oxidizing capacity compared to other studies could be due to~~

The mean OH inter-hemispheric (N/S) ratio of the model is 1.18. This quantity is comparable with the present-day multi-model mean ratio (1.28 ± 0.1) shown in Naik et al. (2013b). In addition, the model regional annual mean air mass-weighted OH concentrations have been calculated and are in general agreement with the multi-model values (Naik et al., 2013b) (see Figure S2 in the supplementary information). However, concentrations over the tropics (30S-30N) are slightly higher than the

multi-model mean and concentrations above 500 hPa are lower than the multi-model mean. Labrador et al. (2004) studied the sensitivity of OH to NO_x from lightning, showing that OH concentrations increase mostly in the middle to upper troposphere (500-200 hPa) if lightning emissions are considered. Therefore, the lack of lightning emissions in our model run could at least partly explain the lower OH values above 500 hPa reported here. Another potential explanation is the lack of aerosols in our simulation, which may overestimate photolysis rates in polluted regions (e.g., Bian et al., 2003; Real and Sartelet, 2011).

5.2 Carbon monoxide (CO)

CO is one of the most important trace gases in the troposphere exerting a significant influence upon the concentration of oxidants such as OH and O_3 (Wotawa et al., 2001). ~~Main~~ The main sources of CO in the troposphere are the photochemical production from the oxidation of hydrocarbons (including methane) and direct emissions, mainly fossil fuel combustion, biomass burning and biogenic emissions. CO main loss is by reaction with OH, which occurs primarily in the tropics, but also in the extratropics.

In the northern extratropics, the elevated CO concentrations are dominated by anthropogenic emissions and precursor hydrocarbons, which leads to a net CO export to the tropics (Shindell et al., 2006; Bergamaschi et al., 2000). Although most of the biomass burning occurs in the tropics, gases and aerosols emitted from large wildfires can be transported to the southern extratropics, where emissions and chemical production are lower. ~~Moreover~~Also, due to ~~the strong convection~~, strong convection enhanced by forest fire activity, emissions can reach the upper troposphere and the lower stratosphere (Jost et al., 2004; Cammas et al., 2009). CO has a chemical lifetime of a few months ($\sim$1-3), and therefore it is a useful tracer for evaluating transport processes in the model. It is important to keep in mind that despite large Alaskan and Canadian wildfires occurred during the summer, globally 2004 had lower CO concentrations than other years during the decade (Elguindi et al., 2010).

An analysis of the CO burden in different regions is presented in Table 6. The global and annual mean burden of CO for 2004 is 399.03 Tg, with higher abundances in the tropics (229.43 Tg CO), followed by the ~~Northern Extratropics~~ northern extratropics (101.71 Tg CO), and the ~~Southern Extratropics~~ southern extratropics (67.88 Tg CO). Other model estimates of the CO burden ~~(;)~~ (Horowitz et al., 2003; Huijnen et al., 2010; Flemming et al., 2015) are also shown in Table 6. Our estimates are higher ~~(by~~ $\sim$ 46-48 Tg CO ~~) in comparison with these studies~~compared to these studies, and it happens in all regions. The largest absolute difference appears in the tropics where the ~~NMMB/BSC-CTM~~ NMMB-MONARCH predicts $\sim$ 30-40 Tg CO more than these studies, even though OH is also overestimated. The main sources of CO in the tropics are from biomass burning, biogenic emissions and anthropogenic direct emissions of CO.

We performed tests comparing the annual mean burden of tropospheric CO with and without biomass burning emissions in the model. Neglecting biomass burning emissions only reduced 7% of the tropospheric CO annual mean burden. Therefore, other factors should explain our higher CO burden. On the one side, biogenic emissions are computed online every hour in order to account for evolving meteorological changes, such as solar radiation and surface temperature (see section 2.2.6). Also this simulation neglects the attenuation of radiation due to aerosols, which may produce an overestimation of VOCs biogenic emissions and the derived CO.

14

The CO anthropogenic emissions used in this study (610.5 Tg/year) are ~~are~~ also higher than those in other inventories (see

5   3.1). The dry deposition of CO is significantly weaker in the ~~NMMB/BSC-CTM~~ NMMB-MONARCH (24 Tg CO) than the global model TM5 (184 Tg CO) and the study of Bergamaschi et al. (2000) (292-308 Tg CO). By contrast, other global models such as MOZART-2 have significantly lower dry deposition (2 Tg CO) and the study of Wesely and Hicks (2000) suggests that CO and other relatively inert substances are deposited very slowly. Clearly, there are major uncertainties in the sources and sinks of CO that could be responsible for modeled CO differences.

10   Fig. 3 shows the time series of CO daily mean concentration over 14 ground-monitoring stations from the WDCGG database (primarily in the northern mid-latitudes, but with a few of them in the tropics and southern mid-latitudes). The solid red line and the solid black line represent, respectively, the average of observations and the model simulation. Bars show the 25th-75th quartile interval of all observations (orange) and the model simulation (~~grey~~gray). The model is in good agreement with the CO field in the surface layer (daily correlations between 0.3-0.7). However, the model is not able to fully capture the seasonal CO

15   variability, with a slight underestimation during cold months (-12.12 μg m^{-3}) and overestimation during warm months (32.83 μg m^{-3}). Such a model limitation could be explained by the fact that most of the stations are closer to anthropogenic polluted areas, where its concentration is primarily determined by local emissions, and the CO land-based anthropogenic emissions inventory does not have any seasonal variation in this study (see Sec.3.1).

Fig. 4 shows the CO mean bias (MB), correlation and root mean square error for all rural WDCGG stations. The model has

20   a negative MB over stations in Europe and Japan and a positive bias in stations in Canada and Africa, where the correlations are low. The negative bias for several of the northern mid-latitude stations indicates that the higher CO burden found in our model compared to other models in these areas is a feature mainly driven by free tropospheric abundances. Higher correlations are found in northern regions of Europe, southern Africa and eastern Asian countries. ~~Correlation~~ The daily correlation in Canadian stations is between 0.3-0.5. In most of the stations, the RMSE is found to be less than ~~60~~40 μg m^{-3}~~;~~, with only 4

25   stations ~~have an~~ having a RMSE higher than 60 μg m^{-3}.

Additionally, the model was compared with ~~the~~ seasonally averaged vertical profiles of temporally collocated CO from MOZAIC aircraft observations ~~for 2004 in Figs. 5 and S2 in the supplementary information~~ from selected airports: Frankfurt, Beijing, Atlanta, Portland, Abu ~~Zabi and Niamey . The comparison is made only when observations are available; i.e., the same data from the model and the observations are used. Measurements are represented by the solid red line and the model~~

30   ~~simulation by the solid black line. To understand the variability of the data, standard deviationis plotted in each vertical layer for both model and observations. It is important to~~ Dhabi and Niamey (shown in Figs. 5 and S3 in the supplementary information). Observations and model results (both mean and standard deviation) are represented in red and black, respectively. We note that the number of flights ~~is significantly different between the different airports ; therefore ,~~ differ among airports (therefore not all comparisons are statistically robust~~. In addition, note that the scale~~), and the CO range represented for Beijing is ~~different~~

35   larger (0-1000 ppb) ~~from the~~ than for others stations (0-400 ppb).

The model captures reasonably well the vertical profiles during the first part of the year ~~, with higher~~ and shows larger biases during the warm months. ~~Generally it~~ It overestimates CO from the middle to the upper troposphere in most ~~of the~~ stations throughout the year. Over Frankfurt, the model is in good agreement with the ~~observation~~ observations during the entire year,

15

despite ~~a slight underestimation during MAM and overestimation during SON~~ slight underestimations during MAM (∼ -31 ppb) and overestimations during SON (∼ 12 ppb) in the middle troposphere.

For Beijing, one of the most polluted cities in the world, the model shows a clear tendency to underestimate CO in the lower atmosphere (below 600 hPa). This is very ~~probably~~ probably due to an underestimation ~~in the~~ of CO anthropogenic emissions. Most ~~of the AQMs seem to be~~ AQMs are unable to capture the extreme growth of anthropogenic emissions in China (Akimoto, 2003; Turquety et al., 2008). Over Atlanta, the model performs ~~much better during the~~ better in winter and spring ~~along the troposphere but positive biases (~~ throughout the troposphere than in summer and autumn, when positive biases reach ∼ 20-25 ppb~~) are seen during the summer and autumn. Regions~~. In regions with biomass burning and biogenic influence, such as Abu Dhabi and Niamey, ~~show a significant overestimation~~ the model significantly overestimates CO during warm months throughout the tropospheric column. During winter and spring, Stein et al. (2014) also obtain an underestimation of CO vertical profiles in airports located in the Northern Hemisphere (NH).

To complete this CO evaluation, seasonal averages are compared with data from the MOPITT instrument at 800 hPa and 500 hPa ~~in~~ (Figs. 6 and ~~S3~~ S4 in the supplementary information, respectively). At 800 hPa, the largest differences are ~~seen~~ detected during boreal winter and spring, ~~where~~ when the model clearly overestimates in the tropics and underestimates in the ~~north extratropics and north of~~ northern extratropics and North Africa. The ~~negative bias during winter~~ wintertime negative bias (∼ - 10-35 ppb) in the NH ~~could further~~ may be explained by either the lack of ~~a seasonal cycle in anthropogenic emissions. However, the underestimation during NH winter, which appears most state-of-the-art AQMs could also be originated from~~ seasonally varying anthropogenic emissions in our simulation, an underestimation of CO emissions (Stein et al., 2014)~~.~~, or a combination thereof. There are significant positive biases over west-central Africa~~and also over~~, western South America, Indonesia and the surrounding Pacific and Indian oceans during the dry season. Sources of CO over west-central Africa are mainly from biomass burning and biogenic emissions. Uncertainties in the emission inventories ~~have probably contributed~~ probably contribute to the CO overestimation ~~for~~ in these regions. Due to the long-range transport of CO, higher ~~CO concentrations are seen throughout all~~ concentrations are also seen throughout the year over the tropics and ~~are extended over~~ some parts of the extratropics from June to November. ~~Hence, during~~ During JJA and SON the model overestimates CO ~~concentrations~~ in most places including south and central ~~EU and USA~~ Europe and US (∼ 10-25 ppb).

At 500 hPa, the model presents similar results, with ~~a clear underestimation in the north extratropics and overestimation~~ clear underestimations in the northern extratropics and overestimations in the tropics and southern latitudes. Excessive vertical mixing by moist convection may explain the overestimation in the tropics. Overestimated emissions in Africa or Asia above the PBL ~~can~~ could also lead to this positive bias in the middle of the troposphere.

Naik et al. (2013b) ~~presents an annual average bias of~~ compared the multi-model ~~(~~annual mean from 17 ~~global models)~~ ~~mean CO for~~ models for year 2000 ~~against average 2000-2006 MOPITT CO~~ with the average CO from MOPITT at 500 hPa ~~.~~ ~~These~~ between 2000 and 2006. The 17 models used the same anthropogenic and biomass burning emissions as our ~~study~~ model, and a priori and averaging kernels ~~are~~ were taken into account for each model before computing the biases. The biases in the tropics and extra tropics are similar to those presented here~~. Hence, these biases might be related to discrepancies in~~, suggesting systematic model errors due to inaccurate anthropogenic and biomass burning emission inventories~~, where the magnitude, and~~

We note that MOPITT V4 CO retrievals are affected by biases of about -6% at 400 hPa when evaluated with in-situ measurements (Deeter et al., 2010), which are low compared to current model discrepancies. Naik et al. (2013b) also discussed how an overestimated OH concentration may lead to the northern mid-latitude underestimation of CO. This may partly explain our results given the higher OH concentration simulated by our model compared to other models. Numerous studies show significant differences in CO among AQMs, which may emerge from a diversity of uncertainties including those in emission inventories and injection heights (Elguindi et al., 2010; Shindell et al., 2006; Prather et al., 2001). For example, Stein et al. (2014) suggest that the persistent negative bias in northern mid-latitude CO in models is most likely due to a combination of too low road traffic emissions and dry deposition errors.

5.3 Nitrogen compounds

The $NO_x (= NO_2 + NO)$ family is one of the key players in the formation of O_3 in the troposphere, causing photochemical smog and contributing to acid rain during pollution episodes. Because it has a relatively short lifetime (a few hours within the PBL and up to a few days in the upper troposphere; Tie et al. (2001, 2002)), it is generally restricted to emission sources, both natural and anthropogenic (mainly fossil fuel combustion). The seasonal cycle of NO_x near the surface is controlled by the seasonality of anthropogenic emissions (especially in the NH) and biomass burning emissions (especially in the tropics and the Southern Hemisphere (SH)). As a result, NO_x concentration is more sensitive to errors in emissions than other pollutants (Miyazaki et al., 2012).

Figure 7 shows the time series of NO_2 and NO_x daily mean surface concentrations over 21 EMEP and 10 EANET rural ground-monitoring stations. In both cases the model is able to successfully reproduce the seasonal cycle of NO_2 and NO_x. However, a positive bias ($< 5\mu g\ m^{-3}$) is found during summertime for NO_2 in Europe (Fig. 7 top panel), which may result from the lack of seasonality in the anthropogenic emissions. The modeled NO_2 concentration is excessive during nighttime (not shown). This may result from the lack of heterogeneous formation of HNO_3 through N_2O_5 hydrolysis, an important sink of NO_2 at night. In addition, the model does not consider secondary aerosol formation in the present study, resulting in an excessively oxidizing atmosphere (overestimation of OH radicals) that in turn may lead to an accumulation of NO_2 near the surface. Between 9 and

18 UTC there is a slight underestimation ~~is observed between 9-18 UTC. Looking at the annual time series of NO$_x$ in the Asian network~~ of NO$_2$. In Asia (Fig. 7 bottom) ~~, it is observed that~~ the model does not reproduce the observed NO$_x$ values, ~~with a sizeable~~ showing a large negative bias during the summer ~~. This underestimation could be attributed to an underestimation in the emission inventories, which do not capture the extreme increase of anthropogenic emissions over Asia during the last decade~~ probably due to underestimated emissions (Akimoto, 2003; Richter et al., 2005), as ~~was the case for CO.~~ in the case of CO. Also, an excessive mixing within the PBL during the night could contribute to a decrease in ozone titration by NO and explain the bias.

~~Concerning the spatial statistics (see Fig. 8), the model's prediction capabilities are lower in some~~ The model correlation is lower in regions such as the Iberian Peninsula and most of the stations in Japan ~~, showing poor correlations.~~ (Fig. 8). The best performance ~~is seen in central EU~~ occurs in central Europe and stations in Japan that are not in the main island. In general there is a negative bias in most of the stations for these two regions.

~~The comparison of modelled and observed vertical profiles of NO$_X$~~ Fig. 9 displays the comparison of NO$_x$, HNO$_3$ and PAN ~~are presented in Fig. 9~~ vertical profiles for several regions ~~over~~ in the US, China, Hawaii and Japan (see Table 5). The comparison over Tahiti and Ireland is shown in Fig. S5 of the supplementary information. As explained in Sec. 4.2, the observed vertical profiles do not correspond to the simulated year (see Table 5 for more ~~detail~~details), but the qualitative patterns can provide insights on the model capability to reproduce the chemistry involved. Fig. 9 (first column) shows that vertical profiles of NO$_x$ are in very good agreement with the observed values. The model has a tendency to overestimate NO$_{\cancel{X}~x}$ concentrations near the surface (~ 400 ppt in Japan and ~ 300 ppt in China); it is likely that NO$_{\cancel{X}~x}$ emissions used in this study are higher than the ~~real~~ actual emissions during the ~~campaigns~~campaign periods. Another reason for these higher values over island locations (Japan and Hawaii) could be that emissions are spread ~~throughout the entire low resolution~~ over the coarse model grid box while the measurements were taken in the cleaner marine boundary layer. In the middle and upper troposphere, the model produces the concentrations well, with a slight underestimation in most of the locations. Note that NO$_x$ lightning emissions are not included in this simulation, which may explain part of this underestimation, particularly in the upper troposphere.

PAN is the main tropospheric reservoir species for NO$_x$ with important implications for the tropospheric O$_3$ production and the main atmospheric oxidant, OH (Singh and Hanst, 1981). PAN is mainly formed in the boundary layer by oxidation of NMVOCs in the presence of NO$_x$. NMVOCs and NO$_x$ have both natural and anthropogenic sources. Rapid convection can transport PAN to the middle and upper troposphere and enables the long-range transport of NO$_x$ away from the urban and polluted areas, where it can produce O$_3$ and OH remotely.

Some features of the vertical profiles are well-captured by the model, although it significantly overestimates PAN concentrations (see Fig. 9, ~~second~~ third column). We find overestimations from the surface to the middle atmosphere in Japan, China, Boulder and Churchill, which are possibly explained by an overestimation of biogenic and anthropogenic NO$_x$ surface emissions~~in this area at surface-level~~. Another possibility for this overestimation is ~~a too long lifetime for PAN. At~~ an excessive lifetime of PAN. In most sites, ~~PAN model concentrations tend~~ the modeled PAN concentration tends to increase with altitude, reaching maximum mixing ratios at about ~~6km~~6 km, from where ~~they progressively decrease. This behaviour~~ it progressively decreases. This behavior explains the long thermal decomposition time of PAN (lifetime of approximately a month) and the

slow loss by photolysis in the cold middle-upper troposphere. Fischer et al. (2014) analyze the sensitivity of PAN to different emission types, showing that most of the NH and Japan are more sensitive to anthropogenic emissions, while the SH and the west coast of the US are more sensitive to biogenic emissions, both contributing to 70-90% of the PAN concentrations.

HNO_3 is mainly produced by the reactions of NO_2 with OH and by the heterogeneous hydrolysis of N_2O_5 (we do not account for the latter in this simulation), and removed by wet and dry deposition. HNO_3 is the main sink of NO_x chemistry. In general, the modeled and observed nitric acid concentrations are of the same magnitude throughout the troposphere, although the model tends to overestimate HNO_3 concentrations, particularly in US regions. In the regions of Hawaii, Japan and China the model overestimates HNO_3 in the lower-middle troposphere (up to 5 km) and underestimates it in the upper troposphere (above 6 km). Overestimation of HNO_3 in the troposphere is a common problem in global models (Hauglustaine et al., 1998; Bey et al., 2001; Park et al., 2004; Folberth et al., 2006). HNO_3 concentrations are highly sensitive to the parameterization of wet deposition. One possible reason for this overestimation is that the scavenging from convective precipitation is underestimated.

Figure S6 in the supplementary information evaluates the wet deposition fluxes of HNO_3 with nitrate observations in Europe, US and Asia. Satisfactory agreement is found in the HNO_3 wet deposition fluxes with correlations of 0.63 in Europe, 0.80 in US and 0.52 in Asia. There is a tendency to underestimate in most of the stations, wet depositions. However, this tendency to underestimate mainly in Asia (MB = -163.27 mg N/m2) and Europe (MB = - 200.70 mg N/m2). We note that these observations include particulate nitrate in addition to HNO_3, and our model omitted nitrate in this study. Therefore, while the underestimation may be partly due to this omission, it is consistent with the higher values of HNO_3 observed in the lower and middle troposphere.

Seasonal averages of Vertical Tropospheric Columns (VTC) of NO_2 are compared with SCIAMACHY satellite data in Fig.10. The model is in line with the observations, capturing the high NO_2 values over the most polluted regions, such as Europe, US and eastern Asia. The phase in the seasonal cycle of the NO_2 columns is captured satisfactorily by the model. Throughout the year, the model tends to underestimate NO_2 VTCs in megacities, especially during the colder months, and overestimate them in rural regions. The largest discrepancies are seen in eastern China, which suggests an underestimation of emissions regionally. The biomass burning cycle is captured remarkably well, with higher NO_2 VTC in central Africa during DJF and in South America in JJA. The model is in good agreement with SCIAMACHY over the ocean, where only small differences are detected ($\pm$ 0.5 x 10^{15} molec cm^{-2}).

5.4 Ozone (O$_3$)

Tropospheric O_3 is originated from in situ photochemical production and of O_3 from the stratosphere.

19

O₃ photochemical production in the troposphere involves stratospheric intrusions. Its photochemical production involves the oxidation of CO and hydrocarbons in the presence of NO_x and sunlight. In remote areas, CO and CH_4 are the most important species oxidized during O_3 formation. In polluted areas, short-lived NMVOCs (e.g. HCHO) are present in high concentrations and are the most important species.

The simulated global burden of tropospheric O_3 is shown in Table 7. O_3 chemical sources and sinks are dominated by the tropics (171.60 Tg O_3). Lower values are predicted in the northern extratropics (101.56 Tg O_3) and especially in the southern extratropics (75.41 Tg O_3), where the presence of precursors is limited. Similar results are found in other global models such as MOZART-2 (Horowitz et al., 2003) and TM5 (Huijnen et al., 2010), with MOZART-2 having a higher and TM5 a lower global burden than our model, and both a lower burden in the southern extratropics (by 10-14 Tg O_3). Higher CO concentrations in the SH (see Table 6) might lead to excessive production of O_3 in this region. Our global tropospheric O_3 burden (348 Tg O_3) is also in good agreement with the C-IFS global model (Flemming et al., 2015), the GFDL AM3 chemistry-climate model (Naik et al., 2013a) and multi-model means (Stevenson et al., 2006; Young et al., 2013).

According to our calculations, 1201 Tg O_3 are removed from the troposphere by dry deposition, a value well above TM5 (829 Tg O_3) and MOZART-2 (857 Tg O_3) estimates, but in agreement with LMDz-INCA (1261 Tg O_3), GFDL AM3 (1205± 20) and the multi-model ensemble study by Stevenson et al. (2006) (1003 ± 200 Tg O_3). The net stratospheric input, Stratosphere-Troposphere Exchange (STE), annual rate of the model (384 Tg O_3) is also shown in Table 7. STE exchange flux is calculated as the annual balance of the ozone mass crossing the 100 hPa height. The model's STE is in good agreement with other modeling studies, especially with the multi-model ensemble in Stevenson et al. (2006) (552 ± 168 Tg O_3).

Fig.11 shows the time series of O_3 daily mean concentration averaged over all available monitoring sites (from top to bottom, WDCGG, CASTNET, EMEP and EANET) over the entire simulation period. The solid red line and solid black line represent the average of observations and the model, respectively. Bars show the 25th-75th quartile interval of all observations (orange) and model simulation (gray). There is an overall good performance although there are significant positive bias from May to October in the US and Japan. The modeled seasonal cycle agrees well with the observations, showing the highest concentrations during July-August and the lowest ones during November-December. Although the model captures the seasonal O_3 variability, it shows a tendency to overestimate concentrations during the warmer months, i.e. May-September. This positive bias is significantly higher in the US, where the overestimation occurs throughout the year (10-20 μg m^{-3}). Over Europe, the overestimation during summer is lower than in other regions. Over East Asia the model captures reasonably well the peaks in April and May, although it is

positively biased during the rest of the year. ~~In this area, concentrations during cold months are overestimated,~~, overestimating during the cold months in contrast to Europe where the model ~~concentrations agree~~ agrees with the observations. Overall the observational networks show a reduction of O_3 ~~concentrations~~ from May-June, but the model has a tendency to simulate an annual cycle with higher concentrations until July. ~~Moreover, a recent study by explains the importance of the dry deposition in controlling surface O_3~~Possible reasons for the overestimation could be the reduction of the ozone titration due to an excessive emission injection height prescribed in the model, or the dry deposition processes included in our model. Val Martin et al. (2014) shows that accurate dry deposition processes can reduce the summertime surface O_3 bias from ~~30 ppb to 14 ppb and from 13 ppb to 5 ppb over eastern U.S.~~ 60 μg m^{-3} to 28 μg m^{-3} and from 26 μg m^{-3} to 10 μg m^{-3} over eastern US and Europe, respectively. ~~Thus, part of this positive bias could be related to the dry deposition processes included in our model.~~ Further investigation is required to understand model ~~behaviour~~ behavior during this period.

Fig.12 displays the spatial statistics for O_3 over all in-situ monitoring sites using daily mean data. Areas without emissions ~~,~~ such as the ~~south pole~~ South Pole and isolated islands in the tropics ~~, have~~ show small mean biases and ~~errors~~ root mean square errors, and good correlations (>0.80). In polluted areas, a good performance is observed in the US midlands, and parts of central and southern Europe (0.60< r<0.80 and RMSE <20 μg m^{-3}). Large errors are seen in northwestern and southern US and ~~Northern~~ northern Europe. Although, large errors are seen in all the stations over Japan, the two ~~stations farthest~~ more distant stations from the main island show high correlation (r> 0.7).

In order to assess the vertical distribution of O_3, the model results are compared with available ozonesondes ~~. The seasonal vertical profiles of O_3 for both the model and observations are compared~~ in Figs.13 and ~~S5 in~~ S7 of the supplementary information ~~for the period of study~~ during the study period (see Table 3 and Fig. 1 for more details). The ~~comparison is made only when ozonesonde observations are available. Fig.13 and S5 from the supplementary information~~ figures show (from top to bottom) four panels: DJF, MAM, JJA and SON for each region. Measurements are represented by the solid red line and the model results by the solid black line. The variability of the data is shown in the form of standard deviation for both the model and ~~observations.~~

the observations. The magnitude and vertical profile ~~of O_3~~ are in good agreement with the observations. However, the model shows a positive bias of $\sim$ 5-20 ppb along the troposphere in most of the regions ~~during the entire~~ throughout the year. As shown in Sec. 5.2 there is a significant overestimation of CO, especially in the free troposphere for some regions, which may account for the positive O_3 biases, although the CO overestimation mostly occurs in the tropics where O_3 biases are not so large. Another reason for this result could be that anthropogenic aerosols and secondary aerosol formation are neglected in this simulation, leading to a higher O_3 formation in regions with more precursors. However, this should have more ~~localised~~ localized effects and therefore it cannot fully explain the biases throughout the troposphere. Possible biases in the stratospheric O_3 or the lack of other specific chemistry (e.g., halogen chemistry) could also contribute to this positive bias.

The vertical profile is in good agreement with the observations, with O_3 increasing from lower to higher tropospheric layers. In the lower-middle troposphere the model overestimates O_3 in regions with high emissions (Japan, Canada, ~~USA and W.~~US and Western Europe), a feature that ~~is more significant in DJF~~stands out in DJF (< 20 ppb). In Western Europe and the US, this bias is reduced at the surface level. In tropical areas (Equator, NH tropical and W. Pacific) the model captures well the observed

concentration and vertical structure of O_3 in the lower to middle troposphere. However, the model tends to overestimate the O_3 in the vicinity of the tropopause layer in these regions (10-20 ppb). At polar regions (NH and SH Polar) the model also presents a tendency to overestimate the vertical structure of O_3. O_3 in the tropopause layer is underestimated in the NH Polar case, and overestimated in SH Polar case.

Finally, statistics were computed to identify those areas where the errors are more important. Fig. 14 ~~,~~ shows the mean O_3 bias (left), correlation (middle) and RMSE (right) of the model with respect to ozonesondes (data is averaged between 400 and 1000 hPa ~~over the year 2004~~). As we have shown, the mean bias is positive for most stations (MB ~~<30%~~ $< 30\mu g\ m^{-3}$). Large RMSE are seen in northern high latitudes ($<50\ \mu g\ m^{-3}$) and in two stations from the US. Europe and Japan present an RMSE around $30\mu g\ m^{-3}$ and the tropics and subtropics are regions with lower errors, i.e. RMSE below $30\mu g\ m^{-3}$. The highest correlations are seen in polar regions.

6 Conclusions

~~A new global chemical transport model, NMMB/BSC-CTM, has been presented. A comprehensive description has been provided for the different components~~ We provided a comprehensive description and evaluation of the gas-phase ~~chemical module coupled online within the NMMB atmospheric driver. This model , which includes~~ chemistry component of the NMMB-MONARCH model version 1.0 at global scale. The model considers 51 chemical species ~~and~~, solves 156 reactions, and simulates the global distributions of ozone and its precursors, including CO, NO_x, and VOCs. The ~~model~~ simulation presented here ~~is~~ was configured with a horizontal resolution of ~~1~~1.4° x ~~1.4~~1°, ~~with~~ 64 vertical layers and a top of the atmosphere at 1 hPa. ~~Emissions from~~ Modeled tropospheric ozone and related tracers were evaluated for year 2004 using data from surface-monitoring stations, ozonesondes, satellite and aircraft campaigns. We used emissions from ACCMIP (Lamarque et al., 2010) ~~are considered and include~~ for fossil fuel combustion, biofuel, biomass burning, soil and oceanic emissions. Biogenic emissions are calculated online with the MEGANv2.04 model (Guenther et al., 2006). ~~In this simulation, aerosols are neglected, thus, no interaction between gas-phase and aerosol-phase is considered.~~ We note that in this contribution, we omitted aerosols and lightning emissions; anthropogenic emissions disregard seasonality; and biomass burning emissions are not specific to 2004.

~~Modelled tropospheric ozone and related tracers have been evaluated for the year 2004 and compared with surface-monitoring stations, ozonesondes, satellite and aircraft campaigns.~~

The evaluation of OH concentrations ~~shows a good~~ is in agreement with previous studies (Spivakovsky et al., 2000; Voulgarakis et al., 2013). The ~~peak concentrations of OH seen~~ OH peak concentrations occurring in April and July at northern latitudes are slightly higher than the climatological mean calculated in Spivakovsky et al. (2000). ~~This may be possibly explained by the fact that~~ Neglecting anthropogenic aerosols and secondary aerosol formation ~~are negelcted in this simulation; hence, a higher oxidized atmosphere is obtained~~ may be leading to a more oxidized atmosphere due to higher photolysis ~~when aerosols are not present~~ rates. However, overall, the widespread positive ozone biases identified seem to be responsible for the higher OH concentrations.

The global annual mean burden of CO (399 Tg) is higher than in other studies, with larger concentrations located in the tropics (229.43 Tg CO). The model is in relatively good agreement with CO observations at the surface, and shows negative biases at stations over Europe and Japan, and positive biases in Canada and Africa. The largest correlations are found in northern Europe, southern Africa and eastern Asia.

Concerning the vertical structure of CO, the model presents a good performance during the DJF and MAM, while positive biases are seen during JJA in most stations. In general, the model overestimates CO from the middle to the upper troposphere throughout the year. Significant underestimation of CO is seen in Beijing below 600 hPa, a common result in other studies which strongly suggests an underestimation of anthropogenic emissions in China. The phase and amplitude of the seasonal cycles of CO at 800 and 500 hPa in NMMB-MONARCH and MOPITT are quite similar.

Overestimations of CO are mainly located over west-central Africa, western South America, Indonesia and the surrounding Pacific and Indian oceans during the dry season. At 800 hPa, a significant negative bias is observed at northern latitudes during winter. These results are most likely related to errors in anthropogenic and biomass burning emission inventories, where the magnitude and the location of emission are not correctly represented.

Nitrogen oxide abundances are well simulated in almost all locations. Looking at the annual time series of NO_2 in Europe, the model captures the higher peaks during winter, although a positive bias is observed during summer. Nitrogen compounds are more sensitive to errors in emissions than other pollutants. We note that the emission inventory neglects seasonal variations for land-based anthropogenic emissions, and therefore we do not account for the potential reduction of NO_x emissions during summer. Over Asia, there is a negative bias of NO_x from March to August, probably due to underestimated emissions in this area. Vertical profiles of NO_x are in good agreement with the observed values, although there is some underestimation in the upper troposphere, possibly due to the lack of lightning NO_x emissions. Vertical profiles of PAN and HNO_3 were also compared with observations. Some agreement is seen in these vertical profiles, although the model has a tendency to overestimate. HNO_3 wet deposition fluxes tend to be underestimated, and are better captured in the US compared to Europe and Asia.

The comparison with observed NO_2 VTC from SCIAMACHY shows that the model reproduces the seasonality and the spatial variability reasonably well, capturing higher NO_2 over the most polluted regions. However, the results show a tendency to underestimate NO_2 VTC in megacities, especially during DJF and SON, possibly due to a negative bias in the NO_x emissions. The biomass burning cycle is well captured by the model with higher NO_2 VTC in central Africa during DJF and in South America during JJA.

The ozone burden is in good agreement with other estimates from state-of-the-art global atmospheric chemistry models. The ozone burden in the southern extratropics is higher in our model, suggesting that higher CO concentrations in the SH could lead to excessive production of ozone in this area. It seems unlikely that the positive ozone biases are

caused by too much STE. STE is in good agreement with other evaluation studies. In addition, STE has stronger effects in the upper troposphere~~, hence, the related~~ . Therefore, biases should increase with height, which is not the case in our simulations.

The surface O_3 results show a reasonable agreement with the observations, with significant positive biases from May to October in the regions of the US and Japan. Surface O_3 concentrations are very sensitive to the emissions; consequently, the variability of ozone concentrations can be enhanced by improving the spatio-temporal distribution of the ozone precursor emissions.

5   The model captures the spatial and seasonal variation ~~in observed~~ of background tropospheric O_3 profiles with a positive bias of $\sim$ ~~5-20ppb along~~ 5-20 ppb throughout the troposphere in most of the regions~~during the whole year. The~~ . The positive bias may be due to the significant overestimation of CO, especially in the free troposphere~~could be the reason for this positive ozone bias.~~ , potential biases in stratospheric O_3 or the lack of halogen and aerosol chemistry.

In summary, ~~NMMB/BSC-CTM~~ the NMMB-MONARCH provides a good overall simulation of the main species involved 10 in tropospheric chemistry, although with some caveats that we have highlighted here. Future versions of the model will ~~aim to~~ address problems identified in this study and will include the effect of aerosols in the system.

7   Code Availability

Copies of the code are readily available upon request from the corresponding authors.

References

Akimoto, H.: Global air quality and pollution, Science, pp. 1716–1719, 2003.

Arakawa, A.: Computational design for long-term numerical integration of the equations of fluid motion: Two-dimensional incompressible flow. Part I , Journal of Computational Physics, 1, 119 – 143, doi:http://dx.doi.org/10.1016/0021-9991(66)90015-5, 1966.

Ashworth, K., Wild, O., and Hewitt, C. N.: Sensitivity of isoprene emissions estimated using MEGAN to the time resolution of input climate data, Atmospheric Chemistry and Physics, 10, 1193–1201, doi:10.5194/acp-10-1193-2010, 2010.

Atkinson, R., Baulch, D. L., Cox, R. A., Crowley, J. N., Hampson, R. F., Hynes, R. G., Jenkin, M. E., Rossi, M. J., and Troe, J.: Evaluated kinetic and photochemical data for atmospheric chemistry: Volume I - gas phase reactions of O_x, HO_x, NO_x and SO_x species, Atmospheric Chemistry and Physics, 4, 1461–1738, doi:10.5194/acp-4-1461-2004, 2004.

Atlas, E. L., Ridley, B. A., and Cantrell, C. A.: The Tropospheric Ozone Production about the Spring Equinox (TOPSE) Experiment: Introduction, Journal of Geophysical Research: Atmospheres, 108, doi:10.1029/2002JD003172, 2003.

Badia, A. and Jorba, O.: Gas-phase evaluation of the online NMMB/BSC-CTM model over Europe for 2010 in the framework of the AQMEII-Phase2 project, Atmospheric Environment, doi:http://dx.doi.org/10.1016/j.atmosenv.2014.05.055, 2014.

Baklanov, A., Schlünzen, K., Suppan, P., Baldasano, J., Brunner, D., Aksoyoglu, S., Carmichael, G., Douros, J., Flemming, J., Forkel, R., Galmarini, S., Gauss, M., Grell, G., Hirtl, M., Joffre, S., Jorba, O., Kaas, E., Kaasik, M., Kallos, G., Kong, X., Korsholm, U., Kurganskiy, A., Kushta, J., Lohmann, U., Mahura, A., Manders-Groot, A., Maurizi, A., Moussiopoulos, N., Rao, S. T., Savage, N., Seigneur, C., Sokhi, R. S., Solazzo, E., Solomos, S., Sørensen, B., Tsegas, G., Vignati, E., Vogel, B., and Zhang, Y.: Online coupled regional meteorology chemistry models in Europe: current status and prospects, Atmospheric Chemistry and Physics, 14, 317–398, doi:10.5194/acp-14-317-2014, 2014.

Bergamaschi, P., Hein, R., Heimann, M., and Crutzen, P. J.: Inverse modeling of the global CO cycle: 1. Inversion of CO mixing ratios, Journal of Geophysical Research: Atmospheres, 105, 1909–1927, doi:10.1029/1999JD900818, 2000.

Betts, A. K.: A new convective adjustment scheme. Part I: Observational and theoretical basis, Quarterly Journal of the Royal Meteorological Society, 112, 677–691, doi:10.1002/qj.49711247307, 1986.

Betts, A. K. and Miller, M. J.: A new convective adjustment scheme. Part II: Single column tests using GATE wave, BOMEX, ATEX and arctic air-mass data sets, Quarterly Journal of the Royal Meteorological Society, 112, 693–709, doi:10.1002/qj.49711247308, 1986.

Bey, I., Jacob, D. J., Yantosca, R. M., Logan, J. A., Field, B. D., Fiore, A. M., Li, Q., Liu, H. Y., Mickley, L. J., and Schultz, M. G.: Global modeling of tropospheric chemistry with assimilated meteorology: Model description and evaluation, Journal of Geophysical Research: Atmospheres, 106, 23 073–23 095, doi:10.1029/2001JD000807, 2001.

Bian, H., Prather, M. J., and Takemura, T.: Tropospheric aerosol impacts on trace gas budgets through photolysis, Journal of Geophysical Research: Atmospheres, 108, n/a–n/a, doi:10.1029/2002JD002743, http://dx.doi.org/10.1029/2002JD002743, 4242, 2003.

Boersma, K. F., Eskes, H. J., and Brinksma, E. J.: Error analysis for tropospheric NO2 retrieval from space, Journal of Geophysical Research: Atmospheres, 109, n/a–n/a, doi:10.1029/2003JD003962, 2004.

Byun, D.: Fundamentals of one-atmosphere dynamics for multiscale Air Quality Modeling, Tech. rep., EPA/600/R-99/030, http://www.epa.gov/AMD/CMAQ/ch05.pdf, 1990.

Byun, D. and Ching, J.: Science algorithms of the EPA Models-3 community multiscale air quality (CMAQ) modeling system, Rep. EPA/600/R-99, 30, 1999.

Cammas, J.-P., Brioude, J., Chaboureau, J.-P., Duron, J., Mari, C., Mascart, P., Nédélec, P., Smit, H., Pätz, H.-W., Volz-Thomas, A., Stohl, A., and Fromm, M.: Injection in the lower stratosphere of biomass fire emissions followed by long-range transport: a MOZAIC case study, Atmospheric Chemistry and Physics, 9, 5829–5846, doi:10.5194/acp-9-5829-2009, 2009.

30 Cariolle, D. and Déqué, M.: Southern hemisphere medium-scale waves and total ozone disturbances in a spectral general circulation model, Journal of Geophysical Research: Atmospheres, 91, 10 825–10 846, doi:10.1029/JD091iD10p10825, 1986.

Chang, J. S., Brost, R. A., Isaksen, I. S. A., Madronich, S., Middleton, P., Stockwell, W. R., and Walcek, C. J.: A three-dimensional Eulerian acid deposition model: Physical concepts and formulation, Journal of Geophysical Research: Atmospheres, 92, 14 681–14 700, doi:10.1029/JD092iD12p14681, 1987.

35 Chipperfield, M. P.: New version of the TOMCAT/SLIMCAT off-line chemical transport model: Intercomparison of stratospheric tracer experiments, Quarterly Journal of the Royal Meteorological Society, 132, 1179–1203, doi:10.1256/qj.05.51, 2006.

Crutzen, P. J.: Photochemical reactions initiated by and influencing ozone in unpolluted tropospheric air, Tellus, 26, 47–57, doi:10.1111/j.2153-3490.1974.tb01951.x, 1974.

Damian, V., Sandu, A., Damian, M., Potra, F., and Carmichael, G. R.: The kinetic preprocessor KPP-a software environment for solving chemical kinetics , Computers and Chemical Engineering, 26, 1567 – 1579, doi:http://dx.doi.org/10.1016/S0098-1354(02)00128-X, 2002.

Deeter, M. N., Edwards, D. P., Gille, J. C., Emmons, L. K., Francis, G., Ho, S.-P., Mao, D., Masters, D., Worden, H., Drummond, J. R., and Novelli, P. C.: The MOPITT version 4 CO product: Algorithm enhancements, validation, and long-term stability, Journal of Geophysical

5 Research: Atmospheres, 115, n/a–n/a, doi:10.1029/2009JD013005, 2010.

Deeter, M. N., Martinez-Alonso, S., Edwards, D. P., Emmons, L. K., Gille, J. C., Worden, H. M., Pittman, J. V., Daube, B. C., and Wofsy, S. C.: Validation of MOPITT Version 5 thermal-infrared, near-infrared, and multispectral carbon monoxide profile retrievals for 2000-2011, Journal of Geophysical Research: Atmospheres, 118, 6710–6725, doi:10.1002/jgrd.50272, 2013.

Derwent, R., Jenkin, M., and Saunders, S.: Photochemical ozone creation potentials for a large number of reactive hydrocarbons under

10 European conditions, Atmospheric Environment, 30, 181 – 199, doi:http://dx.doi.org/10.1016/1352-2310(95)00303-G, 1996.

Ek, M. B., Mitchell, K. E., Lin, Y., Rogers, E., Grunmann, P., Koren, V., Gayno, G., and Tarpley, J. D.: Implementation of Noah land surface model advances in the National Centers for Environmental Prediction operational mesoscale Eta model, Journal of Geophysical Research: Atmospheres, 108, n/a–n/a, doi:10.1029/2002JD003296, 2003.

Elguindi, N., Clark, H., Ordóñez, C., Thouret, V., Flemming, J., Stein, O., Huijnen, V., Moinat, P., Inness, A., Peuch, V.-H., Stohl, A.,

15 Turquety, S., Athier, G., Cammas, J.-P., and Schultz, M.: Current status of the ability of the GEMS/MACC models to reproduce the tropospheric CO vertical distribution as measured by MOZAIC, Geoscientific Model Development, 3, 501–518, doi:10.5194/gmd-3-501-2010, 2010.

Emmons, L. K., Hauglustaine, D. A., Müller, J.-F., Carroll, M. A., Brasseur, G. P., Brunner, D., Staehelin, J., Thouret, V., and Marenco, A.: Data composites of airborne observations of tropospheric ozone and its precursors, Journal of Geophysical Research: Atmospheres, 105,

20 20 497–20 538, doi:10.1029/2000JD900232, 2000.

Emmons, L. K., Hess, P., Klonecki, A., Tie, X., Horowitz, L., Lamarque, J.-F., Kinnison, D., Brasseur, G., Atlas, E., Browell, E., Cantrell, C., Eisele, F., Mauldin, R. L., Merrill, J., Ridley, B., and Shetter, R.: Budget of tropospheric ozone during TOPSE from two chemical transport models, Journal of Geophysical Research: Atmospheres, 108, n/a–n/a, doi:10.1029/2002JD002665, 2003.

Emmons, L. K., Walters, S., Hess, P. G., Lamarque, J.-F., Pfister, G. G., Fillmore, D., Granier, C., Guenther, A., Kinnison, D., Laepple, T.,

25 Orlando, J., Tie, X., Tyndall, G., Wiedinmyer, C., Baughcum, S. L., and Kloster, S.: Description and evaluation of the Model for Ozone and Related chemical Tracers, version 4 (MOZART-4), Geoscientific Model Development, 3, 43–67, doi:10.5194/gmd-3-43-2010, 2010.

Fast, J. D., Gustafson, W. I., Easter, R. C., Zaveri, R. A., Barnard, J. C., Chapman, E. G., Grell, G. A., and Peckham, S. E.: Evolution of ozone, particulates, and aerosol direct radiative forcing in the vicinity of Houston using a fully coupled meteorology-chemistry-aerosol model, Journal of Geophysical Research: Atmospheres, 111, n/a–n/a, doi:10.1029/2005JD006721, 2006.

30 Fels, S. B. and Schwarzkopf, M. D.: The Simplified Exchange Approximation: A New Method for Radiative Transfer Calculations, J. Atmos. Sci., 32, 1475–1488, doi:10.1175/1520-0469(1975)032<1475:TSEAAN>2.0.CO;2, 1975.

Ferrier, B. S., Y., J., Y., L., T., B., E., R., and G., D.: Implementation of a new grid-scale cloud and precipitation scheme in the NCEP Eta model, paper presented at 15th Conference on Numerical Weather Prediction, Am. Meteorol. Soc., San Antonio, Tex., 2002.

Fischer, E. V., Jacob, D. J., Yantosca, R. M., Sulprizio, M. P., Millet, D. B., Mao, J., Paulot, F., Singh, H. B., Roiger, A., Ries, L., Talbot,

35 R., Dzepina, K., and Pandey Deolal, S.: Atmospheric peroxyacetyl nitrate (PAN): a global budget and source attribution, Atmospheric Chemistry and Physics, 14, 2679–2698, doi:10.5194/acp-14-2679-2014, 2014.

Flemming, J., Inness, A., Flentje, H., Huijnen, V., Moinat, P., Schultz, M. G., and Stein, O.: Coupling global chemistry transport models to ECMWF's integrated forecast system, Geoscientific Model Development, 2, 253–265, doi:10.5194/gmd-2-253-2009, 2009.

Flemming, J., Huijnen, V., Arteta, J., Bechtold, P., Beljaars, A., Blechschmidt, A.-M., Diamantakis, M., Engelen, R. J., Gaudel, A., Inness, A., Jones, L., Josse, B., Katragkou, E., Marecal, V., Peuch, V.-H., Richter, A., Schultz, M. G., Stein, O., and Tsikerdekis, A.: Tropospheric chemistry in the Integrated Forecasting System of ECMWF, Geoscientific Model Development, 8, 975–1003, doi:10.5194/gmd-8-975-2015, 2015.

5 Folberth, G. A., Hauglustaine, D. A., Lathière, J., and Brocheton, F.: Interactive chemistry in the Laboratoire de Météorologie Dynamique general circulation model: model description and impact analysis of biogenic hydrocarbons on tropospheric chemistry, Atmospheric Chemistry and Physics, 6, 2273–2319, doi:10.5194/acp-6-2273-2006, 2006.

Foley, K. M., Roselle, S. J., Appel, K. W., Bhave, P. V., Pleim, J. E., Otte, T. L., Mathur, R., Sarwar, G., Young, J. O., Gilliam, R. C., Nolte, C. G., Kelly, J. T., Gilliland, A. B., and Bash, J. O.: Incremental testing of the Community Multiscale Air Quality (CMAQ) modeling

10 system version 4.7, Geoscientific Model Development, 3, 205–226, doi:10.5194/gmd-3-205-2010, 2010.

Gery, M. W., Whitten, G. Z., Killus, J. P., and Dodge, M. C.: A photochemical kinetics mechanism for urban and regional scale computer modeling, Journal of Geophysical Research: Atmospheres, 94, 12 925–12 956, doi:10.1029/JD094iD10p12925, 1989.

Gong, S. L., Lavoué, D., Zhao, T. L., Huang, P., and Kaminski, J. W.: GEM-AQ/EC, an on-line global multi-scale chemical weather modelling system: model development and evaluation of global aerosol climatology, Atmospheric Chemistry and Physics, 12, 8237–8256,

15 doi:10.5194/acp-12-8237-2012, 2012.

Granier, C., Lamarque, J., Mieville, A., Muller, J., Olivier, J., Orlando, J., Peters, J., Petron, G., Tyndall, G., and Wallens, S.: POET, a database of surface emissions of ozone precursors, http://www. aero. jussieu. fr/projet/ACCENT/POET. php, 6988, 30, 2005.

Guenther, A., Karl, T., Harley, P., Wiedinmyer, C., Palmer, P. I., and Geron, C.: Estimates of global terrestrial isoprene emissions using MEGAN (Model of Emissions of Gases and Aerosols from Nature), Atmospheric Chemistry and Physics, 6, 3181–3210, doi:10.5194/acp-

20 6-3181-2006, 2006.

Hauglustaine, D. A., Brasseur, G. P., Walters, S., Rasch, P. J., Müller, J.-F., Emmons, L. K., and Carroll, M. A.: MOZART, a global chemical transport model for ozone and related chemical tracers: 2. Model results and evaluation, Journal of Geophysical Research: Atmospheres, 103, 28 291–28 335, doi:10.1029/98JD02398, 1998.

Haustein, K., Pérez, C., Baldasano, J. M., Jorba, O., S., B., Miller, R., Janjic, Z., Black, T., Nickovic, S., Todd, M., and Washington, R.:

25 Atmospheric dust modeling from meso to global scales with the online NMMB/BSC-Dust model - Part 2: Experimental campaigns in Northern Africa, Atmos. Chem. Phys., 12, 2933–2958, doi:10.5194/acp-12-2933-2012., 2012.

Hertel, O., Berkowicz, R., Christensen, J., and Øystein Hov: Test of two numerical schemes for use in atmospheric transport-chemistry models , Atmospheric Environment. Part A. General Topics, 27, 2591 – 2611, doi:http://dx.doi.org/10.1016/0960-1686(93)90032-T, 1993.

Heue, K.-P., Richter, A., Bruns, M., Burrows, J. P., v. Friedeburg, C., Platt, U., Pundt, I., Wang, P., and Wagner, T.: Validation of SCIAMACHY tropospheric NO_2-columns with AMAXDOAS measurements, Atmospheric Chemistry and Physics, 5, 1039–1051, doi:10.5194/acp-5-1039-2005, 2005.

Hilboll, A., Richter, A., Rozanov, A., Hodnebrog, Ø., Heckel, A., Solberg, S., Stordal, F., and Burrows, J. P.: Improvements to the retrieval of tropospheric NO2 from satellite–stratospheric correction using SCIAMACHY limb/nadir matching and comparison to Oslo CTM2 simulations, Atmospheric Measurement Techniques, 6, 565–584, doi:10.5194/amt-6-565-2013, 2013.

Horowitz, L. W., Walters, S., Mauzerall, D. L., Emmons, L. K., Rasch, P. J., Granier, C., Tie, X., Lamarque, J.-F., Schultz, M. G., Tyndall, G. S., Orlando, J. J., and Brasseur, G. P.: A global simulation of tropospheric ozone and related tracers: Description and evaluation of MOZART, version 2, Journal of Geophysical Research: Atmospheres, 108, doi:10.1029/2002JD002853, 2003.

Hsu, J. and Prather, M. J.: Stratospheric variability and tropospheric ozone, Journal of Geophysical Research: Atmospheres, 114, doi:10.1029/2008JD010942, 2009.

Huijnen, V., Williams, J., van Weele, M., van Noije, T., Krol, M., Dentener, F., Segers, A., Houweling, S., Peters, W., de Laat, J., Boersma, F., Bergamaschi, P., van Velthoven, P., Le Sager, P., Eskes, H., Alkemade, F., Scheele, R., Nédélec, P., and Pätz, H.: The global chemistry transport model TM5: description and evaluation of the tropospheric chemistry version 3.0, Geoscientific Model Development, 3, 445–473, doi:10.5194/gmd-3-445-2010, 2010.

Im, U., Bianconi, B., Solazzo, E., Kioutsioukis, I., Badia, A., Balzarini, A., Baró, R., Bellasio, R., Brunner, D., Chemel, C., Curci, G., Flemming, J., Forkel, R., Giordano, L., Jiménez-Guerrero, P., Hirtl, M., Hodzic, A., Honzak, L., Jorba, O., Knote, C., Kuenen, J., Makar, P., Manders-Groot, A., Neal, L., Pérez, J., Pirovano, G., Pouliot, G. San Jose, R., Savage, N., Schroder, W., Sokhi, R., Syrakov, D., Torian, A., Tuccella, R., Werhahn, J., Wolke, R., Yahya, K., Zabkar, R., Zhang, Y., Zhang, J., Hogrefe, C., and Galmarini, S.: Evaluation of operational online-coupled regional air quality models over Europe and North America in the context of AQMEII phase 2. Part I: Ozone, Atmospheric Environment, pp. –, doi:http://dx.doi.org/10.1016/j.atmosenv.2014.09.042, 2014.

Jacob, D. J., Crawford, J. H., Kleb, M. M., Connors, V. S., Bendura, R. J., Raper, J. L., Sachse, G. W., Gille, J. C., Emmons, L., and Heald, C. L.: Transport and Chemical Evolution over the Pacific (TRACE-P) aircraft mission: Design, execution, and first results, Journal of Geophysical Research: Atmospheres, 108, n/a–n/a, doi:10.1029/2002JD003276, 2003.

Jacobson, M. Z.: GATOR-GCMM: A global- through urban-scale air pollution and weather forecast model: 1. Model design and treatment of subgrid soil, vegetation, roads, rooftops, water, sea ice, and snow, Journal of Geophysical Research: Atmospheres, 106, 5385–5401, doi:10.1029/2000JD900560, 2001.

Janjic, Z.: Pressure gradient force and advection scheme used for forecasting with steep and small scale topography, Contrib. Atmos. Phys., 50, 186–199., 1977.

Janjic, Z.: Forward–backward scheme modified to prevent two–grid–interval noise and its application in sigma coordinate models., Contrib. Atmos. Phys., 52, 69–84, 1979.

Janjic, Z.: Nonlinear Advection Schemes and Energy Cascade on Semi-Staggered Grids, 112, 1234–1245, doi:doi: 10.1175/1520-0493(1984)112<1234:NASAEC>2.0.CO;2, 1984.

Janjic, Z.: The step-mountain coordinates: physical package., Monthly Weather Review, 118, 1429–1443, doi:10.1175/1520-0493(1990)118<1429:TSMCPP>2.0.CO;2, 1990.

Janjic, Z.: The Step-Mountain Eta Coordinate Model: Further Developments of the Convection, Viscous Sublayer, and Turbulence Closure Schemes, Monthly Weather Review, 122, 1994.

Janjic, Z.: Comments on Development and Evaluation of a Convection Scheme for Use in Climate Models, Journal of the Atmospheric Sciences, 57, 3686–3686, 2000.

Janjic, Z.: A nonhydrostatic model based on a new approach, Meteorology and Atmospheric Physics, 82, 271–285, 2003.

Janjic, Z. and Black, T.: A unified model approach from meso to global scales, 7, 24–29, http://meetings.copernicus.org/www.cosis.net/abstracts/EGU05/05582/EGU05-J-05582.pdf, 2005.

Janjic, Z. and Gall, I.: Scientific documentation of the NCEP nonhydrostatic multiscale model on the B grid (NMMB). Part 1 Dynamics, Tech. rep., Tech. rep., NCAR/TN-489+STR, doi:http://dx.doi.org/10.5065/D6WH2MZX10.5065/D6WH2MZX, 2012.

Janjic, Z., Gerrity Jr., J., and Nickovic, S.: An alternative approach to nonhydrostatic modeling, Monthly Weather Review, 129, 1164–1178, 2001.

Janjic, Z., Huang, H., and Lu, S.: A unified atmospheric model suitable for studying transport of mineral aerosols from meso to global scales, in: IOP Conference Series: Earth and Environmental Science, vol. 7, p. 012011, IOP Publishing, 2009.

Jorba, O., Dabdub, D., Blaszczak-Boxe, C., Pérez, C., Janjic, Z., Baldasano, J. M., Spada, M., Badia, A., and Gonçalves, M.: Potential significance of photoexcited NO_2 on global air quality with the NMMB/BSC chemical transport model, Journal of Geophysical Research: Atmospheres, 117, doi:10.1029/2012JD017730, 2012.

Jost, H.-J., Drdla, K., Stohl, A., Pfister, L., Loewenstein, M., Lopez, J. P., Hudson, P. K., Murphy, D. M., Cziczo, D. J., Fromm, M., Bui, T. P., Dean-Day, J., Gerbig, C., Mahoney, M. J., Richard, E. C., Spichtinger, N., Pittman, J. V., Weinstock, E. M., Wilson, J. C., and Xueref, I.: In-situ observations of mid-latitude forest fire plumes deep in the stratosphere, Geophysical Research Letters, 31, n/a–n/a, doi:10.1029/2003GL019253, 2004.

Labrador, L. J., von Kuhlmann, R., and Lawrence, M. G.: Strong sensitivity of the global mean OH concentration and the tropospheric oxidizing efficiency to the source of NOx from lightning, Geophysical research letters, 31, 2004.

Lamarque, J.-F., Bond, T. C., Eyring, V., Granier, C., Heil, A., Klimont, Z., Lee, D., Liousse, C., Mieville, A., Owen, B., Schultz, M. G., Shindell, D., Smith, S. J., Stehfest, E., Van Aardenne, J., Cooper, O. R., Kainuma, M., Mahowald, N., McConnell, J. R., Naik, V., Riahi, K., and van Vuuren, D. P.: Historical (1850–2000) gridded anthropogenic and biomass burning emissions of reactive gases and aerosols: methodology and application, Atmospheric Chemistry and Physics, 10, 7017–7039, doi:10.5194/acp-10-7017-2010, 2010.

Lamarque, J.-F., Shindell, D. T., Josse, B., Young, P. J., Cionni, I., Eyring, V., Bergmann, D., Cameron-Smith, P., Collins, W. J., Doherty, R., Dalsoren, S., Faluvegi, G., Folberth, G., Ghan, S. J., Horowitz, L. W., Lee, Y. H., MacKenzie, I. A., Nagashima, T., Naik, V., Plummer, D., Righi, M., Rumbold, S. T., Schulz, M., Skeie, R. B., Stevenson, D. S., Strode, S., Sudo, K., Szopa, S., Voulgarakis, A., and Zeng, G.: The Atmospheric Chemistry and Climate Model Intercomparison Project (ACCMIP): overview and description of models, simulations and climate diagnostics, Geoscientific Model Development, 6, 179–206, doi:10.5194/gmd-6-179-2013, 2013.

Lelieveld, J., Peters, W., Dentener, F. J., and Krol, M. C.: Stability of tropospheric hydroxyl chemistry, Journal of Geophysical Research: Atmospheres, 107, ACH 17–1–ACH 17–11, doi:10.1029/2002JD002272, 2002.

Marais, E. A., Jacob, D. J., Guenther, A., Chance, K., Kurosu, T. P., Murphy, J. G., Reeves, C. E., and Pye, H. O. T.: Improved model of isoprene emissions in Africa using Ozone Monitoring Instrument (OMI) satellite observations of formaldehyde: implications for oxidants and particulate matter, Atmospheric Chemistry and Physics, 14, 7693–7703, doi:10.5194/acp-14-7693-2014, 2014.

Miyazaki, K., Eskes, H. J., and Sudo, K.: Global NO_x emission estimates derived from an assimilation of OMI tropospheric NO_2 columns, Atmospheric Chemistry and Physics, 12, 2263–2288, doi:10.5194/acp-12-2263-2012, 2012.

Mlawer, E. J., Taubman, S. J., Brown, P. D., Iacono, M. J., and Clough, S. A.: Radiative transfer for inhomogeneous atmospheres: RRTM, a validated correlated-k model for the longwave, Journal of Geophysical Research: Atmospheres, 102, 16 663–16 682, doi:10.1029/97JD00237, 1997.

30 Monge-Sanz, B. M., Chipperfield, M. P., Cariolle, D., and Feng, W.: Results from a new linear O_3 scheme with embedded heterogeneous chemistry compared with the parent full-chemistry 3-D CTM, Atmospheric Chemistry and Physics, 11, 1227–1242, doi:10.5194/acp-11-1227-2011, 2011.

Monin, A. S. and Obukhov, A. M.: Osnovnye zakonomernosti turbulentnogo peremesivanija v prizemnom sloe atmosfery, Trudy geofiz. inst. AN SSSR, 24 (151), 163–187, 1954.

35 Naik, V., Horowitz, L. W., Fiore, A. M., Ginoux, P., Mao, J., Aghedo, A. M., and Levy, H.: Impact of preindustrial to present-day changes in short-lived pollutant emissions on atmospheric composition and climate forcing, Journal of Geophysical Research: Atmospheres, 118, 8086–8110, doi:10.1002/jgrd.50608, 2013a.

Naik, V., Voulgarakis, A., Fiore, A. M., Horowitz, L. W., Lamarque, J.-F., Lin, M., Prather, M. J., Young, P. J., Bergmann, D., Cameron-Smith, P. J., Cionni, I., Collins, W. J., Dalsøren, S. B., Doherty, R., Eyring, V., Faluvegi, G., Folberth, G. A., Josse, B., Lee, Y. H., MacKenzie, I. A., Nagashima, T., van Noije, T. P. C., Plummer, D. A., Righi, M., Rumbold, S. T., Skeie, R., Shindell, D. T., Stevenson, D. S., Strode, S., Sudo, K., Szopa, S., and Zeng, G.: Preindustrial to present-day changes in tropospheric hydroxyl radical and methane lifetime from the Atmospheric Chemistry and Climate Model Intercomparison Project (ACCMIP), Atmospheric Chemistry and Physics, 13, 5277–5298,

5 doi:10.5194/acp-13-5277-2013, 2013b.

Park, R. J., Pickering, K. E., Allen, D. J., Stenchikov, G. L., and Fox-Rabinovitz, M. S.: Global simulation of tropospheric ozone using the University of Maryland Chemical Transport Model (UMD-CTM): 1. Model description and evaluation, Journal of Geophysical Research: Atmospheres, 109, n/a–n/a, doi:10.1029/2003JD004266, 2004.

Pérez, C., Haustein, K., Janjic, Z., Jorba, O., Huneeus, N., Baldasano, J. M., Black, T., Basart, S., Nickovic, S., Miller, R. L., Perlwitz, J. P.,

10 Schulz, M., and Thomson, M.: Atmospheric dust modeling from meso to global scales with the online NMMB/BSC-Dust model Part 1: Model description, annual simulations and evaluation, Atmospheric Chemistry and Physics, 11, 13 001–13 027, doi:10.5194/acp-11-13001-2011, 2011.

Petritoli, A., Bonasoni, P., Giovanelli, G., Ravegnani, F., Kostadinov, I., Bortoli, D., Weiss, A., Schaub, D., Richter, A., and Fortezza, F.: First comparison between ground-based and satellite-borne measurements of tropospheric nitrogen dioxide in the Po basin, Journal of

15 Geophysical Research: Atmospheres, 109, n/a–n/a, doi:10.1029/2004JD004547, 2004.

Prather, M., Ehhalt, D., and Dentener, F.: Atmospheric chemistry and greenhouse gases in Climate Change 2001, 2001.

Prinn, R., Huang, J., Weiss, R., Cunnold, D., Fraser, P., Simmonds, P., McCulloch, A., Harth, C., Salameh, P., O'Doherty, S., Wang, R., Porter, L., and Miller, B.: Evidence for substantial variations of atmospheric hydroxyl radicals in the past two decades, Science, 292, 1882–1888, 2001.

20 Raper, J. L., Kleb, M. M., Jacob, D. J., Davis, D. D., Newell, R. E., Fuelberg, H. E., Bendura, R. J., Hoell, J. M., and McNeal, R. J.: Pacific Exploratory Mission in the Tropical Pacific: PEM-Tropics B, March-April 1999, Journal of Geophysical Research: Atmospheres, 106, 32 401–32 425, doi:10.1029/2000JD900833, 2001.

Real, E. and Sartelet, K.: Modeling of photolysis rates over Europe: impact on chemical gaseous species and aerosols, Atmospheric Chemistry and Physics, 11, 1711–1727, doi:10.5194/acp-11-1711-2011, 2011.

25 Richter, A., Burrows, J. P., Nüß, H., Granier, C., and Niemeier, U.: Increase in tropospheric nitrogen dioxide over China observed from space, Nature, 437, 129–132, 2005.

Sander, S. P., Golden, D., Kurylo, M., Moortgat, G., Wine, P., Ravishankara, A., Kolb, C., Molina, M., Finlayson-Pitts, B., Huie, R., et al.: Chemical kinetics and photochemical data for use in atmospheric studies evaluation number 15, 2006.

Sandu, A. and Sander, R.: Technical note: Simulating chemical systems in Fortran90 and Matlab with the Kinetic PreProcessor KPP-2.1, Atmospheric Chemistry and Physics, 6, 187–195, doi:10.5194/acp-6-187-2006, 2006.

Schultz, M. and Rast, S.: Emission datasets and methodologies for estimating emissions , Tech. rep., RETRO Report D1-6, http://retro.enes. org, 2007.

Schumann, U., Schlager, H., Arnold, F., Ovarlez, J., Kelder, H., Hov, O., Hayman, G., Isaksen, I. S. A., Staehelin, J., and Whitefield, P. D.: Pollution from aircraft emissions in the North Atlantic flight corridor: Overview on the POLINAT projects, Journal of Geophysical Research: Atmospheres, 105, 3605–3631, doi:10.1029/1999JD900941, 2000.

Seinfeld, J. and Pandis, S.: Atmospheric Chemistry and Physics, Wiley-Interscience, New York., 1998.

Shindell, D. T., Faluvegi, G., Stevenson, D. S., Krol, M. C., Emmons, L. K., Lamarque, J.-F., Pétron, G., Dentener, F. J., Ellingsen, K., Schultz, M. G., Wild, O., Amann, M., Atherton, C. S., Bergmann, D. J., Bey, I., Butler, T., Cofala, J., Collins, W. J., Derwent, R. G., Doherty, R. M., Drevet, J., Eskes, H. J., Fiore, A. M., Gauss, M., Hauglustaine, D. A., Horowitz, L. W., Isaksen, I. S. A., Lawrence, M. G., Montanaro, V., Müller, J.-F., Pitari, G., Prather, M. J., Pyle, J. A., Rast, S., Rodriguez, J. M., Sanderson, M. G., Savage, N. H., Strahan, S. E., Sudo, K., Szopa, S., Unger, N., van Noije, T. P. C., and Zeng, G.: Multimodel simulations of carbon monoxide: Comparison with observations and projected near-future changes, Journal of Geophysical Research: Atmospheres, 111, n/a–n/a, doi:10.1029/2006JD007100, 2006.

Singh, H. B. and Hanst, P. L.: Peroxyacetyl nitrate (PAN) in the unpolluted atmosphere: An important reservoir for nitrogen oxides, Geophysical Research Letters, 8, 941–944, doi:10.1029/GL008i008p00941, 1981.

Spada, M., Jorba, O., Pérez García-Pando, C., Janjic, Z., and Baldasano, J. M.: Modeling and evaluation of the global sea-salt aerosol distribution: sensitivity to size-resolved and sea-surface temperature dependent emission schemes, Atmospheric Chemistry and Physics, 13, 11 735–11 755, doi:10.5194/acp-13-11735-2013, 2013.

Spada, M., Jorba, O., García-Pando, C. P., Janjic, Z., and Baldasano, J.: On the evaluation of global sea-salt aerosol models at coastal/orographic sites, Atmospheric Environment, 101, 41 – 48, doi:http://dx.doi.org/10.1016/j.atmosenv.2014.11.019, 2015.

Spada, M., Jorba, O., Pérez García-Pando, C., Tsigaridis, K., Soares, J., and Janjic, Z.: Global aerosols in the online multiscale NMMB/BSC Chemical Transport Model, in prep.

Spivakovsky, C. M., Logan, J. A., Montzka, S. A., Balkanski, Y. J., Foreman-Fowler, M., Jones, D. B. A., Horowitz, L. W., Fusco, A. C., Brenninkmeijer, C. A. M., Prather, M. J., Wofsy, S. C., and McElroy, M. B.: Three-dimensional climatological distribution of tropospheric OH: Update and evaluation, Journal of Geophysical Research: Atmospheres, 105, 8931–8980, doi:10.1029/1999JD901006, 2000.

Stein, O., Schultz, M. G., Bouarar, I., Clark, H., Huijnen, V., Gaudel, A., George, M., and Clerbaux, C.: On the wintertime low bias of Northern Hemisphere carbon monoxide found in global model simulations, Atmospheric Chemistry and Physics, 14, 9295–9316, doi:10.5194/acp-14-9295-2014, 2014.

Stevenson, D. S., Dentener, F. J., Schultz, M. G., Ellingsen, K., van Noije, T. P. C., Wild, O., Zeng, G., Amann, M., Atherton, C. S., Bell, N., Bergmann, D. J., Bey, I., Butler, T., Cofala, J., Collins, W. J., Derwent, R. G., Doherty, R. M., Drevet, J., Eskes, H. J., Fiore, A. M., Gauss, M., Hauglustaine, D. A., Horowitz, L. W., Isaksen, I. S. A., Krol, M. C., Lamarque, J.-F., Lawrence, M. G., Montanaro, V., Müller, J.-F., Pitari, G., Prather, M. J., Pyle, J. A., Rast, S., Rodriguez, J. M., Sanderson, M. G., Savage, N. H., Shindell, D. T., Strahan, S. E., Sudo, K., and Szopa, S.: Multimodel ensemble simulations of present-day and near-future tropospheric ozone, Journal of Geophysical Research: Atmospheres, 111, n/a–n/a, doi:10.1029/2005JD006338, 2006.

Stohl, A., Bonasoni, P., Cristofanelli, P., Collins, W., Feichter, J., Frank, A., Forster, C., Gerasopoulos, E., Gäggeler, H., James, P., Kentarchos, T., Kromp-Kolb, H., Krüger, B., Land, C., Meloen, J., Papayannis, A., Priller, A., Seibert, P., Sprenger, M., Roelofs, G. J., Scheel, H. E., Schnabel, C., Siegmund, P., Tobler, L., Trickl, T., Wernli, H., Wirth, V., Zanis, P., and Zerefos, C.: Stratosphere-troposphere exchange: A review, and what we have learned from STACCATO, Journal of Geophysical Research: Atmospheres, 108, n/a–n/a, doi:10.1029/2002JD002490, 2003.

Tang, Y., M. J., Lu, S., Black, T. and, J. Z., Iredell, M., Perez, C., and O., J.: Recent status of NEMS/NMMB-AQ development, paper presented at 8th Annual CMAS Conference, U.S. Environ. Prot. Agency, Chapel Hill, N. C., 2009.

Thompson, A. M., Witte, J. C., McPeters, R. D., Oltmans, S. J., Schmidlin, F. J., Logan, J. A., Fujiwara, M., Kirchhoff, V. W. J. H., Posny, F., Coetzee, G. J. R., Hoegger, B., Kawakami, S., Ogawa, T., Johnson, B. J., Vömel, H., and Labow, G.: Southern Hemisphere Additional Ozonesondes (SHADOZ) 1998–2000 tropical ozone climatology 1. Comparison with Total Ozone Mapping Spectrometer (TOMS) and ground-based measurements, Journal of Geophysical Research: Atmospheres, 108, doi:10.1029/2001JD000967, 2003a.

Thompson, A. M., Witte, J. C., Oltmans, S. J., Schmidlin, F. J., Logan, J. A., Fujiwara, M., Kirchhoff, V. W. J. H., Posny, F., Coetzee, G. J. R., Hoegger, B., Kawakami, S., Ogawa, T., Fortuin, J. P. F., and Kelder, H. M.: Southern Hemisphere Additional Ozonesondes (SHADOZ) 1998–2000 tropical ozone climatology 2. Tropospheric variability and the zonal wave-one, Journal of Geophysical Research: Atmospheres, 108, doi:10.1029/2002JD002241, 2003b.

Tie, X., Zhang, R., Brasseur, G., Emmons, L., and Lei, W.: Effects of lightning on reactive nitrogen and nitrogen reservoir species in the troposphere, Journal of Geophysical Research: Atmospheres, 106, 3167–3178, doi:10.1029/2000JD900565, 2001.

Tie, X., Zhang, R., Brasseur, G., and Lei, W.: Global NO_x Production by Lightning, Journal of Atmospheric Chemistry, 43, 61–74, doi:10.1023/A:1016145719608, 2002.

Tilmes, S., Lamarque, J.-F., Emmons, L. K., Conley, A., Schultz, M. G., Saunois, M., Thouret, V., Thompson, A. M., Oltmans, S. J., Johnson, B., and Tarasick, D.: Technical Note: Ozonesonde climatology between 1995 and 2011: description, evaluation and applications, Atmospheric Chemistry and Physics, 12, 7475–7497, doi:10.5194/acp-12-7475-2012, 2012.

Turquety, S., Clerbaux, C., Law, K., Coheur, P.-F., Cozic, A., Szopa, S., Hauglustaine, D. A., Hadji-Lazaro, J., Gloudemans, A. M. S., Schrijver, H., Boone, C. D., Bernath, P. F., and Edwards, D. P.: CO emission and export from Asia: an analysis combining complementary satellite measurements (MOPITT, SCIAMACHY and ACE-FTS) with global modeling, Atmospheric Chemistry and Physics, 8, 5187–5204, doi:10.5194/acp-8-5187-2008, 2008.

Val Martin, M., Heald, C. L., and Arnold, S. R.: Coupling dry deposition to vegetation phenology in the Community Earth System Model: Implications for the simulation of surface O_3, Geophysical Research Letters, 41, 2988–2996, doi:10.1002/2014GL059651, 2014.

Van Aardenne, J. A., Dentener, F. J., Olivier, J. G. J., and Peters, J. A. H. W.: The EDGAR 3.2 Fast Track 2000 dataset (32FT2000), Tech. rep., http://www.mnp.nl/edgar/model/v32ft2000edgar/docv32ft20, 2005.

Voulgarakis, A., Naik, V., Lamarque, J.-F., Shindell, D. T., Young, P. J., Prather, M. J., Wild, O., Field, R. D., Bergmann, D., Cameron-Smith, P., Cionni, I., Collins, W. J., Dalsøren, S. B., Doherty, R. M., Eyring, V., Faluvegi, G., Folberth, G. A., Horowitz, L. W., Josse, B., MacKenzie, I. A., Nagashima, T., Plummer, D. A., Righi, M., Rumbold, S. T., Stevenson, D. S., Strode, S. A., Sudo, K., Szopa, S., and Zeng, G.: Analysis of present day and future OH and methane lifetime in the ACCMIP simulations, Atmospheric Chemistry and Physics, 13, 2563–2587, doi:10.5194/acp-13-2563-2013, 2013.

Vukovic, A., Rajkovic, B., and Janjic, Z.: Land ice sea surface model: Short description and verification, paper presented at 2010 International Congress on Environmental Modelling and Software Modelling for Environment's Sake, Int. Environ. Modell. and Software Soc., Ottaw, 2010.

1065 Wesely, M.: Parameterization of surface resistances to gaseous dry deposition in regional-scale numerical models , Atmospheric Environment (1967), 23, 1293 – 1304, doi:http://dx.doi.org/10.1016/0004-6981(89)90153-4, 1989.

Wesely, M. and Hicks, B.: A review of the current status of knowledge on dry deposition, Atmospheric Environment, 34, 2261 – 2282, doi:http://dx.doi.org/10.1016/S1352-2310(99)00467-7, 2000.

WHO: Ambient (outdoor) air quality and health, http://www.who.int/mediacentre/factsheets/fs313/en/, 2014.

1070 Wild, O., Zhu, X., and Prather, M. J.: Fast-J: Accurate Simulation of In- and Below-Cloud Photolysis in Tropospheric Chemical Models, Journal of Atmospheric Chemistry, 37, 245–282, doi:10.1023/A:1006415919030, 2000.

Wotawa, G., Novelli, P. C., Trainer, M., and Granier, C.: Inter-annual variability of summertime CO concentrations in the Northern Hemisphere explained by boreal forest fires in North America and Russia, Geophysical Research Letters, 28, 4575–4578, doi:10.1029/2001GL013686, 2001.

1075 Yarwood, G., Rao, S., Yocke, M., and Whitten, G.: Updates to the Carbon Bond Chemical Mechanism: CB05. Final Report to the US EPA, RT-0400675, http://www.camx.com/publ/pdfs/CB05_Final_Report_120805.pdf, 2005.

Young, P. J., Archibald, A. T., Bowman, K. W., Lamarque, J.-F., Naik, V., Stevenson, D. S., Tilmes, S., Voulgarakis, A., Wild, O., Bergmann, D., Cameron-Smith, P., Cionni, I., Collins, W. J., Dalsøren, S. B., Doherty, R. M., Eyring, V., Faluvegi, G., Horowitz, L. W., Josse, B., Lee, Y. H., MacKenzie, I. A., Nagashima, T., Plummer, D. A., Righi, M., Rumbold, S. T., Skeie, R. B., Shindell, D. T., Strode, S. A., Sudo, K.,

1080 Szopa, S., and Zeng, G.: Pre-industrial to end 21st century projections of tropospheric ozone from the Atmospheric Chemistry and Climate Model Intercomparison Project (ACCMIP), Atmospheric Chemistry and Physics, 13, 2063–2090, doi:10.5194/acp-13-2063-2013, 2013.

Zhang, Y.: Online-coupled meteorology and chemistry models: history, current status, and outlook, Atmospheric Chemistry and Physics, 8, 2895–2932, doi:10.5194/acp-8-2895-2008, 2008.

Zilitinkevich, S.: Bulk characteristics of turbulence in the atmospheric planetary boundary layer, Tr. GGO, 167, 49–52, 1965.
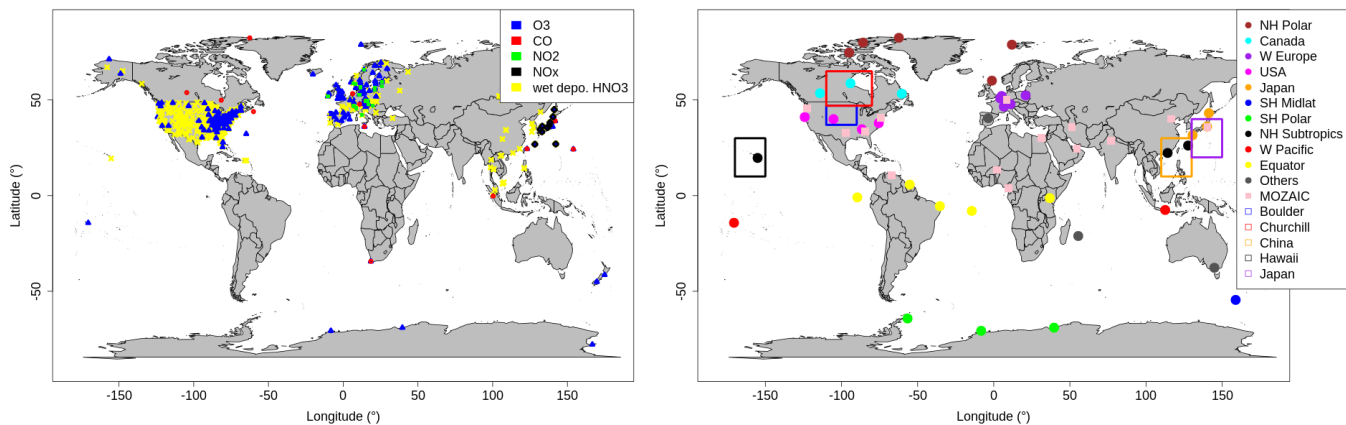
Figure 1. Stations used for the evaluation of the ~~NMMB/BSC-CTM~~ NMMB-MONARCH model. On the left, surface-monitoring rural stations of O_3 (blue triangle), CO (red circle), NO_2 (green square cross) and $NO_{~~x~~ x}$ (black diamond) are shown. Moreover, wet deposition of HNO_3 measurement locations (yellow cross) ~~measurement locations~~ are presented. On the right, locations of the ~~different~~ ozonesondes used ~~(O_3 vertical profiles)~~ are shown. ~~Ozonesonde~~ Ozonesondes are grouped by the following regions: NH Polar (brown circle), Canada (cyan circle), W. Europe (purple circle), ~~USA~~ US (pink circle), Japan (orange circle), SH Midlat (blue circle), SH Polar (green circle), NH Subtropics (black circle), W. Pacific (red circle), Equator (yellow circle) and Others (~~grey~~ gray circle). In addition, CO vertical profiles from the aircraft campaign MOZAIC (pink square) are presented. Finally, large rectangles show areas for the climatology analysis (NO_x, PAN and HNO_3) ~~of~~ for Boulder (blue), Churchill (red), China (orange), Hawaii (black) and Japan (purple).
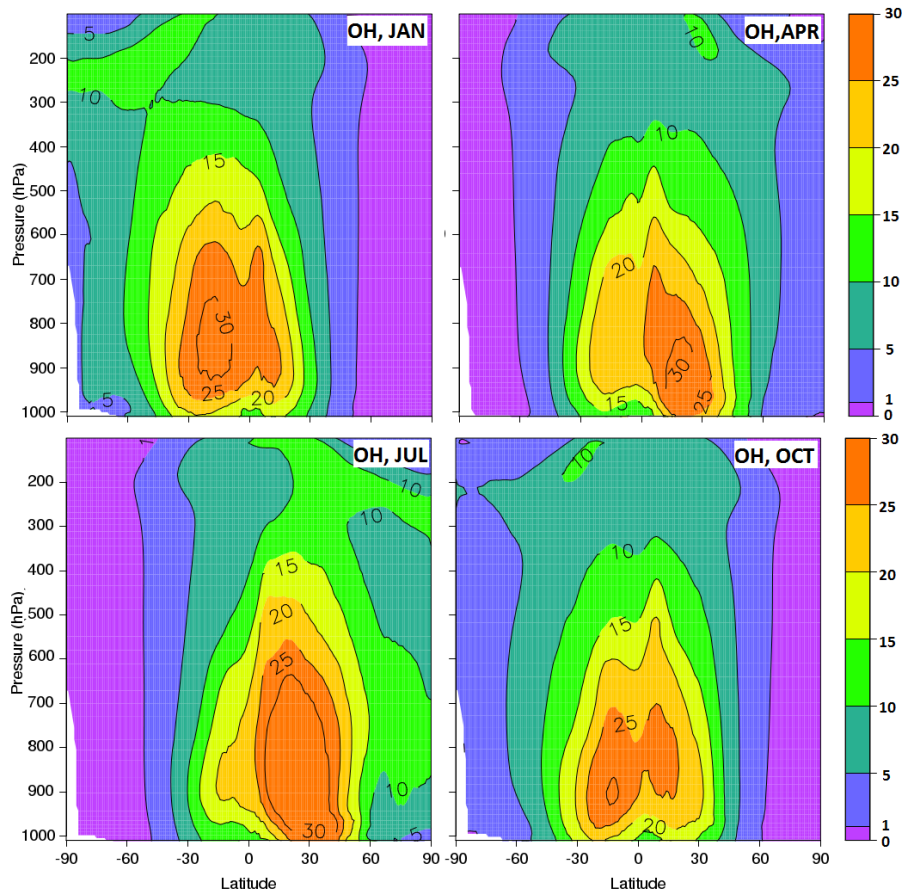
Figure 2. Zonally monthly mean OH concentrations (10^5 ~~molecules /~~ molec cm^{-3}) for January, April, July and October by the ~~NMMB/BSC-CTM~~ NMMB-MONARCH model.
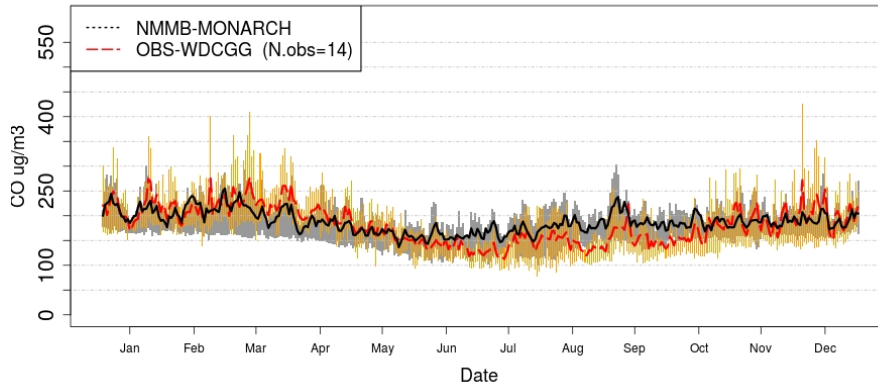
Figure 3. Time series of CO daily mean concentration in μg m^{-3} ~~,~~ averaged over all the rural WDCGG stations used. Observations are ~~in~~ depicted with a solid red line and model data ~~in~~ with a solid black line. Bars show the 25th-75th quartile interval for observations (orange bars) and ~~for the~~ model ~~simulation~~ (~~grey~~ gray bars).

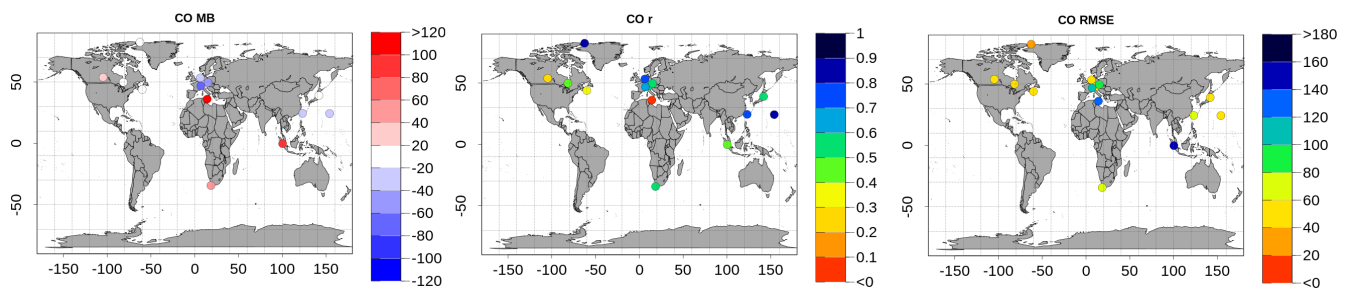**Figure 4.** CO spatial distribution of mean bias (MB, $\mu g\ m^{-3}$) (left panel), correlation (r) (middle panel) and root mean square error (RMSE, μg m^{-3}) (right panel) at all the rural WDCGG stations used.

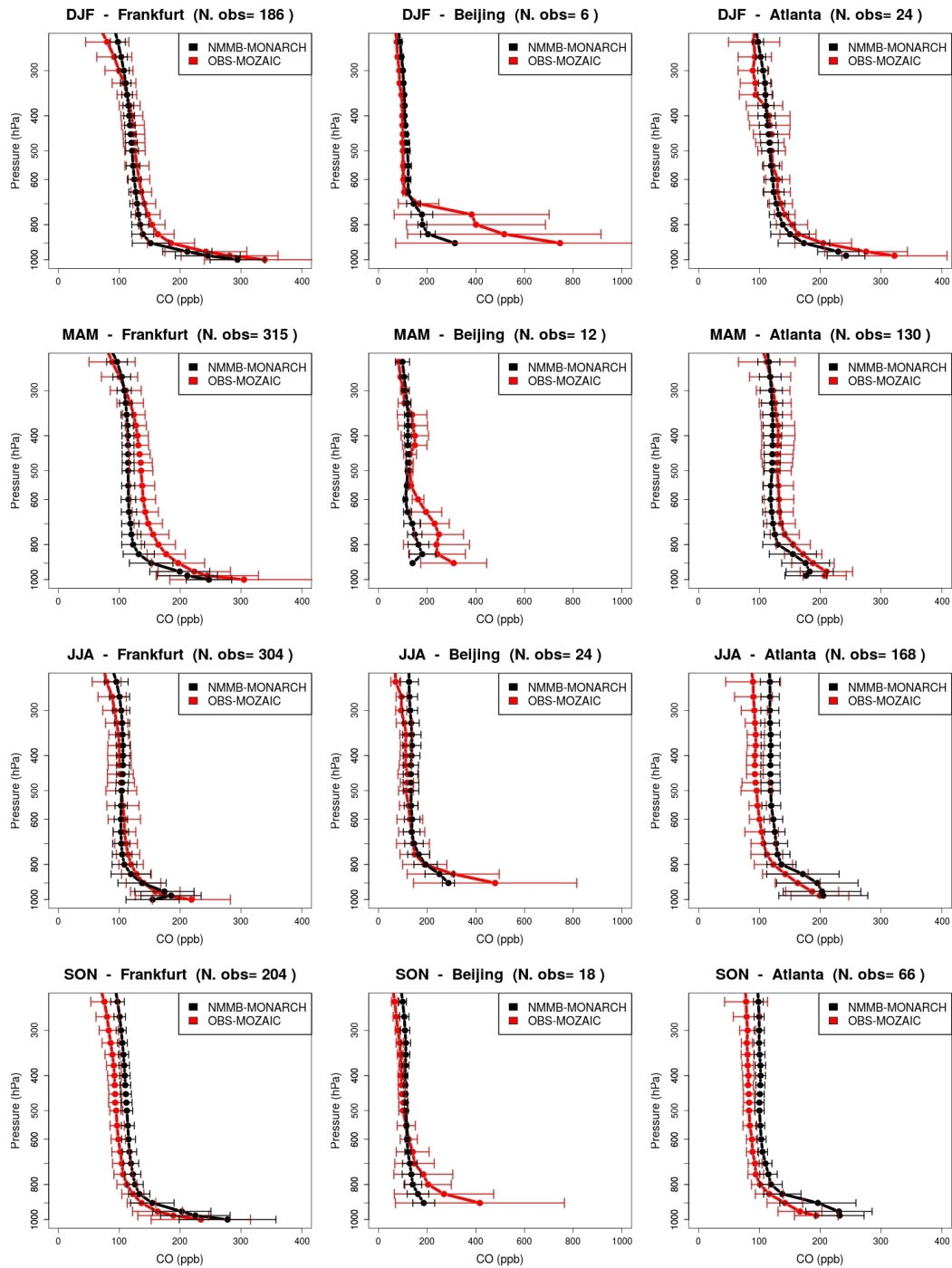**Figure 5.** CO vertical profile seasonal averages over Frankfurt, Beijing and Atlanta (from left to right) for ~~the whole~~ year ~~2004.~~ 2004 from MOZAIC. Observations ~~are in~~ depicted with a solid red line and model ~~data in~~ with a solid black line. Horizontal lines show the standard deviations. The number of ~~observations~~ flights is ~~given~~ provided on the top of each plot.

37
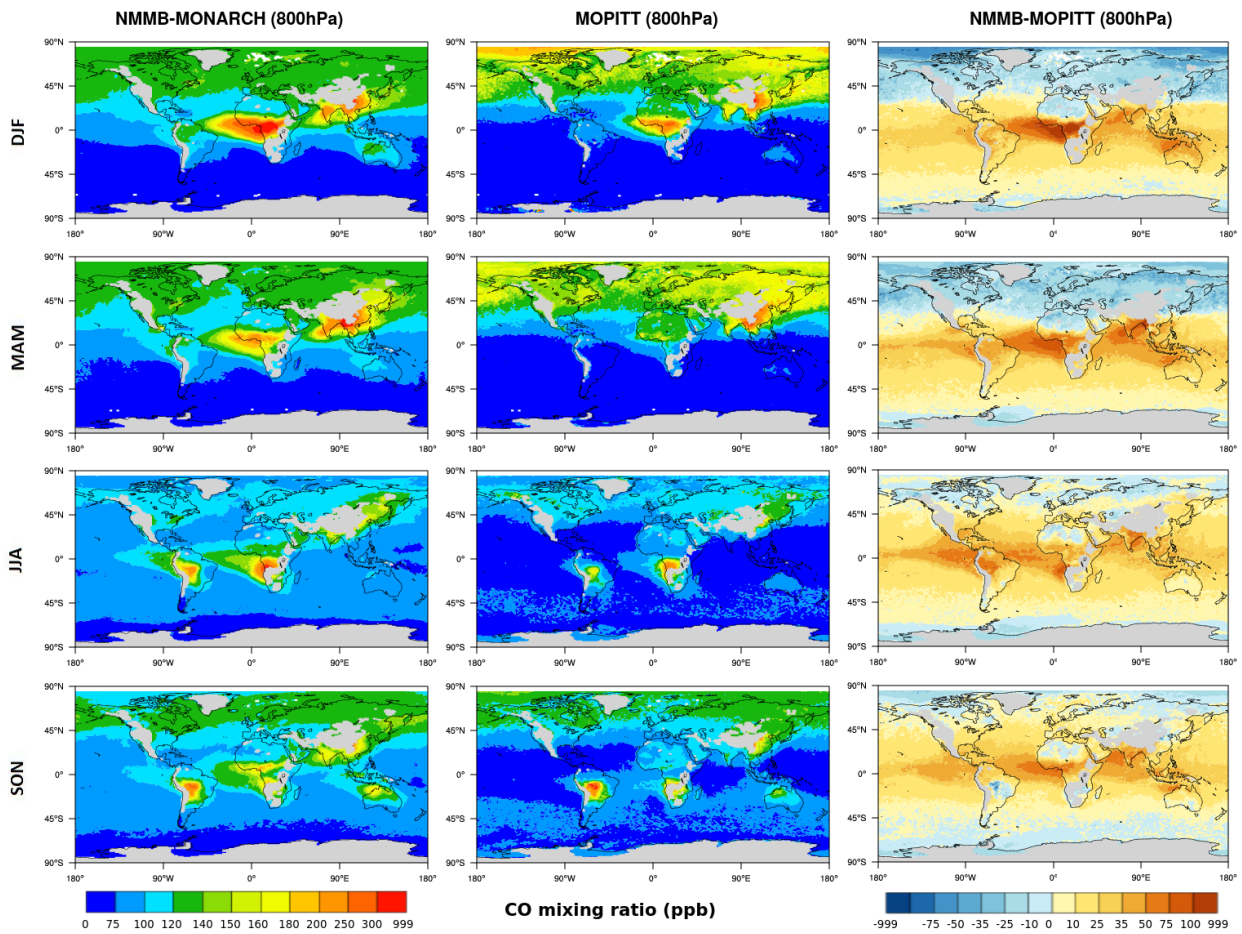
Figure 6. Comparison of ~~modelled NMMB/BSC-CTM~~ modeled CO mixing ratio at 800 hPa against satellite data (MOPITT) ~~for (from in ppb. From~~ top ~~) (to bottom:~~ DJF for December-January-February, MAM for March-April-May, JJA for June-July-August and SON for September-October-November ~~)~~ for ~~the whole~~ year ~~2004 in ppb. NMMB/BSC-CTM~~ 2004. NMMB-MONARCH data is displayed in the left panel, MOPITT data in the middle panel and the bias in the right panel.

Figure 7. Time series of NO$_2$ (top) and NO$_x$ (bottom) daily mean concentration averaged over ~~all~~ the rural EMEP and EANET stations, respectively, ~~used~~ in μg m^{-3}. Observations are ~~in~~ depicted with a solid red line and model data ~~in~~ with a solid black line. Bars ~~show~~ indicate the 25th-75th quartile interval for observations (orange bars) and ~~for~~ model ~~simulation~~ (~~grey~~ gray bars).

Figure 8. NO$_2$ (top) NO$_x$ (bottom) and spatial distribution of mean bias (MB, μg m^{-3}) (left panel) , correlation (r) (middle panel) and root mean square error (RMSE, μg m^{-3}) (right panel) at all rural EMEP and EANET stations, respectively, stations used.
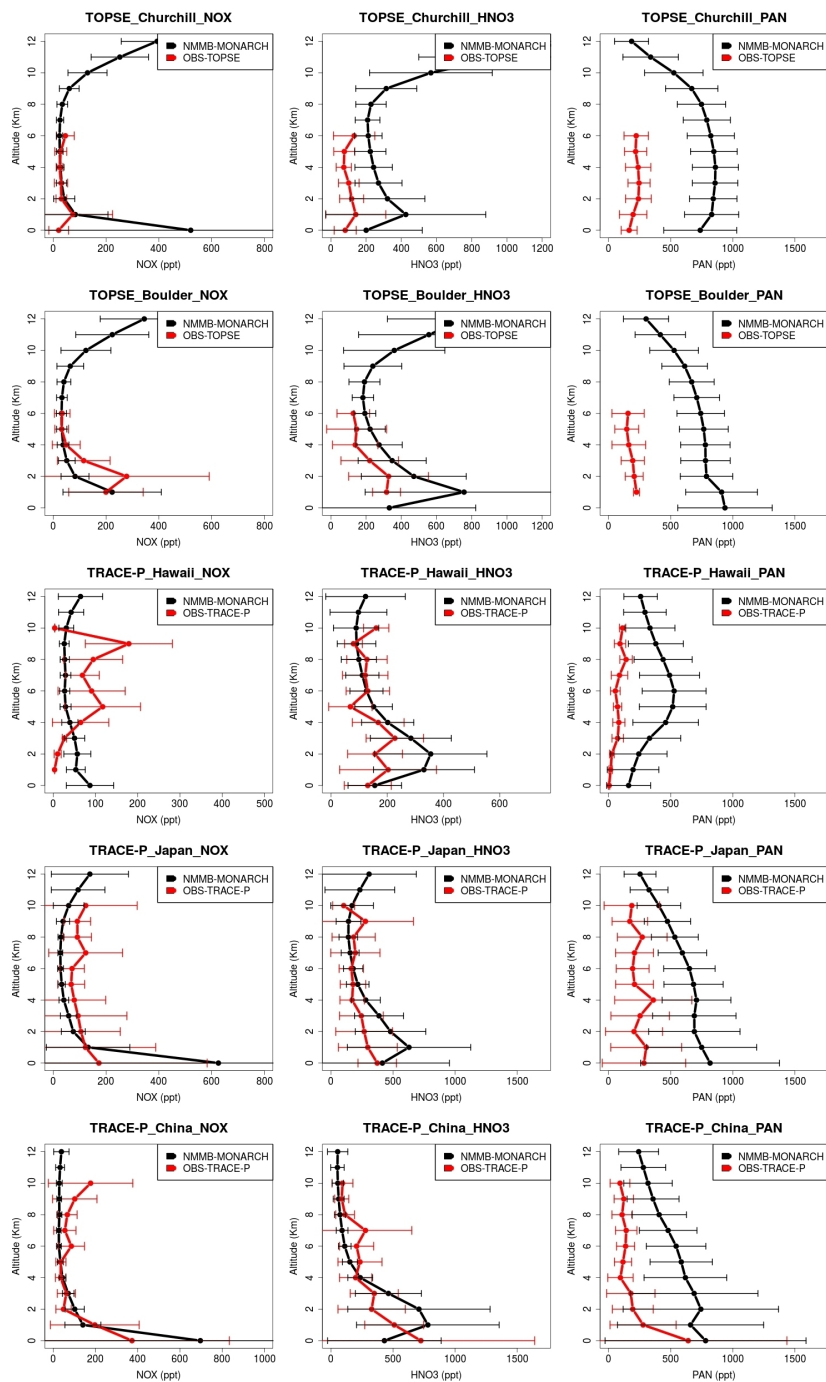
Figure 9. Comparison of modeled (black lines) and observed (red lines) vertical profiles of NO$_x$ (first column), HNO$_3$ (second column) and PAN (third column) for several regions in the US, China, Hawaii and Japan. Horizontal lines show the standard deviations.
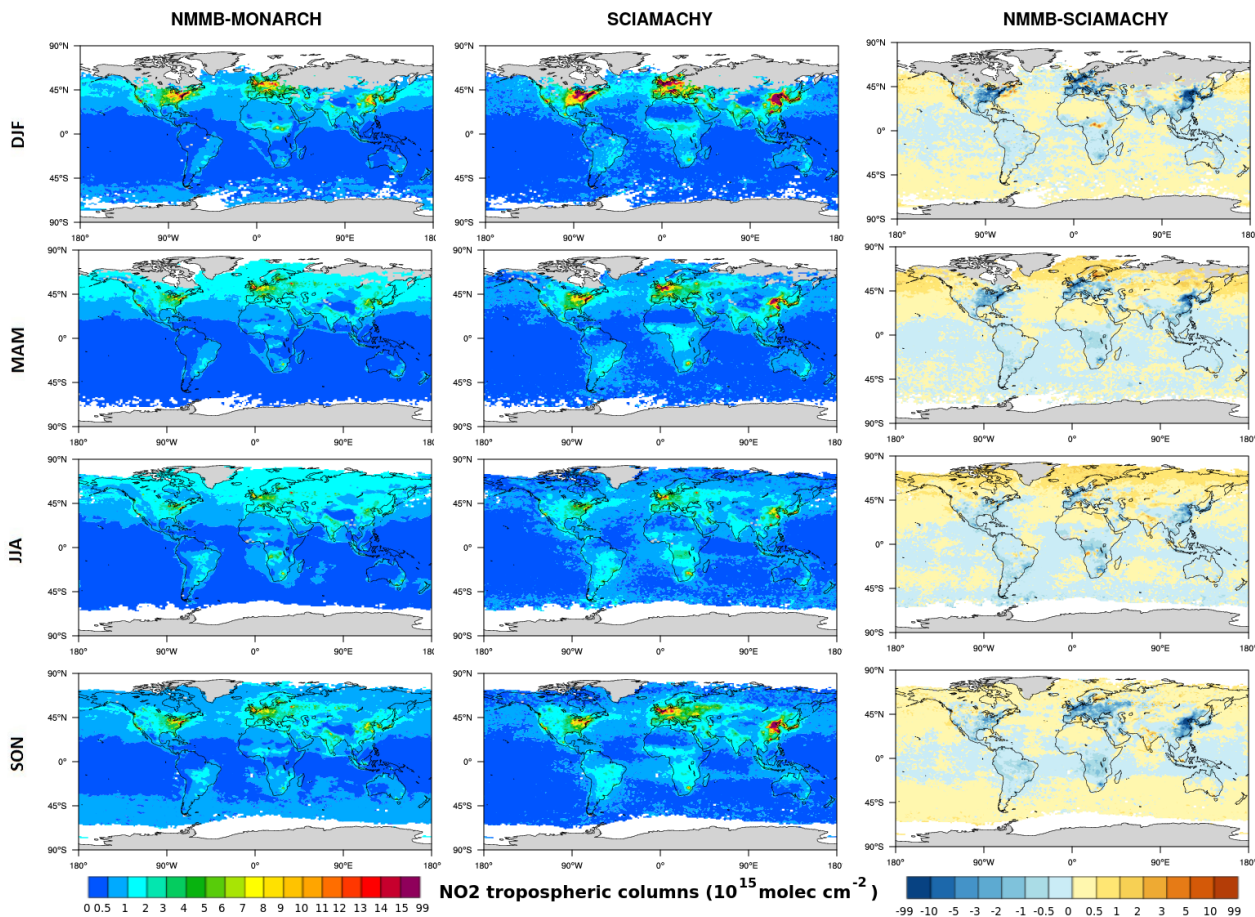
Figure 10. Comparison of ~~modelled NMMB/BSC-CTM~~ modeled NMMB-MONARCH NO$_2$ vertical tropospheric columns against satellite data (SCIAMACHY) ~~for (from~~ in 10^{15}molec cm^{-2}. From top ~~)~~ to bottom DJF, MAM, JJA, and SON for ~~the entire~~ year ~~2004 in 1e^{15}molec/cm^2. NMMB/BSC-CTM~~ 2004. NMMB-MONARCH data is displayed in the left panel, SCIAMACHY data in the middle panel and the bias in the right panel.
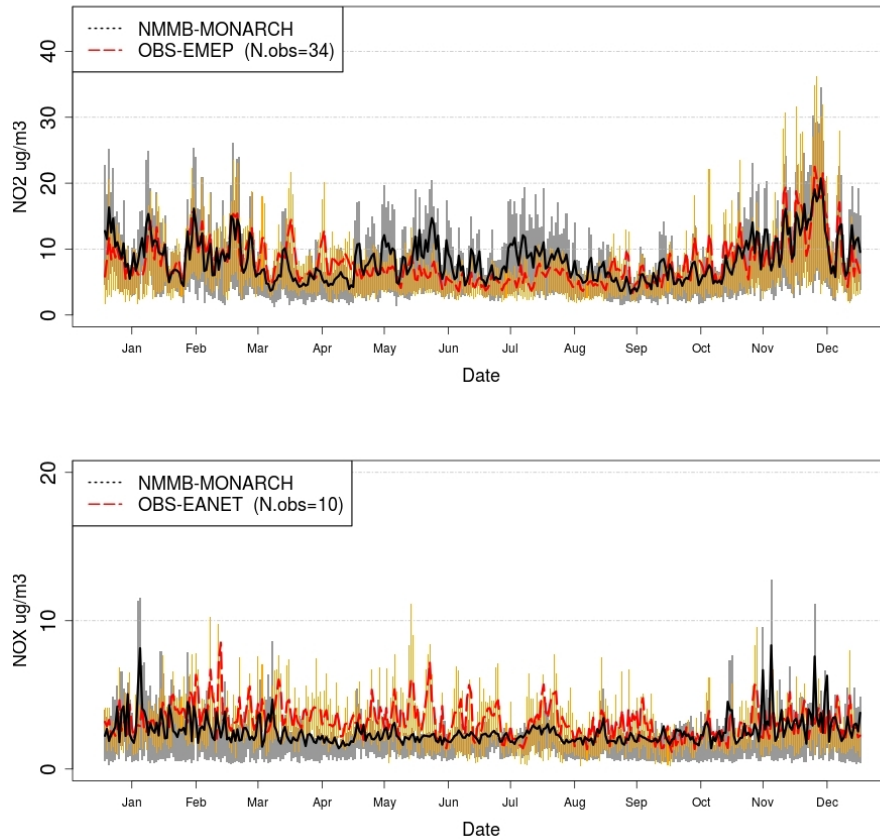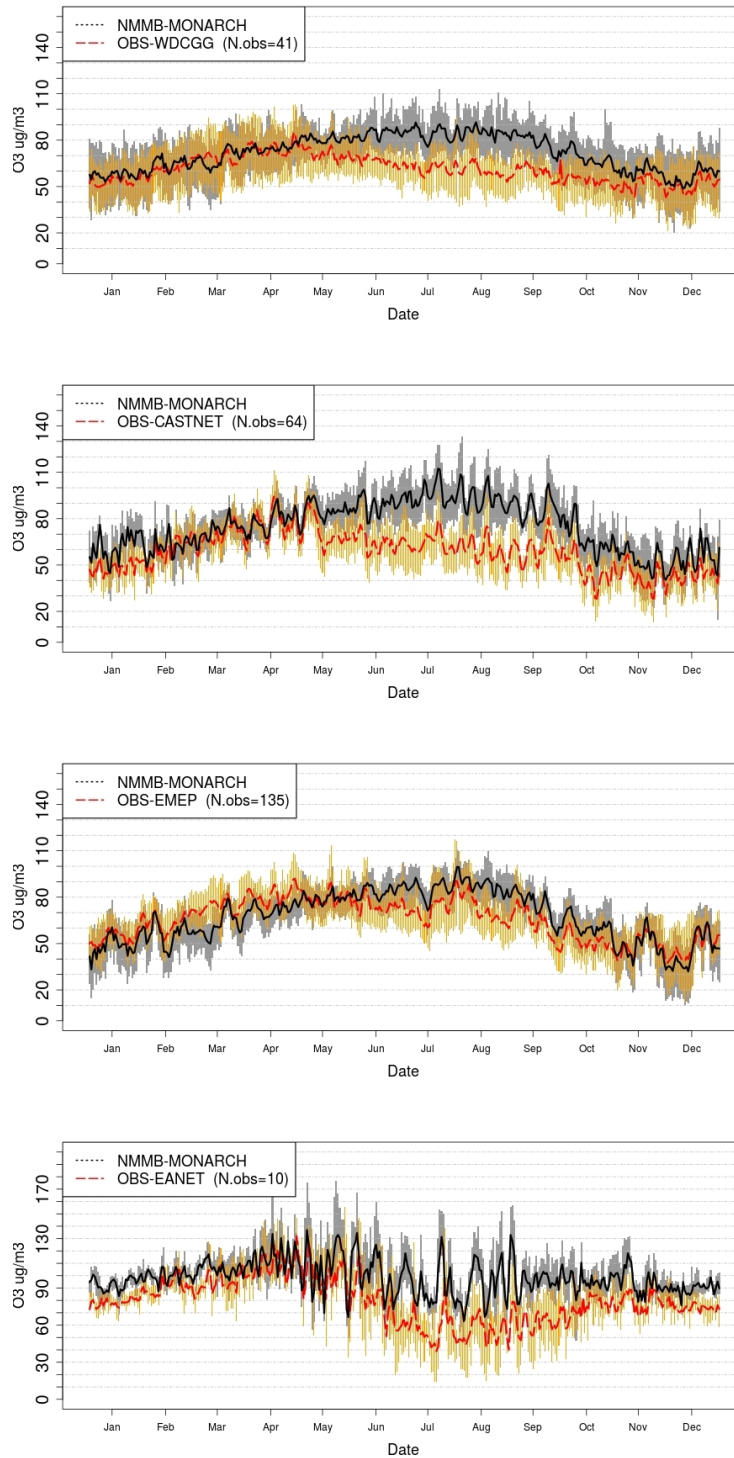
Figure 11. Time series of O$_3$ daily mean concentration averaged over ~~all the~~ rural WDCGG, CASTNET, EMEP and EANET stations (from top to bottom) ~~used~~ in μg m^{-3}. Observations are ~~in~~ depicted with a solid red line and model data ~~in~~ with a solid black line. Bars ~~show~~ indicate the 25th-75th quartile interval for observations (orange bars) and ~~for~~ model ~~simulation~~ (~~grey~~ gray bars).
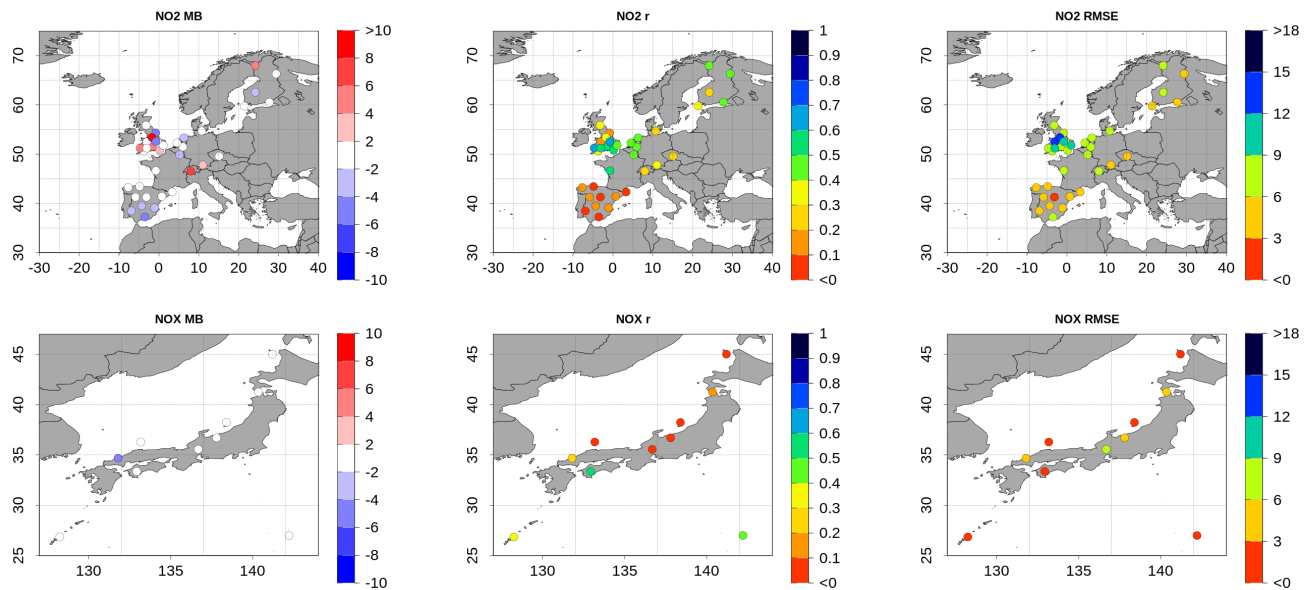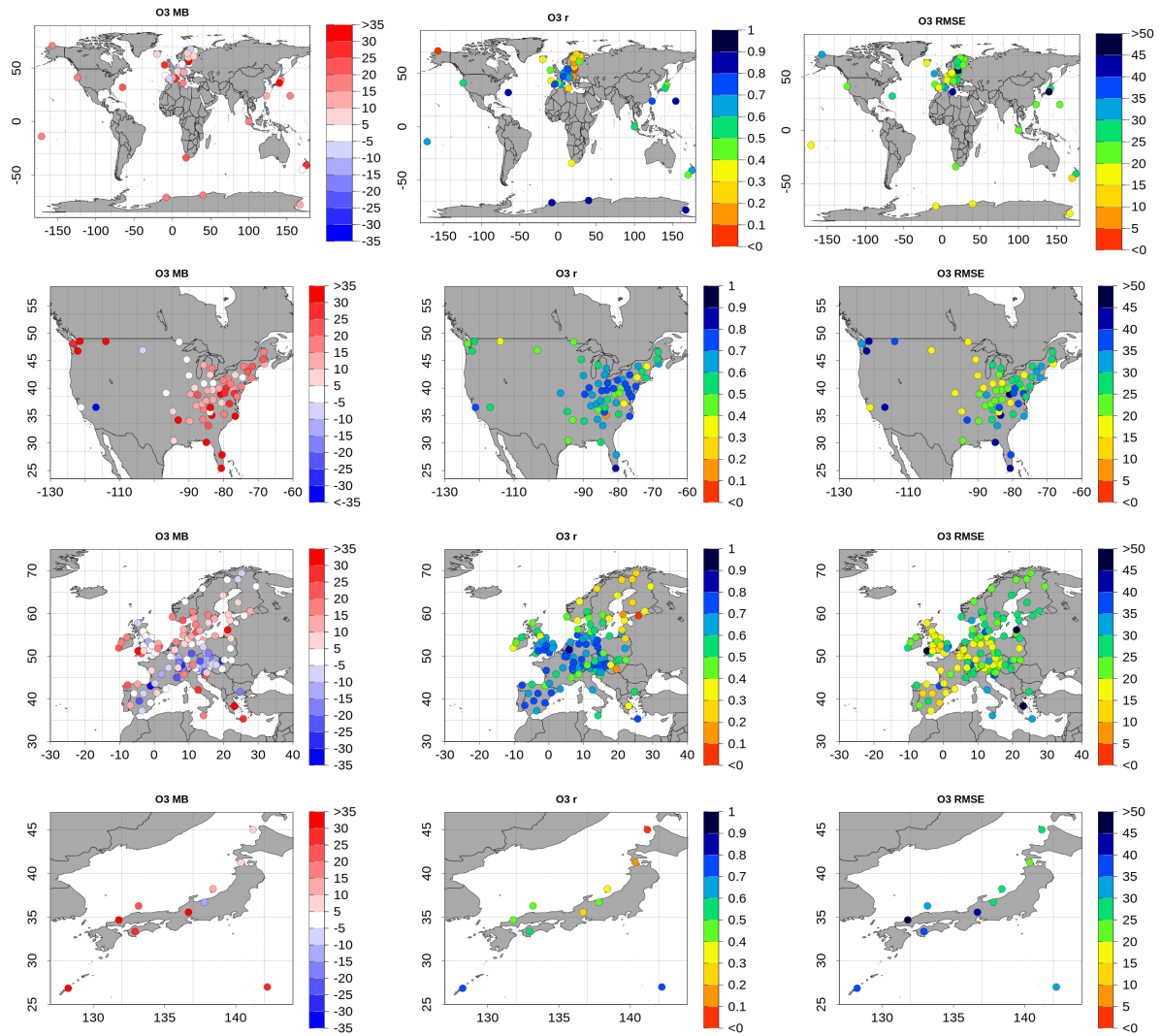
Figure 12. ~~O₃ spatial~~ Spatial distribution of ~~the~~ O₃ mean bias (MB, $\mu g\ m^{-3}$) (left panel), correlation (r) (middle panel) and root mean square error (RMSE, $\mu g\ m^{-3}$) (right panel) at ~~all~~ rural WDCGG, CASTNET, EMEP and EANET stations (from top to bottom)~~stations used~~.
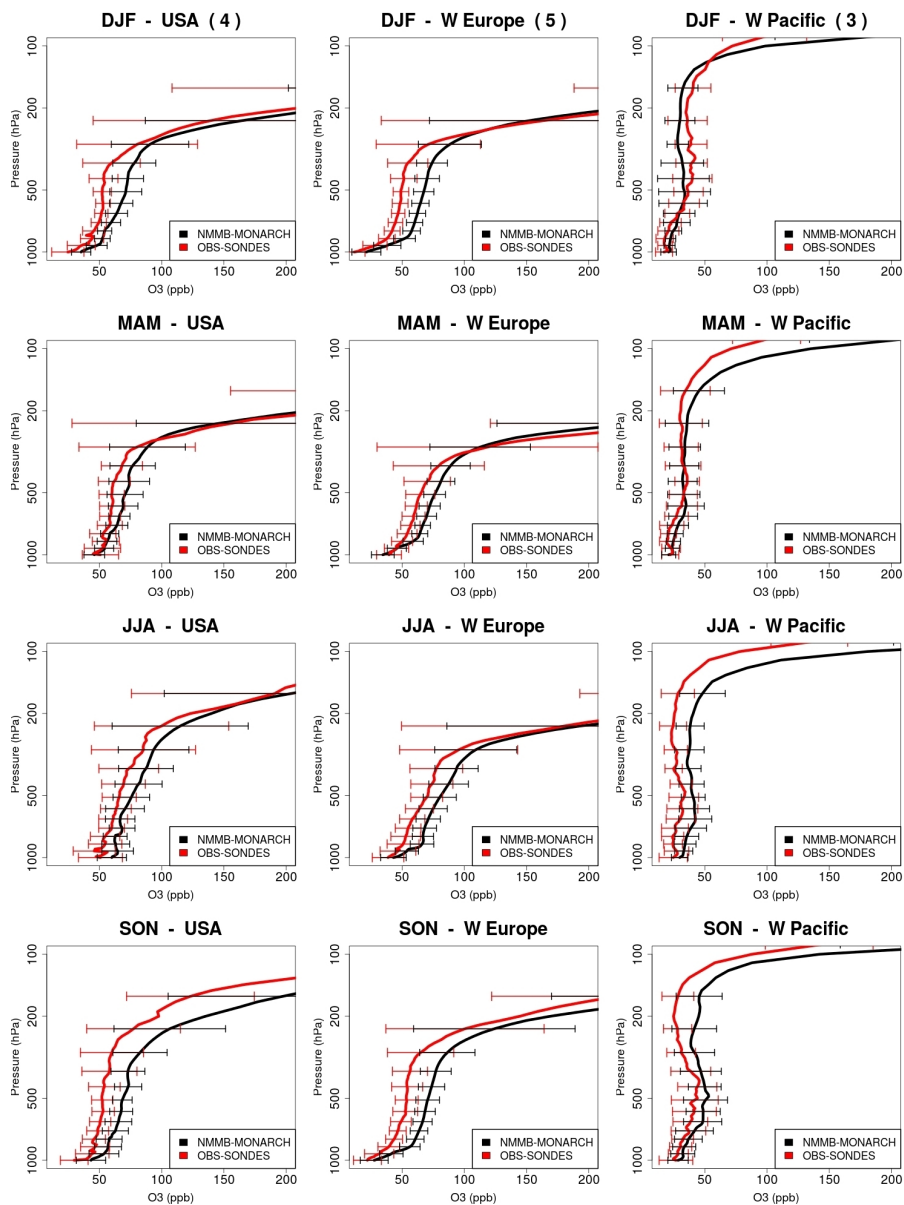
Figure 13. Comparison of ozonesonde measurements (red lines) and simulated (black lines) seasonal vertical profiles of O$_3$ (ppb) and standard deviations (horizontal lines). The region name and the number of stations ~~, using brackets,~~ are given above each plot between brackets.
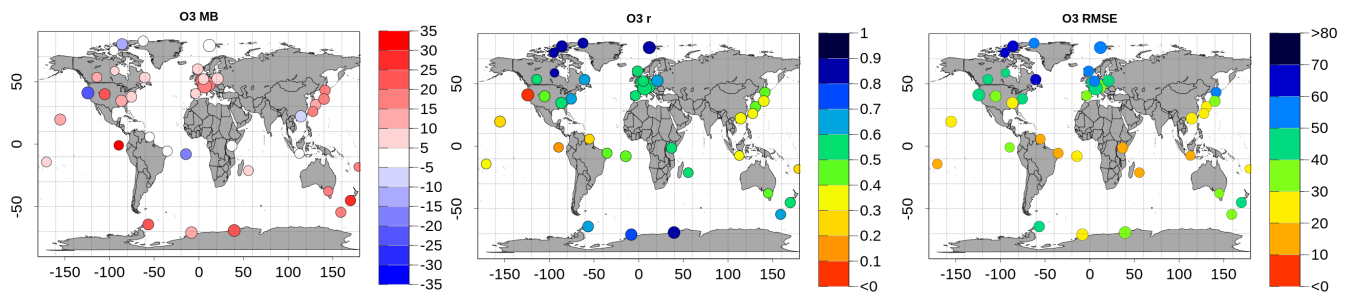
Figure 14. Mean tropospheric ozone bias spatial distribution ~~of NMMB/BSC-CTM minus ozonesondes~~ (MB, $\mu g\ m^{-3}$) (left panel), correlation (middle panel) and root mean square error (RMSE, $\mu g\ m^{-3}$) (~~middle panel) and correlation~~ (right panel) for ~~the whole~~ year 2004, averaged between 400-1000 hPa. The diameter of the circles indicates the number of profiles over the respective stations. The bias is calculated as model minus observation.

Table 1. Model characteristics and experiment configuration

Meteorology	
Dynamics	~~non-hydrostatic~~ nonhydrostatic NMMB (Janjic and Gall, 2012)
Physics	Ferrier microphysics (Ferrier et al., 2002)
	BMJ cumulus scheme (Betts and Miller, 1986)
	MYJ PBL scheme (Janjic et al., 2001)
	LISS land surface model (Vukovic et al., 2010)
	RRTMG radiation (Mlawer et al., 1997)
Chemistry	
Chemical mechanism	~~Carbond~~ Carbon Bond 05 (Yarwood et al., 2005)
Photolysis scheme	online Fast-J photolysis scheme (Wild et al., 2000)
Aerosols	No aerosols considered in this study
Dry deposition	Wesley resistance approach from Wesely (1989)
Wet deposition	Grid and sub-grid scale from Foley et al. (2010)
Biogenic emissions	MEGAN (Guenther et al., 2006)
Anthropogenic and other natural emissions	ACCMIP (Lamarque et al., 2010) and POET (Granier et al., 2005)
Stratospheric ozone	COPCAT (Monge-Sanz et al., 2011)
Resolution and Initial conditions	
Horizontal resolution	1.4° x 1°
Vertical layers	64
Top of the atmosphere	1 hPa
Chemical initial condition	MOZART4 (Emmons et al., 2010)
Meteorological initial condition	FNL/NCEP
Chemistry spin-up	1 year

Table 2. ~~Emissions~~ Emission totals by category ~~for 2004~~ in Tg(species)/year ~~.~~ for 2004. Anthropogenic and biomass burning emissions applied in this study are based on Lamarque et al. (2013). Ocean and soil natural emissions are based on the POET global inventory (Granier et al., 2005). Biogenic emissions are computed online from ~~the~~ MEGAN (Guenther et al., 2006).

Species	Anthrop.	Bio. burning	Biogenic	Soil	Ocean
CO	610.5	459.6	148.13	-	19.85
NO	85.8	5.4	16.54	11.7	-
SO_2	92.96	3.84	-	-	-
Isoprene (C_5H_8)	-	0.15	683.16	-	-
Terpene ($C_{10}H_6$)	-	0.03	120.85	-	-
Xylenes (C_8H_{10})	1.05	0.16	1.36	-	-
Methanol (CH_3OH)	-	-	159.91	-	-
Ethanol (C_2H_6O)	4.28	3.7	17.06	-	-
Formaldehyde (HCHO)	4.24	0.35	9.58	-	-
Aldehyde (R-CHO)	-	-	5.06	-	-
Toluene (C_7H_8)	0.66	0.19	0.79	-	-
Ethane (C_2H_6)	1.27	0.57	0.48	-	-
Ethylene (C_2H_4)	3.32	2.71	32.03	-	-

Table 3. ~~Ozonesondes main~~ Main information about the ozonesondes used in this ~~model evaluation for~~ study, including the ~~year 2004. Location of these ozonesondes is displayed in the third~~ location and ~~fourth columns. Columns 6-9 display the~~ number of available measurements for each season (DJF for December-January-February, MAM for March-April-May, JJA for June-July-August and SON for September-October-November).

Station	Country	Latitude	Longitude	Region	DJF	MAM	JJA	SON
Kagoshima	Japan	31.6N	130.6E	Japan	13	12	11	12
Saporo	Japan	43.1N	141.3E	Japan	12	10	12	10
Tsukubay	Japan	36.1N	140.1E	Japan	14	13	12	12
Alert	Canada	82.5N	62.3W	NH Polar	11	10	13	9
Edmonton	Canada	53.5N	114.1W	Canada	7	12	10	10
Resolute	Canada	74.8N	95.0W	NH Polar	9	10	8	6
Macquarie Island	Australia	54.5S	158.9E	SH Midlat	6	15	12	9
Lerwick	Great Britain	60.1N	1.2W	W Europe	9	13	13	12
Uccle	Belgium	50.8N	4.3E	W Europe	35	37	36	36
Goose Bay	Canada	53.3N	60.4W	Canada	12	13	13	12
Churchill	Canada	58.7N	94.1W	Canada	7	6	4	8
NyAlesund	Norway	78.9N	11.9E	NH Polar	25	24	23	17
Hohenpeissenberg	Deutschland	47.8N	11.0E	Europe	34	34	26	31
Syowa	Japan (Antarctica)	69.0S	39.6E	SH Polar	16	16	19	26
Wallops Island	US	37.9N	75.5W	US	11	15	17	7
Hilo	US	19.7N	155.1W	NH Subtropic	13	18	14	12
Payerne	Switzerland	46.5N	6.6E	Europe	38	40	38	40
Nairobi	Kenya	1.3S	36.8E	Equador	11	13	13	13
Naha	Japan	26.17N	127.7E	NH Subtropics	9	12	8	10
Samoa	Independent State of Samoa	14.2S	170.6W	W Pacific	9	11	8	9
Legionowo	Poland	52.4N	20.9E	Europe	16	18	16	18
Marambio	Antarctica	64.2S	56.6W	SH Polar	10	7	15	22
Lauder	New Zealand	45.0S	169.7E	SH Midlat	11	13	13	9
Madrid	Spain	40.5N	3.6W	Others	11	9	8	12
Eureka	Canada	80.0N	85.9W	NH Polar	17	17	11	13
De Bilt	Nederland	52.1N	5.2E	Europe	13	10	14	12
Neumayer	Antarctica	70.7S	8.3E	SH Polar	11	13	13	31
Hong Kong	China	22.3N	114.2E	NH Subtropics	12	26	11	13
Broad Meadows	Australia	37.7S	144.9E	Others	6	7	7	11
Huntsville	US	34.7N	86.6W	US	14	13	23	13
Parambio	Surinam	5.8N	55.2W	Equador	11	8	9	9
Reunion Island	France	21.1S	55.5E	Others	9	14	9	6
Watukosek	Indonesia	7.5S	112.6E	W Pacific	7	11	10	6
Natal	Brasil	5.5S	35.41W	Equador	10	12	13	7
Ascencion Island	Great Britain	7.98S	14.42W	Equador	12	12	12	18
San Cristobal	Galapagos	0.92S	89.6W	Equador	7	4	10	13
Boulder	US	40.0N	105.26W	US	12	11	17	16
Trinidad Head	US	40.8N	124.2W	US	4	7	5	8
Suva	Fiji	18.13S	178.4E	W Pacific	13	12	48	11

Table 4. MOZAIC aircraft information including the location of measurements, and the number of available measurements for each season (DJF, MAM, JJA and SON).

Station	Country	Latitude	Longitude	DJF	MAM	JJA	SON
Abu Dhabi	United Arab Emirates	24.44N	54.65E	11	17	58	20
Atlanta	US	33.63N	84.44W	24	130	168	66
Beijing	China	40.09N	116.6E	5	12	23	17
Cairo	Egypt	30.11N	31.41E	19	16	2	8
Caracas	Venezuela	10.6N	67W	21	9	9	21
Dallas	US	32.9N	97.03W	8	24	24	10
Douala	Cameroon	4.01N	9.72E	7	0	10	6
Frankfurt	Germany	50.02N	8.53E	169	295	286	192
New Delhi	India	28.56N	77.1E	30	24	72	38
New York	US	40.7N	74.16W	79	23	41	16
Niamey	Niger	13.48N	2.18E	4	0	12	12
Portland	US	45.59N	122.6W	5	8	5	4
Tehran	Iran	35.69N	51.32E	8	11	31	18
Tokyo	Japan	35.76N	140.38E	38	50	56	34

Table 5. Description of additional aircraft campaign data, including location and date.

Region Name	Expedition	Latitude	Longitude	Date
Boulder	TOPSE	37-47N	110-90W	5 February to 23 May 2000
Churchill	TOPSE	47-65 N	110-80W	5 February to 23 May 2000
China	TRACE-P	10-30N	110-130E	24 February to 10 April 2001
Hawaii	TRACE-P	10-30N	170-150W	24 February to 10 April 2001
Japan	TRACE-P	20-40N	130-150E	24 February to 10 April 2001
Tahiti	PEM-Tropics-B	20S-0	160W-130W	6 March to 18 April 1999
Ireland	POLINAT-2	50-60N	15-5W	19 September to 25 October 1997

Table 6. Annual mean burden of tropospheric CO (Tg CO) in the NMMB-MONARCH, MOZART-2, TM5 and C-IFS global models.

Model	Burden						Dry depo.	Reference
	Global	NH	SH	Trop.	N. Extratrop.	S. Extratrop.		
NMMB-MONARCH	399	221	177	229	101	67	24	This study
MOZART-2	351	210	142	199	102	50	2	Horowitz et al. (2003)
TM5	353	-	-	188	106	59	184	Huijnen et al. (2010)
C-IFS	361	-	-	-	-	-	-	Flemming et al. (2015)

Table 7. Annual mean burden, dry deposition of tropospheric O_3 and stratospheric inflow (Tg O_3) for the ~~NMMB/BSC-CTM~~NMMB-MONARCH, MOZART-2, TM5~~and~~, LMDz-INCA, GFDL AM3, C-IFS global models, and two different ~~Multimodel~~ multi-model ensembles (including 25 and 15 global models each).

Model	Burden						Dry deposition	Stratospheric inflow	Reference
	Global	NH	SH	Trop.	N. Extra.	S. Extra.			
~~NMMB/BSC-CTM~~ NMMB-MONARCH	348	189	158	171	101	75	1201	384	This study
MOZART-2	362	203	159	203	99	60	857	343	Horowitz et al. (2003)
TM5	312	-	-	165	84	63	829	421	Huijnen et al. (2010)
LMDz-INCA	303	178	125	-	-	-	1261	715	Folberth et al. (2006)
GFDL AM3	360±7	-	-	-	-	-	1205±20	-	Naik et al. (2013a)
C-IFS	390	-	-	-	-	-	-	-	Flemming et al. (2015)
~~Multimodel~~ Multi-model	344 ± 39	-	-	-	-	-	1003 ± 200	552 ± 168	Stevenson et al. (2006)
~~Multimodel~~ Multi-model	337 ± 23	-	-	-	-	-	-	-	Young et al. (2013)